1-1-2015

Probabilistic Musculoskeletal Simulation Methods to Address Intersegmental Dependencies of the Knee, Hip, and Spine

Casey A. Myers
University of Denver

PROBABILISTIC MUSCULOSKELETAL SIMULATION METHODS TO ADDRESS INTERSEGMENTAL DEPENDENCIES OF THE KNEE, HIP, AND SPINE

A Dissertation

Presented to

The Faculty of the Daniel Felix Ritchie School of Engineering and Computer Science

University of Denver

In Partial Fulfillment

of the Requirements for the Degree

Doctor of Philosophy

---

by

Casey A. Myers

June 2015

Advisor: Bradley S. Davidson, PhD

Author: Casey A. Myers
Title: PROBABILISTIC MUSCULOSKELETAL SIMULATION METHODS TO ADDRESS INTERSEGMENTAL DEPENDENCIES OF THE KNEE, HIP, AND SPINE
Advisor: Bradley S. Davidson, PhD
Degree Date: June 2015

ABSTRACT

Orthropaedic clinical practice in the area of the knee, hip, and spine has benefited from the concept of regional interdependence, where interventions applied to one region can influence the outcome and function of other regions of the body that may be seemingly unrelated to the applied intervention. An understanding of the biomechanical mechanisms that describe clinical practice involving knee, hip, and spine regional interdependence can improve treatment of a wide range of pathological conditions. Improvement in this area can be particularly impactful on the outcomes of patients with total joint replacement, where pathology and compensatory strategies develop during multi-joint interactions. Additionally, probabilistic methods are well suited to address knee, hip, and spine regional interdependence by using input distributions to quantify the impact of variability on the range of possible output variables. Outputs from probabilistic methods include variable interaction effects and provides sensitivity information, resulting in a more comprehensive evaluation of a system The main objectives of the work presented in this dissertation were to further our understanding of the interdependencies of the knee, hip, and spine with probabilistic musculoskeletal modeling. These objectives were achieved by developing a probabilistic plugin for use in OpenSim and performing investigations of the regional interdependence of the knee, hip, and spine involving patients with total joint replacement. An initial study identified how

uncertainty in musculoskeletal simulation inputs can propagate through the stages of analysis and impact interpretation of outputs from a simulation of gait. Second, improvements to current modeling methodology for patients with total hip arthroplasty were made through the implementation of patient-specific strength scaling and input uncertainty assessment. The third study then applied these methods in an investigation of knee, hip, and spine regional interdependence in rehabilitation of patients with total hip arthroplasty to quantify the influence of simulated strengthening of hip musculature on the dynamic and mechanical interdependencies of the knee, hip and spine. A final study demonstrated how population-based musculoskeletal modeling can further impact the study of knee, hip, and spine regional interdependence by presenting the feasibility study of performing population-based musculoskeletal modeling. These studies include several novel methods for investigating the regional interdependencies of the knee, hip, and spine that have been used to translate outputs from musculoskeletal simulations into rehabilitation practice.

ACKNOWLEDGMENTS

First and foremost, I thank my advisor Dr. Bradley Davidson for his guidance and support during my years at the University of Denver. You have been a wonderful mentor and critical to helping me to grow throughout this process. I would like to thank all of my committee. Dr. Laz, thank you for unselfishly giving so much of your time and energy to bringing your expertise to this project and holding it to the highest possible standard. I appreciate the unique role you played in my own personal development and in the guidance of the work. Dr. Shelburne, I cannot thank you enough for your role as a mentor and friend throughout the years. So much of the reason I find myself at this point in my career is due to your influence. It has been a wonderful journey and I look forward to continuing it in the future. I would also like to thank Dr. Decker for always challenging me to look at problems in unique ways and for being a trusted friend and colleague. I have enjoyed being around the most talented and enjoyable people I have ever worked with in my fellow graduate students in the lab. I would like to especially thank Craig Simons, Brecca Gaffney and Stu Currie. I thank my parents David and Kathy Myers for their unending love and support as well as all of their many sacrifices that have allowed me to pursue all of goals and aspirations. Additionally, I could not have completed this work without the love and devotion of Lori Miller. Her support during a very difficult time gave me inspiration when things were most challenging. Lastly, this research would not have been possible without the generous support provided by the Gustafson family through the Donald W. Gustafson Fellowship in Orthopaedic Biomechanics. In addition, Kim and David Gustafson have provided so much more than financial support that has contributed to my career development and I could never thank them enough.

TABLE OF CONTENTS

LIST OF FIGURES

PAGE

LIST OF TABLES

PAGE

CHAPTER 1 – INTRODUCTION AND DISSERTATION OVERVIEW

1.1: Knee, Hip, and Spine as an Interdependent System.

There have been major advances in the biomechanical assessments of knee, hip and spine joint behavior using multi-scale approaches that combine experimental data with high fidelity computational models. For example, studies that evaluate the behavior associated with anterior cruciate ligament injury (Fernandez et al., 2011), osteoarthritis (Fregly et al., 2007), total joint replacement (Fitzpatrick et al., 2011) and spinal stability (Tanaka et al., 2010) have been successful at informing clinical decisions and improving patient outcomes. These studies contributed largely to our understanding of healthy and pathological function at the knee, hip and spine. However, often times the primary focus of the investigation is on the affected joint in isolation.

Improvements to the combined experimental and computational approach to assessing joint function can be made by considering the knee, hip and spine as an interdependent system. Clinical practice in the area of the knee, hip and spine has benefited from the concept of regional interdependence, where interventions applied to one region can influence the outcome and function of other regions of the body that may be seemingly unrelated to the applied intervention. Biomechanically, a perturbation or disturbance to any one anatomical body or musculoskeletal structure can influence the dynamics of a body segment (the forces, torques and resulting motion of

that segment) in which the perturbation/disturbance was not directly applied. Complex joint pathology in the knee, hip and spine, such as osteoarthritis, likely develops and progresses as a result of multi-joint interactions. Quantification of the knee, hip and spine interdependence in healthy and pathological populations can offer valuable insight for improved understanding of joint disease and treatment methods.

1.2: Musculoskeletal Modeling of Knee, Hip, and Spine Interdependence

Whole-body movement is often assessed through the use of the musculoskeletal modeling software platforms such as OpenSim (Delp et al., 2007) and Anybody (AnyBody Technology, Aalborg, Denmark). Musculoskeletal modeling is used to calculate joint kinematics and moments and as well as intersegmental joint loads and muscle forces. Musculoskeletal simulation offers valuable data to clinicians and researchers assessing pathological conditions and understanding human movement. Simulation of human movement has significantly impacted approaches to clinical treatment of cerebral palsy, lower extremity amputees, and osteoarthritis (Delp et al., 1996; Fregly et al., 2007; Silverman and Neptune, 2012) as well as basic science related to the understanding of movement progression and control during dynamic tasks (Anderson et al., 2004; Neptune et al., 2009; Zajac et al., 2002). There have been a number of impactful innovations in simulation methods from sophisticated subject-specific models with highly accurate anatomic detail (Arnold et al., 2010), to creation of efficient forward dynamics simulations using computed muscle control (Thelen and Anderson, 2006).

The only musculoskeletal modeling methods specifically related to regional interdependence use forward dynamic simulations and induced acceleration analysis to identify how individual muscles contribute to joint accelerations throughout the body (Neptune et al., 2001). This approach has been applied in a wide range of basic science applications (Anderson et al., 2004; Dorn et al., 2012; Liu et al., 2008) and has furthered our understanding of knee, hip and spine dynamics by identifying important non-hip spanning muscles with large contributions to hip joint function (Pandy, 2001; Zajac and Gordon, 1989). Similarly, continued innovation to musculoskeletal modeling through the addition of probabilistic methods, that are uniquely well-suited to address multi-joint interactions, can be used to expand our clinical understanding of knee, hip and spine regional interdependence and also provide a valuable tool to the musculoskeletal community.

1.3: Combining Probabilistic Methods with Musculoskeletal Modeling

Probabilistic methods use input distributions to quantify the impact of variability on the range of possible output variables. This approach includes variable interaction effects and provides sensitivity information, resulting in a more comprehensive evaluation of a system. Developers of musculoskeletal models are mindful that simulation outputs are dependent on inputs that have inherent variability and uncertainty in which there are currently no openly available methods to quantify the effects of this inherent variability. In addition to quantifying the impact of variability and uncertainty on model outputs, probabilistic methods offer the ability to quantify the interdependence of the knee, hip and spine. This can be achieved by evaluating the influence of perturbations

to the parameters of one segment on the output dynamics (the forces, torques and resulting motion of that segment) other segments in which the perturbation was not directly applied.

Accordingly, the main objectives of this dissertation were to further our understanding of the interdependencies of the knee, hip and spine with probabilistic musculoskeletal modeling. These objectives were achieved by developing a probabilistic plugin for use in OpenSim and performing investigations of the regional interdependence of the knee, hip and spine involving patients with total joint replacement, where these methods can have clinical impact and improve patient outcomes.

1.4: Dissertation Overview

Chapters 1-4 will cover foundational concepts and an experimental study that support the theory and methodology of the dissertation. Chapters 5-7 demonstrate the application of the theory and methodology from the early chapters in musculoskeletal simulation studies. Chapter 2 will expand on the clinical and scientific importance of regional interdependence and review the literature that has demonstrated the vital role of the hip musculature in influencing joint function of the knee, hip and spine. Chapter 3 is an experimental investigation of the regional interdependence of the knee, hip, and spine through the use of an external support garment. An overview of the probabilistic methods and interpretations used extensively throughout this dissertation is provided in chapter 4. Following a review of these methods, the dissertation will focus on the application of these methods.

Chapters 5-7 will describe the application of the probabilistic plugin that was designed for use in OpenSim. Chapter 5 is a study that assessed how uncertainty in standard musculoskeletal simulation inputs can propagate through the stages of analysis and impact interpretation of outputs from a simulation of gait. Chapter 6 contains two studies that 1) use the OpenSim probabilistic plugin to improve on current modeling methodology for patients with total hip arthroplasty and 2) apply those methods in a study to quantify the influence of simulated strengthening of hip musculature on lower extremity and spine loads. Chapter 7 introduces how population-based musculoskeletal modeling can further impact the study of knee, hip and spine regional interdependence and presents a feasibility study to address challenges in performing population-based modeling in OpenSim. The appendix includes the user manual for the probabilistic plugin with tutorial examples and recommendations for best practices.

CHAPTER 2 – A REVIEW OF KNEE, HIP, AND SPINE REGIONAL INTERDEPENDENCE AND THE VITAL ROLE OF THE HIP MUSCULATURE

This chapter will introduce the concept of regional interdependence by defining it and describing examples from the clinical literature where the concept has been applied for pathological interpretation and/or treatment. Additionally, the role of the hip musculature in influencing knee, hip and spine mechanics is described along with methods that have been used to quantify the interdependence of the knee, hip and spine using musculoskeletal modeling.

2.1 Regional Interdependence Definition

There is a growing body of literature demonstrating that interventions applied to one anatomical region of the body can influence the outcome and function of other regions of the body that may be seemingly unrelated to the applied intervention. This is a concept known as regional interdependence that has emerged primarily in the clinical literature. Regional interdependence was originally defined as a concept that unrelated impairments in remote anatomical regions could contribute to a patient's primary complaint. A proposed more comprehensive definition of regional interdependence was that a patient's primary musculoskeletal symptoms may be directly or indirectly influenced by impairments from various body regions and systems regardless of proximity to the primary symptoms (Sueki et al., 2013; Wainner et al., 2007).

These definitions remain rooted in the clinical observations that gave rise to the concept of regional interdependence. In order to address the mechanisms that produce the concept from a biomechanical perspective, it is necessary to further develop the definition in terms of musculoskeletal system dynamics. The concept in these terms is defined as: a perturbation or disturbance to any one anatomical body or musculoskeletal structure can influence the dynamics of a body segment (the forces, torques and resulting motion of that segment) in which the perturbation/disturbance was not directly applied.

2.2 Clinical Examples of Regional Interdependence

The definition of regional interdependence is best illustrated using examples from the clinical literature. The majority of literature supporting the concept of regional interdependence is related to the knee, hip, and spine region. Clinicians have identified practices that rely on the concept of regional interdependence to treat a range of pathologies that affect the knee, hip and spine. Patients with primary low back pain and knee complaints have received treatment directed at the hip and experienced positive outcomes (Currier et al., 2007; Deyle et al., 2005, 2000). Additionally, interventions targeting the lumbar spine have been reported in the management of patients who have primary complaints of hip and knee pain (Suter et al., 2000). A relationship has even been proposed between the foot and ankle and the lumbosacral region (Cibulka, 1999; Rothbart and Estabrook, 1999). While many of these relationships have been identified in individual case studies, there are various examples of successful patient outcomes resulting from relationships of regional interdependence in randomized controlled trials.

Low back pain has been associated with pathologies of the hip that include, osteoarthritis, bone fractures and total hip replacement (Porter and Wilkinson, 1997; Reiman et al., 2009). Over thirty years ago, concurrent pathology at both the hip and spine was identified in older populations and labeled as 'hip-spine syndrome' (Offerski and MacNab, 1983). In an early case study, a female patient was diagnosed with what was called 'secondary hip-spine syndrome'. Her symptoms were low back pain, accompanied by anterior thigh pain, denegation in the lumbar spine and osteoarthritis in both hips. In more recent studies, investigators have identified that severe hip osteoarthritis can result in abnormal spinal alignment, particularly in the sagittal plane, that results in adverse changes to muscle length and joint contact forces (Reiman et al., 2009). Further, Yoshimoto et al. (2005) identified higher pelvic incidence, and associated higher lumbar lordosis, as a predictor for hip osteoarthritis later in life. In patients with late stage hip osteoarthritis, total hip arthroplasty is commonly performed, resulting in reductions in hip pain and higher levels of overall function. In addition, both spinal alignment and low back pain have been found to improve following total hip arthroplasty (Ben-galim et al., 2007; Parvizi et al., 2010).

Clinical relationships between the hip and spine have also been identified in less severe, pre-arthritic conditions as well. Clinicians have used the relationship between the hip and spine in treatment strategies that involve non-surgical methods, as well as minimally invasive hip arthroscopic surgical procedures in some cases. For example, runners with chronic hip pain demonstrate significant reductions in pain and increases in mobility with the use of lumbar back manipulation techniques (Cibulka and Delitto, 1993). Conversely, imbalances in hip range of motion have been identified in patients

with low back pain (Ellison et al., 1990; Esola et al., 1996; Porter and Wilkinson, 1997; Sjolie, 2004). It has been hypothesized that alterations in hip range of motion can lead to increased stress on the sacroiliac joint and lumbar spine and lead to the development of pain in these areas. Physical therapy designed to correct these imbalances through stretching and strengthening has been shown to effectively reduce low back pain in certain patients (Winter, 2015). In cases when physical therapy is ineffective, arthroscopic hip surgery has become a well-recognized treatment option for multiple pathologic processes in and around the hip joint. A study by Kelly et al. (2012) showed improvement in hip internal rotation after arthroscopic treatment of femoroacetabular impingement, which has been demonstrated to reduce low back pain in patients with coexisting spinal pathologies (Redmond et al., 2014).

In further investigation of the concept of regional interdependence, there has also been a relationship identified between the lumbar spine and the presence of knee pathologies (Boyle et al., 2014). Low back pain is present in 54.6% of patients with knee osteoarthritis and almost every knee osteoarthritis clinical status measure is worse in the patients with low back pain (Wolfe et al., 1996). This may be partially explained by the influence of spinal kinematics on knee range of motion. In 365 patients with pain in the knee and/or low back pain, a significant relationship was indicated between lower degrees of lumbar lordosis and reduced knee flexion/extension range of motion (Murata et al., 2003). Successful treatment of these patients has targeted both the hip and spine. Cliborne et al. (2004) demonstrated that subjects with knee osteoarthritis experienced an average decrease in pain and improved knee range of motion after receiving physical therapy treatments that targeted hip mobility. Additionally, spinal manipulation of the

sacroiliac joint has been used to effectively increase knee extensor muscle activity in patients with anterior knee pain and proposed as a method for treating a broad range of knee pathologies (Suter et al., 2000).

Clinical cases, interventions and clinical decision making focused on a single pathological structure have often resulted in poor outcomes (Bogduk, 2000; van Tulder et al., 1997). The studies discussed have reported positive patient outcomes when targeting areas or structures not seemingly involved in the primary complaint. However, it has been commonly noted in the cited work that when using treatments attempting to influence regions away from the primary symptoms, individual responses can be highly variable. The underlying mechanisms that lead to improved patient outcomes when using treatment models that rely on regional interdependence are not well understood. To better understand these mechanisms, it is necessary to identify the major muscles and musculoskeletal structures involved in knee-hip-spine regional interdependence and derive methods that can be used in the quantification of the mechanical relationships that explain knee-hip-spine regional interdependence.

2.3 Influence of the Hip Abductor Musculature in Knee, Hip, and Spine Regional Interdependence

Previous investigations have identified the ability of the hip abductor muscle group to influence the function of the knee, hip and spine. The hip abductor muscle group is made up of the gluteus maximus, gluteus medius, gluteus minimus, tensor fasciae latae, piriformis and gemellus (Figure 2.1). The attachment sites for these muscles include the sacrum, pelvis and the femur. The architecture of the muscles of the hip abductor group

enable their influence on the three-dimensional orientation of the pelvis during movement, which determines each muscles force generating parameters (i.e., muscle length, moment arm length). The relationship between pelvic orientation and hip abductor muscle function has been hypothesized to be a key component in knee-hip-spine regional interdependence. Previous studies on whole body balance have suggested that hip muscle force production is crucial in minimizing the acceleration of the body center of mass in response to postural perturbations (Aramaki et al., 2001). In pathological studies of this relationship, several studies have reported that individuals with patellofemoral pain syndrome demonstrate deficits in hip abductor muscle strength and exhibit greater degrees of hip adduction and internal rotation during dynamic activities such as landing from a jump (Lee et al., 2012; Powers, 2010; Salsich and Long-Rossi, 2011).

Of the hip abductor muscles, the gluteus medius has been specifically linked to knee-hip-spine regional injury and dysfunction. The gluteus medius is one of the strongest lower extremity muscles based on physiological cross-sectional area and its architecture has lines of action in multiple movement planes. Gluteus medius dysfunction has been associated with injuries superior to the pelvis in the upper extremities (Oliver, 2014; Plummer and Oliver, 2014) and lower back (Nelson-Wong et al., 2008), as well as inferior to the pelvis at the hip (Bolgla and Uhl, 2005), knee (Crossley et al., 2012), and ankle (Beckman and Buchanan, 1995). The link between the gluteus medius muscle function and injury risk may be a result of weakness in this muscle, which results in poor stability (Wilson, 2005) and excessive hip, pelvic, and trunk kinematics during weight-bearing activities (Powers, 2010; Souza and Powers, 2009; Thijs et al., 2007). Alterations

in the neuromuscular control parameters of the gluteus medius characterized by reduced activation, delayed onset, and decreased activation duration (Aminaka et al., 2011; Beckman and Buchanan, 1995; Brindle et al., 2003; Cowan et al., 2009; Santos et al., 2013; Willson et al., 2011) are also associated with abnormal hip, pelvic, and trunk kinematics for individuals with movement based problems (Barton et al., 2013). To further investigate the role of the gluteus medius, in the next chapter, we present an investigation of knee-hip-spine regional interdependence using biomechanical variables related to core control and dynamic stability and supportive technology designed to enhance the function of the gluteus medius.

2.4 Quantifying the Role of Hip Abductors in Regional Interdependence

Defining the mechanisms of regional interdependence in terms of the musculoskeletal system dynamics could improve outcomes from rehabilitation strategies that incorporate the concept of regional interdependence. In order to do this, it is necessary to use a musculoskeletal model that includes detailed geometry and musculature of the hip and pelvis. There have been studies that have demonstrated the interdependencies of the knee, hip and spine using musculoskeletal models.

The dynamic coupling between body segments has been represented by calculating how individual muscle forces contribute to the angular accelerations of all joints at each instant of a dynamic motion (Pandy, 2001; Zajac and Gordon, 1989). For example, Correa et al., (2010) demonstrated during gait, that the vasti, soleus and gastrocnemius contribute greater than 0.5 BW to hip contact force. Because the articular contact forces are a function of the joint angular accelerations, each muscle force also

contributes to the contact force transmitted by each joint. Therefore, muscles that do not cross a specific joint are capable of contributing to the contact force at that joint.

The probabilistic methods that will be described in chapter 4 are uniquely suited to quantify the mechanisms of regional interdependence when combined in a musculoskeletal modeling framework. These methods allow for systematic perturbations to be made to one specific anatomic area or structure, while quantifying the impact on any other segment or structure in the model. A previous investigation did demonstrate the feasibility of this method in a probabilistic approach; however it did not specifically address regional interdependence. Valente et al. (2013) simulated the effect of hip abductor weakness by reducing the maximum force generating capacity of the muscles in a probabilistic framework and evaluating the effects on hip and knee joint loading. Their results demonstrated that there were greater increases in the peak knee joint load than in the load at the hip. Additionally, the gluteus medius was the abductor muscle with the most influence on hip and knee loads. This study demonstrates how a probabilistic approach can evaluate regional independence and how the further advances discussed in this dissertation can describe the mechanisms that contribute to knee-hip-spine regional interdependence to influence clinical decision making.

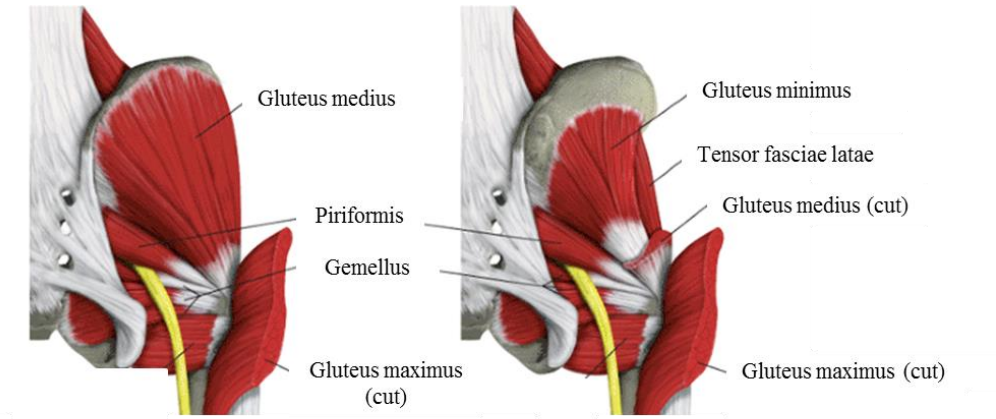

Figure 2.1: Hip abductor muscle group

CHAPTER 3 –THE EFFECTS OF EXTERNAL CORE SUPPORT ON PROPRIOCEPTION AND DYNAMIC STABILITY

This chapter describes an experimental study that evaluated the effect of an external core support garment designed to enhance the function of the hip abductor group on proprioception and dynamic stability. Data from this study was used in the probabilistic simulations described in the chapters to follow.

3.1 Abstract

The study design was a randomized cross-over design comparing two support conditions during dynamic tasks of varying difficulty. Core stability dysfunction is linked to musculoskeletal pathologies that range from lower extremity joint disease and injury to low back pain. The object of this study was to determine the effects of a novel support garment designed to enhance the function of the gluteus medius on core proprioception and dynamic stability. Fourteen healthy participants (9 male, 5 female) performed a core proprioception unstable sitting task and a dynamic landing task while wearing form-fitting, athletic shorts with built in core support (CS) and without support (WOS). Each participant sat on an unstable surface with the eyes open, and with the eyes closed and under two levels of task difficulty. Performance was represented by the average velocityof the 3D marker path length. Each participant performed single leg landings onto a force platform and kinematics and kinetics of the lumbar spine, pelvis, hip, knee,

and ankle segments were calculated. The frontal plane moment arm of the groundreaction force was calculated throughout the landing task at the ankle, knee and hip. The average velocity of 3D path length significantly increased with increasing task difficulty for each unstable sitting condition (P<0.001). However, the increase when visual input was removed was 19.1% smaller with the addition of core support (P=0.040). The peak hip abductor moment was reduced on average by 6.3% when landing with CS (WOS: -123.4 ± 35.8 Nm vs. CS: -115.0 ± 25.4 Nm; P=0.041). The moment arm at peak GRF was reduced with core support by an average of 0.9 cm at the knee joint (CS: -1.22±1.16 vs. WOS: -2.27±1.68 cm; P<0.001) and 1.9 cm at the hip joint (CS: -4.71±1.64 vs. WOS: -6.79±1.53 cm; P<0.001). Core support designed to enhance the function of the gluteus medius resulted in significant improvements in core proprioception and dynamic stability. Use of supportive technology that enhances the role of the hip abductors may lead to improved clinical outcomes and decreased injury rates during high-demand dynamic tasks.

3.2 Introduction

Core stability dysfunction is associated with a number of musculoskeletal pathologies that range from lower extremity joint disease and injury (Grimaldi et al., 2009; S. P. Lee et al., 2012; Leetun, 2004) to low back pain (Jo et al., 2011; D. C. Lee et al., 2012; Radebold et al., 2001; You et al., 2014). The musculoskeletal core of the body includes the passive contributions of the hip, pelvis, and thoracolumbar spine, as well as the active contributions of the musculature in this region. The core provides the proximal stability for the control and function of the extremities that is developed in a proximal to

distal progression (Hodges and Richardson, 1997). This proximal core stability is maintained by the central nervous system and the complex interrelationship between sensory information obtained from the somatosensory, visual, and vestibular systems (Xu et al., 2010). Proprioception is a key component of the somatosensory system's contribution to core stability, and poor proprioception is linked to reduced control of the lumbar spine and longer trunk muscle response times in patients with low back pain compared to healthy individuals (Radebold et al., 2001). Additionally, lower extremity function can be compromised when core proprioception is poor. For example, recent prospective studies reported that female athletes with impaired core proprioception had a higher incidence of lower extremity injury compared to those with normal core proprioception (Beynnon et al., 2001; Zazulak et al., 2007).

Core stability is also influenced by the regional interdependence of the hip, pelvis, and lumbar spine, in which perturbations or interventions to any one region of the core can influence the function and outcome of other regions not directly affected (Sueki et al., 2013; Wainner et al., 2007). The three-dimensional orientation of the pelvis during movement is a key component in hip/spine regional interdependence given its influential role on the muscle force parameters (i.e., muscle length, moment arm length) of the hip abductors (Delp et al., 1999; Kibler et al., 2006). Using a simulated hip model, Merchant, (1965) demonstrated that abnormal hip rotation (both internal and external) reduced the mechanical advantage of the hip abductor muscles and presented a greater challenge for these muscles to control pelvis and trunk orientation during weight bearing.

Of the hip abductor muscles, the gluteus medius plays a significant role in core stability, and is linked to regional injury and dysfunction. The gluteus medius is one of

the strongest lower extremity muscles based on physiological cross-sectional area and architecture with lines of action in multiple movement planes. The gluteus medius is made up of three nearly equal sized sections in a fanned shape with origins that span the outer surface of the ilium and insert at the superior region of the greater trochanter (Ward et al., 2009). Because of the size and architecture, gluteus medius dysfunction has been associated with injuries superior to the pelvis in the upper extremities (Oliver, 2014; Plummer and Oliver, 2014) and lower back (Nelson-Wong et al., 2008), as well as inferior to the pelvis at the hip (Bolgla and Uhl, 2005), knee (Crossley et al., 2012), and ankle (Beckman and Buchanan, 1995). The link between the gluteus medius muscle function and injury risk may be a result of weakness in this muscle, which results in poor core stability (Wilson, 2005) and excessive hip, pelvic, and trunk kinematics during weight-bearing activities (Powers, 2010; Souza and Powers, 2009; Thijs et al., 2007). Alterations in the neuromuscular control parameters of the gluteus medius characterized by reduced activation, delayed onset, and decreased activation duration (Aminaka et al., 2011; Beckman and Buchanan, 1995; Brindle et al., 2003; Cowan et al., 2009; Santos et al., 2013; Willson et al., 2011) are also associated with abnormal hip, pelvic, and trunk kinematics for individuals with movement based problems (Barton et al., 2013).

The function of the gluteus medius to regulate core stability during movement may be enhanced with the use of external support. Traditional attempts to treat pathology associated with gluteus medius has focused on strength training. Although strength training has demonstrated short-term success in relieving pain and improving joint kinematics, it may not be effective at preventing these issues from recurring (Blond and Hansen, 1998; Ferber et al., 2010). Hip abduction bracing has long been used in

rehabilitation following hip surgery to provide mechanical assistance with joint stability as well as improved proprioceptive feedback to enhance joint positional awareness (DeWal et al., 2004; Kelly et al., 2005). However, bracing can be cumbersome and restrict joint mobility. A more recent approach to external support incorporates two or more fabrics with varying mechanical properties that when combined in a garment applies a directional pattern of compression to the body. A recent study demonstrated that these garments reduced the demand on hip musculature during high-demand tasks (Chaudhari et al., 2014), but the influence on kinematics and kinetics remains unknown.

It may be possible for external support of the gluteus medius through directional compression to improve sensory feedback and mechanical stability within the core. Therefore, the **objective** of this study was to assess the effects of a novel support garment with directional compression on core proprioception and dynamic stability during dynamic tasks. We hypothesized that (1) core support would improve performance during a proprioception-based task of unstable sitting and that (2) core support would alter the kinematics and kinetics of the lower extremity by redirecting ground reaction forces during a single leg landing task.

3.3 Methods

Fourteen healthy participants (9 male, 5 female) that were free of neurological illness and musculoskeletal injury performed unstable sitting and single leg landings with (CS) and without (WOS) external core support. During the WOS condition, each participant wore a standard form-fitting short (Under Armour, Inc., Baltimore, MD). During the CS condition, each participant wore the CoreTec short (Opedix LLC, USA)

that was designed to provide directional compression that replicates the function of the hip abductor muscles with diagonal bands of fabric with low elasticity spiraling downwards from the waist and hips to the thighs. This banding pattern is overlaid onto a standard compression base layer with high elasticity (Figure 3.1). Fit was determined based on manufacturer's guideline using the waist circumference of the participant. To prevent systematic bias in the data, task order was randomly selected and order of core support was balanced across the participants. All procedures were approved by the Institutional Review Board and all participants signed an informed consent form prior to participation.

3.3.1:Unstable Sitting

Core proprioception was assessed while each participant sat on an unstable surface composed of a chair affixed on a hemisphere (Figure 3.2). The center of the hemisphere was placed behind the front edge of the chair at 75% of the participant's femur length. To prevent lower-body movement while sitting on the chair, leg and foot supports were adjusted so that the feet were flat and both ankle and knee angles were 90º in the sagittal plane. The feet were aligned to the posterior edge of the foot support. To balance the mass of the chair supports with the mass of the feet and legs of the participant, a 12-kg mass was placed on a horizontal arm that extended posteriorly from the leg and foot support and centered along the medial/lateral axis of the chair. The location of the mass was adjusted in the anterior or posterior direction so that each participant could maintain an upright torso when the chair surface was level. A horizontal

safety railing was positioned in front of the chair and vertically adjusted to chest height while the participant was seated.

Each participant grasped the safety railing between the trials to prevent additional learning between trials. At the initiation of each trial, the participant released the safety railing, immediately crossed their arms in front of them with their hands on their shoulders with arms tucked in, and kept the chair as still as possible for 10 seconds while maintaining an upright torso posture. Three trials with eyes open (EO) and eyes closed (EC) were collected under two levels of task difficulty by changing the diameter of the sphere: 39 cm diameter (more difficult) and 44 cm diameter (less difficult). Retro-reflective markers were placed on the corners of the chair surface. Two variables that describe core proprioception performance were calculated during the first five seconds of each sitting trial: average velocity and maximum displacement of the three-dimensional location of the markers.

3.3.2: Single Leg Landing

Each participant performed three single leg landings by jumping with their dominate leg onto a force platform from a horizontal distance equal to their greater trochanter height. Each participant was instructed to jump and land on a target located on the force plate, balance as fast as possible, and remain balanced for five seconds. Trials wherein the participants missed the landing target or demonstrated a loss of balance that included a touch down with their non-weight-bearing leg were recollected.

Each participant was instrumented with 44 retro-reflective markers and three-dimensional coordinates were captured (100 Hz) with an eight-camera motion capture

system (Vicon, Centennial, CO). Ground reaction forces under the landing leg were measured (1000 Hz) with a force platform (Bertec, Columbus, OH). Kinematics and kinetics of the lumbar spine, pelvis, hip, knee, and ankle between ground contact and five seconds following contact were calculated using the gait2392 model in OpenSim (Delp et al., 2007). Models were scaled for each participant based segment dimensions calculated from marker locations.

The frontal plane moment arm of the ground reaction force was calculated at the ankle, knee, and hip (Shelburne et al., 2008, 2006) by projecting the ground reaction force vector to the height of the joint and calculating the horizontal distance between the ground reaction force vector and joint center (Figure 3.3). Four variables that described the moment arm were calculated: average moment arm, standard deviation of the moment arm, maximum excursion during the landing task, and the moment arm at peak ground reaction force.

3.3.3: Data Analysis

For the variables from each task (single leg landing, unstable sitting), the three trials collected for each participant were averaged with each condition to create the dependent variables used in the statistical analyses. Paired *t*-tests were used to assess the effect of external core support conditions (CS, WOS) on the single leg landing task (peak ground reaction forces, moment arm variables, kinematics, and joint kinetics). A three-way repeated measures ANOVA with Bonferroni post-hoc comparisons were used to compare the effects of external core support (CS, WOS), visual input (EO, EC), and task difficulty (less difficult, more difficult) on core proprioception performance during

unstable sitting (average velocity, maximum displacement). Alpha level was set at 0.05 for all inferential comparisons.

3.4: Results

3.4.1: Unstable Sitting

The average velocity of 3D path length significantly increased with increasing task difficulty for each condition ($P<0.001$) (Figure 3.4). A greater increase in 3D path length velocity was observed between eyes open/closed conditions (avg: 71.1% difference; $P<0.001$) than more/less difficult sphere (avg: 20.6% difference; $P<0.001$). However, the increase in average path length velocity that occurred when visual input was removed was 19.1% smaller on average with the addition of core support ($P=0.040$). The reduction in average velocity of the 3D path length by CS was the greatest when task difficulty was the highest with the more difficult sphere and when visual input was removed (23.2 vs. 19.9 mm/s; $P=0.028$). Additionally, the maximum 3D path length increased with greater task difficulty ($P<0.001$) and the increase was an average of 18.9% less with CS across all conditions ($P=0.010$).

3.4.2: Single leg Landing

The jump that proceeded the single leg landing was performed the same in both external support conditions as indicated by the lack of statistical differences in all initial contact kinematics. During the single leg landing, frontal plane hip range of motion and

pelvis range of motion were not statistically different between external support conditions (hip: P=0.450; pelvis: P=0.800) (Table 3.1).

The peak hip abductor moment was reduced on average by 6.3% when landing with CS (WOS: -123.4 ± 35.8 Nm vs. CS: -115.0 ± 25.4 Nm; P=0.041;) (Table 3.2). Further analysis revealed that the magnitude of the peak vertical and mediolateral ground reaction forces were reduced 6.5% and 10.8% during the CS condition (vertical, P=0.033; mediolateral, P=0.098) (Figure 3.5).

Lower extremity joint moments were affected by the direction of the GRF relative to each joint center. Frontal plane GRF moment arm at the ankle joint was not significantly different between core support conditions; however, the knee and hip joint moment arms decreased with core support (Figure 3.6). There were significant reductions in the excursion of the moment arm over the landing task at the knee (CS: -3.28±1.56 vs. WOS: -3.83±1.84 cm; P=0.030) as well as the amount of variability in the moment arm values at the knee (CS: 0.83±0.41 vs WOS: 1.08±0.46 cm; P=0.049) and hip (CS: 1.15±0.52 vs. WOS: 1.77±0.66 cm; P<0.001). Notably, the moment arm at peak GRF reduced by an average of 0.9 cm at the knee joint (CS: -1.22±1.16 vs. WOS: -2.27±1.68 cm; P<0.001) and 1.9 cm at the hip joint (CS: -4.71±1.64 vs. WOS: -6.79±1.53 cm; P <0.001) with core support.

Differences in forces and moments during the landing task may have been associated with small differences observed in lumbar angles between the CS and WOS conditions. There was an average 7.5% reduction in lateral bending excursion with CS (P=0.030). Additionally, there was a trend toward a reduction in the overall amount of variability in lateral bending throughout the landing task (Table 3.3).

3.5: Discussion

Core support designed to support gluteus medius function produced significant improvements in core proprioception and dynamic stability during unstable sitting and single leg landing, respectively. This study was designed to assess the proprioceptive effects of the support garment during an isolated core activity, and the mechanical effects on the lower extremity during a whole-body dynamic task. Expected decreases in unstable sitting performance due to the removal of visual input and increased task difficulty were reduced with core support. During the single leg landings, core support resulted in subtle but significant reductions in the vertical ground reaction force and the peak frontal plane hip moment. These findings indicate that core support directed at the proprioceptive and mechanical contributions of the hip abductor group may be beneficial in avoiding injuries and pathological conditions that arise from a lack of core stability.

A significant improvement in unstable sitting performance occurred with external core support, and indicates the importance of support location when targeting core proprioception. During unstable sitting, the muscles of the trunk are considered to be the primarily stabilizers, with pelvis and lower extremity muscles functioning in a secondary role. Although the primary purpose of the garment design was to influence the gluteus medius muscle, a substantial proprioceptive effect occurred. In contrast, a prior investigation on lumbar bracing and unstable sitting did not find the same proprioceptive effect (Reeves et al., 2006). This may indicate that the central nervous system is more

sensitive to external support that interacts with the hip and pelvis than the lumbar region alone.

Changes in single leg landing performance with external support demonstrated the regional effects of the core support and the ability to alter the mechanical influence of the gluteus medius during the landing. A single leg landing is a high-demand task that requires the hip abductor group to maintain lateral balance, and is often used as a clinical measure of dynamic stability (Scott et al., 2005; Willson and Davis, 2008). There were no differences in landing task up to and including the point of initial contact, which demonstrates that participants maintained similar lower-extremity kinematics and kinetics between the two support conditions. Following initial contact, core support resulted in decreased vertical ground reaction force (6.5% reduction) and decreased frontal plane hip moment (6.3% reduction). These decreases occurred along with a redirection of ground forces by an average of 0.9 cm at the knee and 1.9 cm at the hip at the point of peak ground reaction force. Additionally, a reduction in moment arm excursion (14.1% at the knee) and a reduction in moment arm variability (23.1% at the knee; 35.0% at the hip) throughout the trial indicate that core support led to fewer large corrective movements as well as fewer corrective movements in general. Core support targeted at enhancing the function of the gluteus medius takes advantage of the fact that the gluteus medius has a moment arm much longer than other lower extremity muscles that control frontal plane movement, and is more effective than other lower extremity muscles at repositioning the body center of mass in response to perturbations (Hoy et al., 1990; S. P. Lee et al., 2012).

Core support may help diminish the effects of weakened hip abductors and assist patients with alignment-based joint pathologies. Popovich and Kulig (2012) reported that

females with weak hip abductor muscles demonstrated greater peak lumbopelvic displacement and excursion during single leg landing, which can lead to increased muscular demand and loading in the lumbopelvic region. This agrees with our findings that without core support, participants demonstrated 7.5% greater lateral bending excursion and greater lateral bending variability during the single leg landing. Lee et al.,(2012) demonstrated that hip abductor weakness was associated with poor performance during a single leg step down task. Performance for these individuals was improved with the addition of a hip abductor stabilizing brace. Radebold et al.,(2001) demonstrated that patients with low back pain perform worse than healthy controls during unstable sitting and that the differences between groups were greatest when task difficulty was the highest and visual input was removed. Similar to our findings in healthy participants, core stability in low back pain patients may improve with the use of core support.

There are limitations to this investigation that should be noted when interpreting the results. First, the model used to quantify single leg landing kinematics and kinetics did not include multiple degrees of freedom at the ankle and knee. The model was intended to address the primary focus of this investigation: the hip, pelvis, and lumbar region. Second, the effects of core support were noted only for a single laboratory session. Participants did not have multiple days to acclimate to the effect of the external support. This investigation demonstrated an immediate motor adaptation to core support that now warrants further investigation to assess the influence of core support on motor learning over longer experimental durations.

3.6 Conclusion

A novel external core support garment demonstrated significant improvements in core proprioception in addition to changes in both upper and lower extremity mechanics during dynamic stabilizing tasks. Continued used of clinical practices and supportive technology that take advantage of the interdependence of the lumbopelvic region and the vital role of the hip abductors may lead to improved clinical outcomes and decreases in injury rates.

3.6.1 Key Points

FINDINGS: Core support designed to enhance the function of the gluteus medius produced an immediate motor adaptation resulting in significant improvements in dynamic stability and core proprioception.

IMPLICATIONS: Core support can enhance the function of the hip abductors and assist patients with alignment based joint pathologies.

CAUTION: Participants did not have multiple days to acclimate to the effect of the external support and further investigation is needed to determine the influence of core support over longer experimental durations.

Table 3.1: Average kinematics at the point of initial contact ±1 standard deviation. P-values from the paired t-tests used to compare core support (CS) and without core support (WOS). * indicates significance of P<0.05.

	Without Core Support	Core Support	*P*
Hip Flexion Angle (deg)	-28.1±7.4	-29.8±8.2	0.308
Hip Adduction Angle (deg)	-8.3±3.8	-7.9±4.5	0.698
Knee Flexion Angle (deg)	-21.5±6.0	-22.2±7.9	0.633
Ankle Flexion Angle (deg)	4.8±6.8	6.1±5.0	0.330
Pelvis COM Contact Velocity - Vertical (m/s)	0.33±0.11	0.36±0.08	0.242
Pelvis COM Contact Velocity - AP (m/s)	0.60±0.12	0.61±0.10	0.355

Table 3.2: Average peak joint moments ±1 standard deviation at the ankle, knee, and hip without core support and with core support. *P*-values from the paired *t*-tests used to compare core support (CS) and without core support (WOS). * indicates significance of *P*<0.05.

	Without Core Support	Core Support	*P*
Sagittal Hip	148.3±59.6	147.5±57.9	0.827
Frontal Hip	-125.6±35.7	-117.7±25.7	*0.044
Sagittal Knee	181.1±49.2	189.7±59.5	0.309
Sagittal Ankle	142.1±56.1	129.5±51.2	*0.035

Table 3.3: Average ±1 standard deviation position throughout the landing task, the average amount of variability over the task and the average excursion of lumbar angles for flexion, lateral bending, and twisting in degrees. * indicates significance of P<0.05.

Lumbar Flexion	Without Core Support	Core Support	*P*
Mean	27.97±9.21	25.84±6.47	0.250
Mean Variability (Std)	2.64±1.19	3.02±1.33	0.159
Excursion	11.58±4.05	12.83±4.70	0.281
Lumbar Bending	Without Core Support	Core Support	*P*
Mean	4.64±4.39	3.37±4.34	0.099
Mean Variability (Std)	2.42±1.48	2.25±1.46	0.053
Excursion	11.44±5.15	10.63±4.85	*0.031

Figure 3.1: The CoreTec short (Opedix LLC, USA) with arrows indicating the design providing directional compression that replicates the function of the hip abductor muscles with diagonal bands of fabric with low elasticity spiraling downwards from the waist and hips to the thighs. This banding pattern is overlaid onto a standard compression base layer with high elasticity and is designed to facilitate neuromuscular control of pelvic orientation, hip adduction, and hip external rotation.

Figure 3.2: Unstable sitting experimental setup (left). A chair was affixed over an adjustable hemisphere (top right) while an adjustable 12-kg counter weight was attached to the foot plate of the chair (bottom right) to offset the mass of the feet and legs.

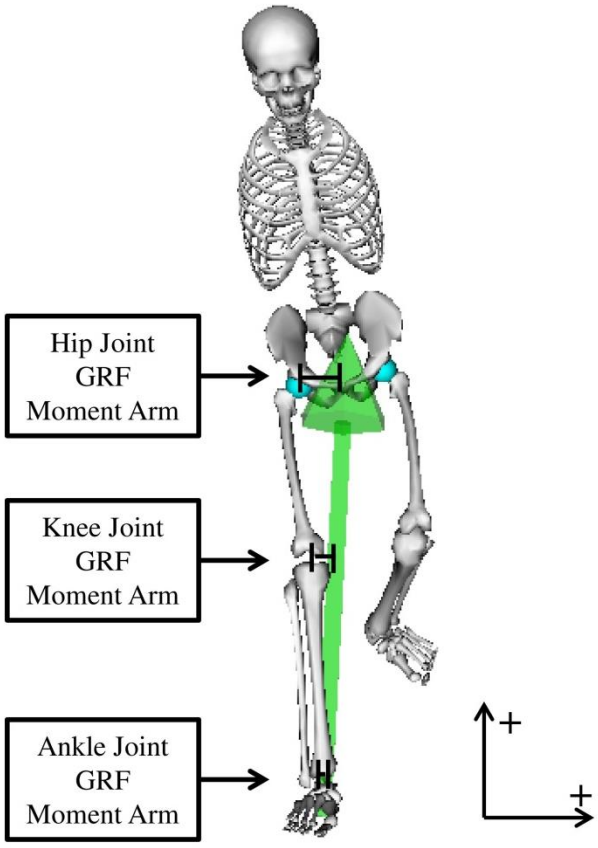

Figure 3.3: Ground reaction force moment arm was assessed at the ankle, knee, and hip by calculating the horizontal distance between the projection of the ground reaction force vector and the joint center location in the frontal plane. A distance of zero indicates that the ground reaction force passed directly through the joint center, a positive value indicates the ground reaction force vector was medial to the joint center, and a negative value indicates the ground reaction force vector was lateral to the joint center.

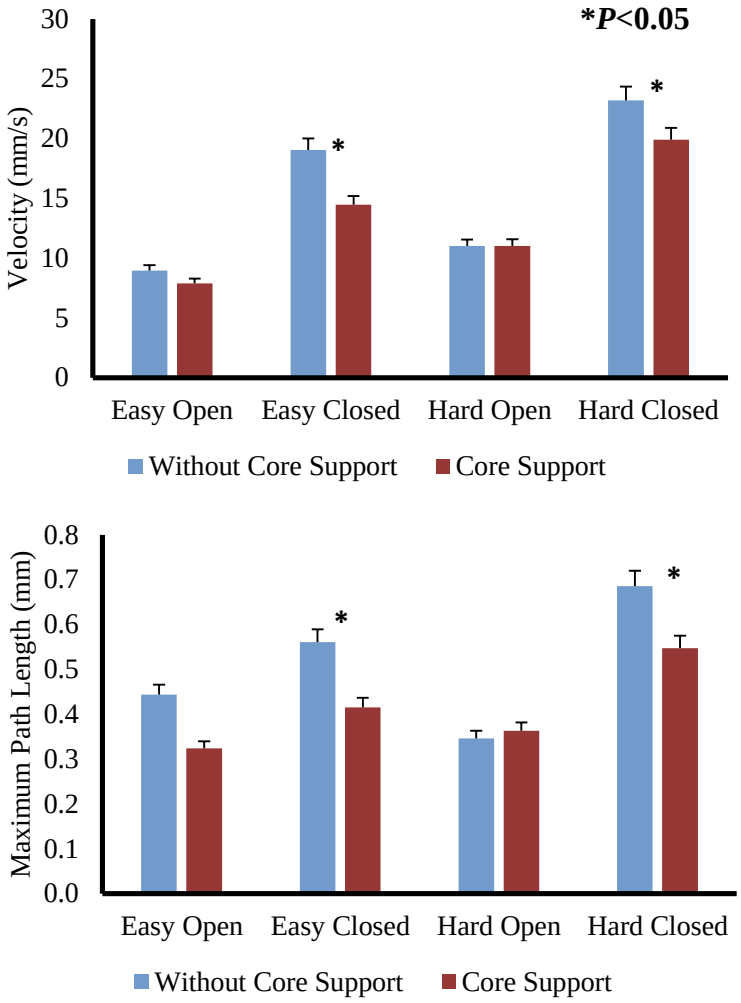

Figure 3.4: Average velocity and average maximum displacement ±1 standard deviation of three-dimensional path length during unstable sitting for each combination of the four task difficulty conditions; easy or hard sphere size and eyes open or eyes closed

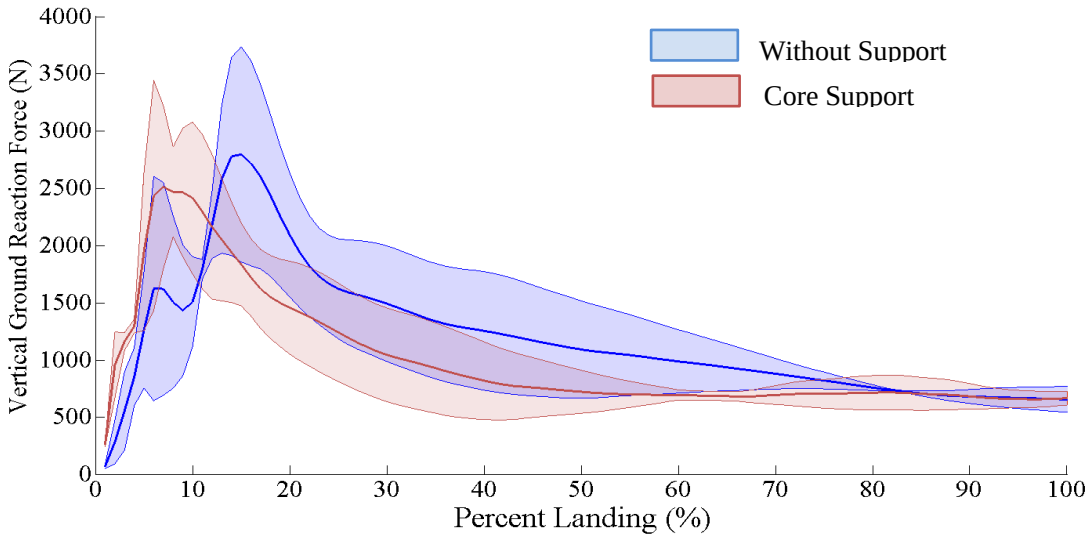

Figure 3.5: Average ± 1 standard deviation of the vertical ground reaction force across three landing trials without core support and with core support for a representative participant. The vertical ground reaction force was reduced by 6.3% on average with core support compared to without core support.

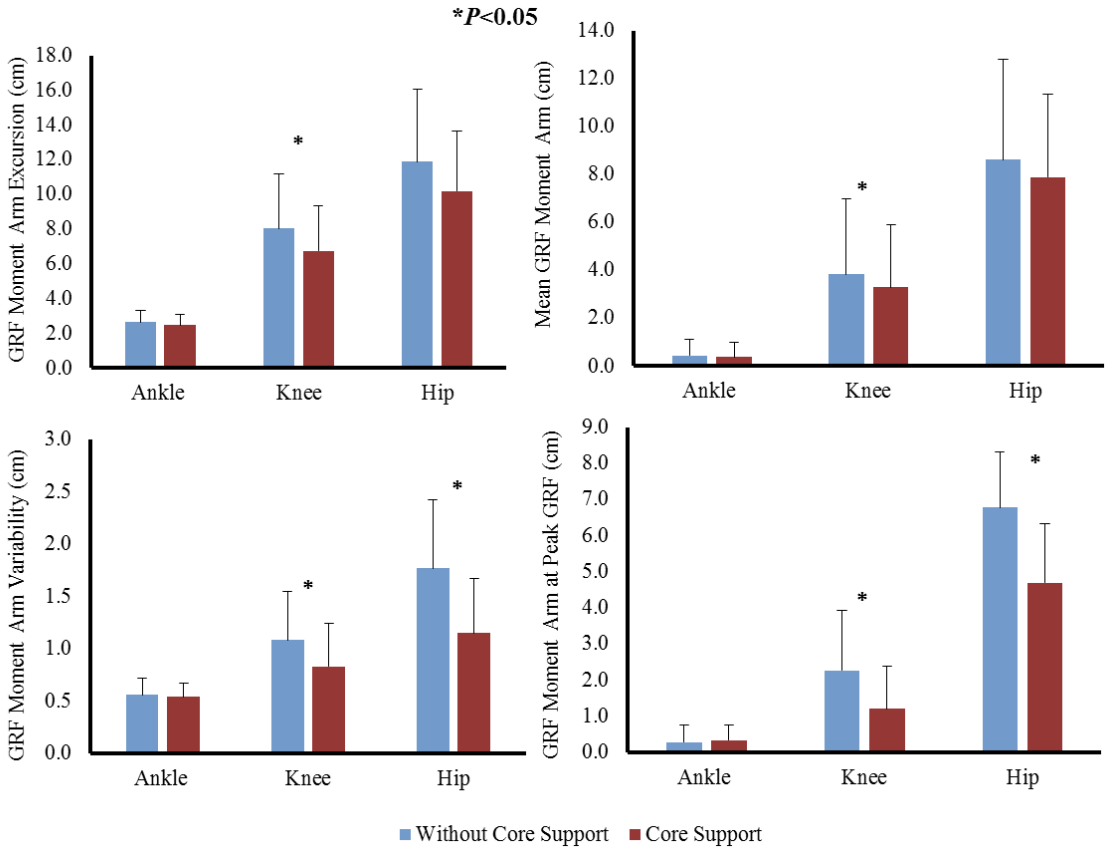

Figure 3.6: Average ± 1 standard deviation excursion (top left), ground reaction force (GRF) moment arm length (top right), variability (bottom left), and value at peak ground reaction force (bottom right) for the ground reaction force moment arm at the ankle, knee, and hip.

CHAPTER 4 – A REVIEW OF PROBABILISITIC METHODS AND THEIR APPLICATIONS IN ORTHOPAEDIC AND MUSCULOSKELETAL MODELING

This chapter will introduce the probabilistic approach and describe the theory and methodology involved in implementing two probabilistic methods that are used in this dissertation and applied to the concept of regional interdependence using musculoskeletal modeling. It further discusses the application of these methods in orthopaedic investigations and software tools for the implementation of the probabilistic approach.

4.1 Introduction to Probabilistic Approach

Variability is present in many aspects of biomechanics and orthopaedics. Additionally, many of the tools and methods that are used are influenced by measurement error and uncertainty. Factors such as patient anthropometry, joint kinematics, soft tissue material properties and joint loading are all inherently variable and subject to error during assessment. The use of probabilistic methods allows investigators to quantify the impact of uncertainty and patient variability as well as determine the most important factors that influence the resulting outputs.

Probabilistic methods use input distributions defined by the investigator to predict an output distribution for a given model (Figure 1). The identification of the input distributions is crucial because there is a direct effect on the predicted output distribution. This approach is in contrast to a more standard study design that would take a

deterministic approach to exactly determine an output for a specific set of given inputs. In probabilistic studies, each of the input parameters is represented as a distribution instead of a single value. The distribution characterizes the range of possible outcomes and the likelihood associated with those outcomes. It is then possible to determine model output sensitivity by identifying the most influential input parameters in determining the range of possible outcomes and explore how different input and output responses interact together. This is in contrast to a traditional sensitivity study that in somewhat limiting by individually varying a single input by a fixed magnitude and measuring the resulting change in the output (Scovil and Ronsky, 2006). Probabilistic modeling was developed for applications in structural reliability (Melchers, 2001; Riha et al., 2006; Thacker et al., 2006) but there have been more recent applications in orthopaedic (Fitzpatrick et al., 2011; Laz et al., 2006) and musculoskeletal modeling (Langenderfer et al., 2008; Reinbolt et al., 2007; Valente et al., 2013).

4.2 Outputs from the Probabilistic Approach

Two commonly used results from a probabilistic approach, which are used throughout this dissertation, are confidence bounds and sensitivity factors.

4.2.1: Confidence Bounds

Confidence bounds represent a two-sided bound that provides the probable range in which the output of the model will occur. Different values can be selected for the probabilities that the bounds represent depending on the size of the distribution that the investigator is intending to quantify, with common approaches using 1-99% (Pal et al.,

2007) or 5-95% (Fitzpatrick et al., 2012a). Currently, standards do not exist on selection of confidence bound sizes. If the 5-95% confidence bounds are identified, this indicates there is a 90% probability that that true model output lies between the lower and upper confidence bounds. Confidence bounds should be distinguished from confidence intervals. Confidence bounds approximate the value of a model output and are calculated from repeated numerical simulations, where confidence intervals typically approximate the mean of an entire population based on a sample data set that includes multiple participants. However, when the output distribution of a probabilistic simulation is Gaussian, the two-sided confidence bounds can be interpreted in a similar manner as a confidence interval (Curran-Everett, 2009). Quantifying the range of possible outcomes for any model output based on the variability in the inputs provides researchers and clinicians with a complete assessment of model performance when using outputs to test hypotheses and inform clinical decisions.

4.2.2 Sensitivity

In addition to the value offered from the calculation of confidence bounds, another strength of the probabilistic approach is the insight into model sensitivity that can be gained. Models are determined to be sensitive to input parameters if the variability or uncertainty associated with an input parameter is propagated through the model and results in a large contribution to the overall output variability (Hamby, 1994). Probabilistic methods can generate relative or absolute sensitivities depending on the method that is used. A common way to quantify relative sensitivity is to calculate Pearson Product-Moment Correlations between the input values selected from the defined

distribution and the resulting output values. A correlation coefficient represents the degree of linear dependence between variables; a value of 1 or -1 represents a direct relationship between an input variable and an output measure, while a value of 0 represents no influence of the input variable on the output measure. Further distinction can be made to categorize the degree of the sensitivity relationship with correlations coefficients using: weakly sensitive (r=0.2-0.4), moderately sensitive (r=0.4-0.6) and highly sensitive (r=0.6-1.0). In addition, the slope of the regression provides information about what the expected change in the output is for a given change in the input.

Importance factors may be evaluated that give the change in probability with respect to the mean and standard deviation (Wu, Y et al., 1990). Importance factors are commonly generated from probabilistic approximation methods, are non-dimensional and allow comparisons to be made between all of the variables considering the characteristics of each variable's input distribution. These sensitivities indicate how much the mean and standard deviation of each random variable contributes to the variability in the output.

4.3 Probabilistic Methods

While there are many methods that can be used to calculate confidence bounds and sensitivity factors in a probabilistic approach, the two that will be a focus throughout this dissertation are Monte Carlo and the approximation method of Advanced Mean Value (AMV).

4.3.1 Monte Carlo

The Monte Carlo method is a commonly applied method in many fields of science and engineering that involves randomly sampling values for each variable of interest according to a predefined distribution and predicting the distribution of the output through repeated trials. The Monte Carlo method requires that the distributions of all included probabilistic variables be known completely. The methodology consists of selecting a single random sample for the assumed probability distribution of each parameter, which then is treated deterministically, to provide one realization (trial) of the output. The Monte Carlo method is referred to as the 'gold standard' because it will always converge to the correct solution. However it is computationally expensive as the accuracy of the solution is dependent on the number of trials.

It should be noted that a variation of Monte Carlo simulation that offers greater efficiency is Latin hypercube sampling. In the random sampling of Monte Carlo simulation, new samples are generated without accounting for previously sampled points and it is not necessary to know beforehand how many sample points are needed. In Latin hypercube sampling, sample points are spread evenly across the possible values. The range of potential inputs is partitioned into intervals of equal probability and a sample is selected from each interval. Latin hypercube sampling can be used to offset the cost of the Monte Carlo method and provide similar results.

Various studies that used the Monte Carlo method in orthopaedic and musculoskeletal modeling applications were instrumental in the design of the methods used in this dissertation. Fitzpatrick et al., (2012) combined finite element and

probabilistic methods in four separate Monte Carlo simulations to assess the impact of variability from sources that included patient, surgical procedure and implant design on total knee replacement performance. This method allows for the source of uncertainty with the greatest influence to be identified as well as the individual parameters within that source to be identified. Reinbolt et al., (2007) implemented a two staged approach that applied optimization and Monte Carlo analysis to evaluate the importance of joint parameters (axis positions and orientations) and inertial parameters (segment masses, mass centers, and moments of inertia) for obtaining accurate inverse dynamics results of gait. The study found that inverse dynamics solutions were impacted more by joint axis positions and orientations that are commonly defined by markers placed on the skin than by segment inertial parameters. Valente et al., (2013) performed a Monte Carlo analysis on OpenSim simulations of gait to simulate weakness in the hip abductor muscles of healthy subjects. This study identified that hip muscle weakness had a greater influence on knee loading that on hip loading which may be a factor is osteoarthritis. However, it was noted as a limitation that it required over 250 hours of computational time to generate the results for this study.

4.3.2: Advanced Mean Value Approximation Method

Approximation methods offer a means to perform probabilistic studies with greater efficiency. Models that are highly complex can prohibit the use of sampling techniques, such as Monte Carlo and Latin hypercube, because of long model run times. The most probable point (MPP) approximation methods are considerably more efficient than the Monte Carlo simulation because fewer iterations are necessary to generate

similar outputs. While these methods are approximations, they have been shown to be accurate in comparison to Monte Carlo.

The MPP represents the combination of input parameter values that predict the model output at a specific probability level. The mean value method is one of the MPP methods that maps the original random variables into independent standard normal variables and constructs a mean-based response function to compute the MPP for the specified probability levels (Figure 2). It is a first-order method that can provide a good approximation of the solution near the mean, but can deviate significantly for probability levels in the outer tails for non-linear problems.

The mean value method requires n+1 trials, where n is the number of random variables. The AMV method (Wu, Y et al., 1990) uses higher-order terms to achieve a better representation of the output and requires n+1+m trials, where m is the number of specified probability levels (Laz and Browne, 2010). Confidence bounds are calculated by specifying the desired probability level for the upper and lower bound. Sensitivity factors are calculated from the unit vector specifying the MPP in the transformed standard normal variate space (Haldar and Mahadevan 2000; Easley et al. 2007)

Langenderfer et al. (2009) used AMV to calculate 1-99% bounds in shoulder kinematics that considered the impact of uncertainty in anatomical landmark location and performed a comparison with Monte Carlo to assess the accuracy of AMV for this model. Excellent agreement was found between results obtained with the AMV and Monte Carlo methods with an average difference of 0.188 deg between the 1-99% bounds in shoulder

angles between the two methods. Convergence of the AMV analysis to the Monte Carlo results in this study was based on 2500 trials. Pal et al. (2007) implemented the AMV method with a finite element based musculoskeletal model of the lower extremity to assess the effects of uncertainty in origin-insertion and kinematic variability on moment arm calculations in major lower extremity muscles. In this study design, the AMV method required 189 iterations to generate 1-99% bound in comparison to the greater than 1000 Monte Carlo trials that would have been necessary.

The AMV method cannot be used in every musculoskeletal modeling application because of tradeoffs between accuracy and efficiency. As the need to assess results from multiple input variables at many different probability levels increases, the computational savings of AMV is reduced and the more robust Monte Carlo method should be used. Additionally, when multiple combinations of input parameters result in the same output, the AMV method will have difficulty converging on a meaningful solution. It is recommended that prior to proceeding with the use of the AMV method with models that is has not been previously validated on, the outputs should be compared to those from a Monte Carlo simulation.

4.4 The OpenSim Probabilistic Plugin

A probabilistic study will generate large volumes of output data that must be reduced to the key results and effectively visualized to be most beneficial to investigators and clinicians. The continued development of accurate probabilistic analysis methods and

the software tools capable of interfacing these methods with modeling platforms can greatly improve the use and interpretation of modeling outputs.

The need for software tools capable of integrating probabilistic methods with modeling tools has been around for over twenty years. The Southwest Research Institute has been addressing the need for efficient probabilistic analysis methods through the use of the NESSUS probabilistic analysis software (SwRI, San Antonio, TX). NESSUS can be used to simulate uncertainties in loads, geometry, material behavior, and other user-defined random variables to predict the probabilistic response, reliability and probabilistic sensitivity measures of a wide range of systems. NESSUS allows the user to perform probabilistic analysis with analytical models, external computer programs such as commercial finite element codes, and general combinations of the two. Many of the studies referenced above used the NESSUS software to interface with a modeling platform and generate their probabilistic outputs. Eleven probabilistic algorithms are available in NESSUS including the Monte Carlo and AMV methods (Thacker et al., 2006).

NESSUS is a commercial software product, where recently there have been large increases in both the amount and complexity of musculoskeletal modeling that is being done in the open source environment of OpenSim. OpenSim does not currently include the capability to perform probabilistic analyses within the software. To achieve the objectives of this dissertation, a probabilistic plugin was modeled after NESSUS and designed to interface with OpenSim to implement the probabilistic methods of Monte Carlo and AMV. The plugin functions with any of the OpenSim tools (*e.g.* Inverse Dynamics, Static Optimization, ect.) and provides a graphical user interface to guide

users through the setup of probabilistic analyses and generate visualizations of results for interpretation. A user manual with tutorial examples was created (Appendix) and the tool was made available to OpenSim users (simtk.org/prob_tool). The following chapters will use the OpenSim probabilistic plugin and describe studies where it was applied.

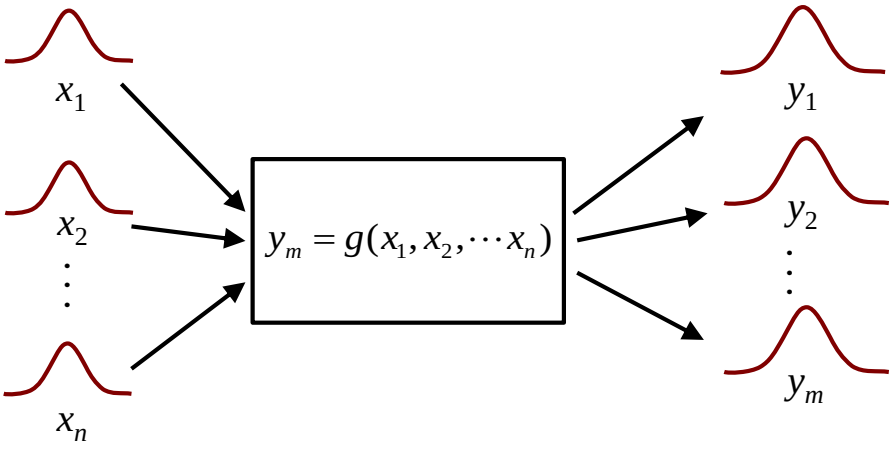

Figure 4.1: Illustration of the probabilistic approach in which inputs are defined as distributions and the resulting output distributions are predicted for a given model.

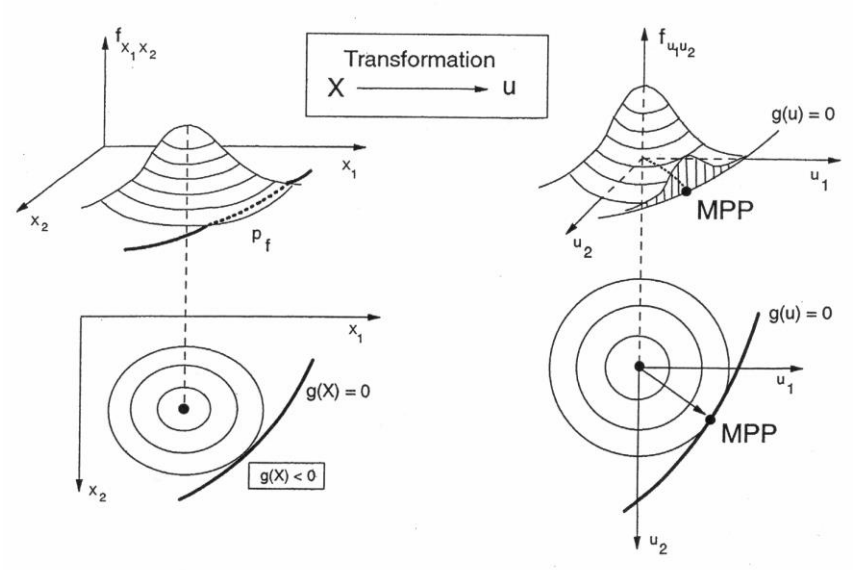

Figure 4.2: The most probable point (MPP) methods find the MPP along the limit state equation. The MPP represents the shortest distance to the origin in the standard normal space and the highest frequency along the limit state equation (*NESSUS Theoretical Manual*, 2001).

CHAPTER 5 – A PROBABILISTIC APPROACH TO QUANTIFY THE IMPACT OF UNCERTAINTY PROPAGATION IN MUSCULOSKELETAL SIMULATIONS

This chapter is the initial application of the application of the probabilistic tool described in the Appendix. This chapter is a study that assessed the propagation of uncertainty in a musculoskeletal simulation of gait.

5.1: Abstract

Uncertainty that arises from measurement error and parameter estimation can significantly affect the interpretation of musculoskeletal simulations; however, these effects are rarely addressed. The objective of this study was to develop an open-source probabilistic musculoskeletal modeling framework to assess how measurement error and parameter uncertainty propagate through a gait simulation. A baseline gait simulation was performed for a male subject using OpenSim for three stages: inverse kinematics, inverse dynamics, and muscle force prediction. A series of Monte Carlo simulations were performed that considered intrarater variability in marker placement, movement artifacts in each phase of gait, variability in body segment parameters, and variability in muscle parameters calculated from cadaveric investigations. Propagation of uncertainty was performed by also using the output distributions from one stage as input distributions to subsequent stages. Confidence bounds (5-95%) and sensitivity of outputs to model input parameters were calculated throughout the gait cycle. The combined impact of

uncertainty resulted in mean bounds that ranged from 2.7 to 6.4 deg in joint kinematics, 2.7 to 8.1 N·m in joint moments, and 35.8 N to 130.8 N in muscle forces. The impact of movement artifact was 1.8 times larger than any other propagated source. Sensitivity to specific body segment parameters and muscle parameters were linked to where in the gait cycle they were calculated. We anticipate that through the increased use of probabilistic tools, researchers will better understand the strengths and limitations of their musculoskeletal simulations and more effectively use simulations to evaluate hypotheses and inform clinical decisions.

5.2: Introduction

Simulation of human movement has significantly impacted approaches to clinical treatment of cerebral palsy, lower extremity amputees, and osteoarthritis(Delp et al., 1998, 1996; Fregly et al., 2007; Shelburne and Pandy, 1998; Silverman and Neptune, 2012; Valente et al., 2013) as well as basic science related to the understanding of movement progression and control during dynamic tasks.(Anderson et al., 2004; Neptune et al., 2009; Thelen and Anderson, 2006; Zajac et al., 2002) Because these simulations often combine human movement data measured in the laboratory with mathematical models of the musculoskeletal system, accurate estimations of biomechanical outputs such as intersegmental joint loads, muscle activation/coordination, and muscle force are possible.(Fregly et al., 2012) The experimental methods used to create anatomic detail in musculoskeletal models have improved over the past decade through direct measurement of sarcomere length(Klein Horsman et al., 2007) and increased cadaveric sample sizes,(Ward et al., 2009) which has led to enhanced accuracy of simulations specific to

individual patients. As the field of musculoskeletal simulation progresses, the use of simulation to create individual and population-based treatments will increase.

Outputs from musculoskeletal simulations are affected by measurement error and model parameter uncertainties that are important to consider when interpreting results. A common approach to musculoskeletal simulations contains three sequential stages (inverse kinematics, inverse dynamics, and muscle force prediction); therefore, the uncertainty introduced at earlier stages can propagate through the process and produce a range of possible results within subsequent stages. In the first stage, inverse kinematics are commonly calculated from marker-based motion capture, where placement and motion of markers relative to anatomic landmarks can introduce measurement error.(Chiari et al., 2005; Della Croce et al., 1999; Gao and Zheng, 2008) In the second stage, inverse dynamics are influenced by inverse kinematics from the first stage and by estimates of body segment parameters (mass, center of mass, moment of inertia), which are commonly calculated from regression equations based on cadaveric investigations.(Chandler et al., 1975; Dempster, 1955) In the third stage, muscle force prediction utilizes the data from inverse kinematics, inverse dynamics, and a Hill-type muscle model that includes anatomic and physiologic parameters (maximum isometric force, optimal fiber length, tendon slack length, pennation angle) that are estimated from cadaveric investigations.(Arnold et al., 2010; Ward et al., 2009) Because each of these simulation inputs introduce uncertainty, it is important that interpretation and clinical decision-making consider that the output taken from a single set of input parameters lies within a range of possible solutions.

Probabilistic analyses provide comprehensive methods to simultaneously quantify the impact of uncertainties that arise from multiple sources. These techniques were developed in structural reliability engineering(Melchers, 2001), and have been applied in other biomechanical applications.(Laz and Browne, 2010) The primary metrics for used to quantify the impact of uncertainty from these analyses are *confidence bounds* and *sensitivity factors*. Confidence bounds provide the output levels associated with specific probability (*e.g.* 5% and 95%) and sensitivity factors(Hamby, 1994) provide insight on how changing an input parameter affects the simulation output. The probabilistic method familiar to most researchers is Monte Carlo simulation, which is a repeated sampling method that models inputs according to predetermined probability distributions and presents the outputs as distributions.(Halder and Mahadevan, 2000) Recent musculoskeletal studies have used repeated sampling methods to quantify output variability and sensitivity of inverse dynamics and muscle force prediction to variability in model parameters.(Ackland et al., 2012; Goehler and Murray, 2010; Langenderfer et al., 2008; Nguyen and Reynolds, 2014; Scovil and Ronsky, 2006; Valente et al., 2013) Although these studies provide insight into factors that affect a particular model at a single stage in the simulation, the current study introduces new methodology to musculoskeletal simulation practices that characterizes the impact and interaction of multiple sources of uncertainty, and quantifies the propagation of uncertainty through each stage of the musculoskeletal simulation process.

When developing musculoskeletal simulations for research or clinical decision making, understanding and reporting the output confidence and sensitivity to a range of

known possible inputs should be standard practice. However, an accessible toolset and standard methods to report these results currently do not exist in the musculoskeletal community. The objective of this investigation was to develop an open-source probabilistic musculoskeletal modeling framework to assess how measurement error and parameter uncertainty propagates through the outputs of each simulation stage: (1) joint angles from inverse kinematics, (2) joint moments from inverse dynamics, and (3) muscle forces from static optimization. The probabilistic framework was developed for OpenSim(Delp et al., 2007), a platform with widespread use among biomechanics researchers and clinicians and the ability to interact with the simulation through an open source application programming interface (API). The probabilistic tool developed is available for download at simtk.org/home/prob_tool. We anticipate that regular use of systematic uncertainty analysis within the musculoskeletal simulation community will allow researchers to interpret simulation outputs with confidence, refine new model development, and more effectively translate the results from musculoskeletal simulations to clinical decision-making and human performance assessments.

5.3: Methods

5.3.1: Experimental Setup and Baseline Simulation

Following approval from the institutional review board, a single male participant (mass: 68.2, height: 154.5 cm) walked at a self-selected pace while an 8-camera motion capture system (Vicon, Centennial, CO) tracked 40 markers at 100 Hz on the torso, pelvis, thigh, shank, and foot. Marker clusters were fixed to each segment and used to define baseline (unperturbed) segment reference frames throughout the gait cycle, but

were not included in the OpenSim model for tracking and calculation of joint kinematics. Two force platforms (Bertec Corp, Columbus, Ohio) captured ground reaction forces sampled at 1000 Hz for a complete gait cycle that began and ended with a right foot heel strike. Body segment parameters (BSPs) and muscle properties were scaled to the subject for the baseline simulation using scale factors calculated from marker positions. OpenSim was used to generate baseline joint kinematics, moments, and muscle forces using the gait2392 model.(Delp et al., 1990) A custom interface using the OpenSim/Matlab API was developed to perturb the baseline simulation by altering input files within a Monte Carlo simulation. All input perturbations were sampled from Gaussian distributions created from means and variance reported in the relevant experimental literature (Tables 5.1 and 5.2).(Benoit et al., 2006; Della Croce et al., 1999; Friederich and Brand, 1990; Rao et al., 2006; Ward et al., 2009) Propagation of uncertainty was performed by using output files of results from the previous OpenSim stage as input in the subsequent stage during each trial of the Monte Carlo simulation (Figure 5.1).

5.3.2: Stage 1 – Probabilistic Inverse Kinematics

Marker placement and movement artifact, two sources of measurement error that influence the results of inverse kinematics, were modeled and combined for each of the 40 markers used in the simulation. This was accomplished by generating a perturbed trajectory for each marker as input into the Inverse Kinematics Tool within each trial of the Monte Carlo simulation.

Marker placement error results from the inability of an investigator to locate an anatomic landmark through palpation. Therefore, the error is a placement that is

constantly offset from the anatomic location it is intended to mark. This was modeled by sampling the magnitude of this offset in each plane from a distribution created by previously reported intrarater variances (Table 5.1).(Della Croce et al., 1999) For marker placements in which intrarater variance was unavailable, the mean variance for markers on the corresponding segment was used to define the input distribution. The Monte Carlo simulation generated a random perturbation for each marker coordinate from the distributions and applied it as a constant perturbation to every sample during the gait cycle. Each perturbation was performed in baseline segment coordinate systems that were consistent with those defined in Della Croce *el al*.[8] The perturbed trajectory was transformed into the lab coordinate system to produce a trajectory that was constantly offset from the original within the segment (Figure 5.2).

Marker movement artifact occurs when skin and soft tissues move relative to the underlying bone during limb movement. The magnitude of the marker movement varies with time based on the character of the motion, location of the marker placement, and the anatomy of the subject. Movement artifact was modeled by perturbing each marker uniquely within each of the eight traditional phases of the gait cycle (*e.g.* between 'heel off' and 'opposite initial contact').(Perry, 1992) The Monte Carlo simulation sampled a perturbation from a distribution constrained with a maximum resultant artifact of 15 mm.(Benoit et al., 2006; Gao and Zheng, 2008) Smoothness at the phase transition was enforced by applying a 4th-order low pass Butterworth filter with a 20 Hz cutoff frequency to the trajectory. The movement artifact uncertainty was combined with the marker placement uncertainty for each of the 40 markers and a new marker trajectory file was generated for use by the Inverse Kinematics Tool. Joint angles from the right side

were analyzed for the following degrees of freedom: ankle plantarflexion/dorsiflexion, knee flexion/extension (flex/ext), hip flex/ext, hip adduction/abduction (add/abd), and hip internal/external (int/ext) rotation.

5.3.3: Stage 2 – Probabilistic Inverse Dynamics

Uncertainties in BSPs were modeled by perturbing the baseline model inputs for segment mass, moment of inertia, and center of mass location. The input distributions were defined using baseline model parameters as the means and variances were defined by coefficients of variation measured by Rao *et al.*(Rao et al., 2006) and Pavol *et al.*(Pavol et al., 2002) (Table 5.2). Each trial of the Monte Carlo simulation combined a perturbed model file with randomly generated body segment parameters with the kinematic output created from the inverse kinematics tool and measured ground reaction forces to generate joint moments at each degree of freedom.

5.3.4:Stage 3 – Probabilistic Muscle Force Prediction

Uncertainties in muscle parameters were modeled by perturbing the baseline model inputs for maximum isometric force, tendon slack length, and pennation angle. The input distributions were defined using the baseline model parameters as the means and variances were defined by coefficients of variation measured by Friederich and Brand(Friederich and Brand, 1990) and Ward *et al.*(Ward et al., 2009) (Table 5.2). Muscle forces were predicted using static optimization with the objective function that minimized the sum of muscle activation squared.(Anderson and Pandy, 2001) Eight lower-extremity muscles on the right side were assessed: gluteus maximus, gluteus

medius, rectus femoris, vastus medialis, vastus lateralis, semitendinosus, biceps femoris long head, and medial gastrocnemius. Because the gluteus medius and gluteus maximus muscles were each modeled using three fascicles with different paths, each fascicle received unique input parameters for each trial in the Monte Carlo simulation. The force generated by each muscle fascicle was summed to obtain a single muscle force output for gluteus medius and gluteus maximus, respectively.

5.3.5: Data Analysis

To assess the individual contributions and the combined effects of the sources of input uncertainty on simulation outputs, a series of Monte Carlo simulations of 3000 trials were performed separately considering all combined sources of uncertainty and for each individual source of uncertainty.(Fitzpatrick et al., 2012) The 5 and 95 confidence bounds were calculated for joint kinematics for each degree of freedom, joint moments for each degree of freedom, and muscle forces. These bounds indicate a 90% probability that the true result of the simulation output lies between the lower and upper confidence bounds. For joint kinematic and joint moment outputs, mean and standard deviation for the 5-95 confidence bounds were calculated for the entire gait cycle, and separately for the stance and swing periods. For muscle force outputs, the mean and standard deviation for the 5-95 confidence bounds were calculated over the time period(s) when the muscles were active. The outputs for each simulation stage were reported in actual units (not normalized) to maintain the interpretability. Mean and standard deviation of peak muscle force timing was calculated for each muscle. Using similar methods as Valente *et al*.,(Valente et al., 2013) Monte Carlo simulations of 3000 trials were sufficient for

convergence with differences in the mean confidence bounds of less than 0.1 deg for joint angles, 0.1 N•m for joint moments, and 0.5 N for muscle force.

Sensitivity of joint moment and muscle force outputs to individual BSPs and muscle parameters were quantified by Pearson Product-Moment Correlation between the input parameter and the maximum value of each output. To objectively assess if a correlation was meaningful, a 95% confidence interval (CI) was calculated for the correlation coefficient. Correlations were considered statistically significant when the CI did not include zero with an alpha level of 0.05.(Curran-Everett, 2009) Strengths of the correlations that were statistically significant were categorized as weakly sensitive (r=0.2-0.4), moderately sensitive (r=0.4-0.6), or highly sensitive (r=0.6-1.0). The slope of each relationship was calculated and multiplied by the standard deviation of the input parameter from Table 5.2. This additional scaling places the slope in the context of the potential variance of the input parameter. To assess if calculating sensitivity at the maximum value of the output is a consistent representation of sensitivity throughout the gait cycle, a Pearson Product-Moment Correlation was calculated for the input parameter and the generated range of outputs at each individual time point.

5.4: Results

5.4.1: 5-95 Confidence Bounds

The impact of marker placement error and movement artifact on joint kinematics can be observed by the size of the 5-95 confidence bounds for each joint angle output (Figure 5.3, Stage 1). The knee flex/ext joint angle exhibited the smallest bounds (2.7±0.3 deg), but the largest motion during the gait cycle. The relative bound sizes for hip angle

in add/abd (3.0±0.3 deg) and int/ext (5.1±1.0 deg) were large considering the smaller motions in these degrees of freedom.

When considering the combined effects of marker error (marker placement and movement artifact) and body segment parameter uncertainty, bounds for hip flex/ext (8.0±2.8 N·m) and add/abd (7.4±2.8 N·m) moments were substantially larger than any other degree of freedom (ankle: 2.7±1.8 N·m; knee: 4.4±1.4 N·m; hip int/ext: 1.8±1.0 N·m)(Figure 5.3, Stage 2). Joint moment bound sizes during the swing period were 81.7% smaller in the ankle and 16.5% smaller in the knee compared to the stance period; however, bound sizes in hip degrees of freedom were 42.9% larger on average in the swing period compared to the stance period.

The combined effect of all sources of uncertainty had the greatest impact on medial gastrocnemius (142.3±110.8 N) and the gluteus medius (130.8±89.2 N), which demonstrated the largest bounds for muscle force output (Figure 5.3, Stage 3). Gastrocnemius and gluteus medius also generated the largest peak forces during the gait cycle (gastrocnemius: 663.1 ± 105.5 N; gluteus medius: 1025.4 ± 62.9 N). The average muscle force bound size for all eight muscles was 83.1±39.6 N. Variability was present in peak muscle force timing for each of the eight muscles that was on average 104±112 msec and as high as 402 msec for the gluteus medius.

By comparing 5-95% bounds with all uncertainty sources considered versus the individual sources, relative contributions of each source can be evaluated (Figure 5.4). For Stage 1, the impact of movement artifact was 1.8 times larger than marker placement on joint kinematics for all degrees of freedom, with the greatest difference occurring at the ankle (5.9±0.8 vs. 2.2±0.1 deg). When this uncertainty was propagated to joint

moment calculation in Stage 2, the relative impact of movement artifact compared to marker placement increased to 2.3-4.0 times, with higher impact in swing period than in the stance period for hip add/abd and hip int/ext. BSPs had a relatively small impact on joint moments compared to the impact of marker error. The exception was hip flex/ext during the swing period where BSP uncertainty has the largest impact and was 2.1 times greater during the stance period compared to the swing period (Figure 5.4).

In Stage 3, the impact of muscle parameter uncertainty on muscle force output was 1.7 times greater for all muscles than movement artifact, which had the second largest impact. The impact of movement artifact was greater than marker placement and resulted in a muscle force bound size of 37.2±20.4 N on average for all muscles. BSP uncertainty had a relatively small impact on muscle force output in all muscles except the hamstrings, where BSP uncertainty had the second largest impact after muscle parameter uncertainty (Figure 5.4).

5.4.2: Input Parameter Sensitivity

Statistically significant correlations existed between each BSP and hip moments. Hip flex/ext was highly sensitive to segment mass, with the strongest correlation at the shank (thigh: r=0.42, CI [0.40, 0.45]; shank: r=0.64, CI [0.62, 0.67]; foot: r=0.11, CI [0.08, 0.22]). Hip add/abd moment was highly sensitive to segment mass, with the strongest correlation at the thigh (thigh: r=0.75, CI [0.72, 0.77]; shank: r=0.33, CI [0.30, 0.38]; foot: r=0.14, CI [0.11, 0.23]). Flex/ext moment was moderately sensitive to thigh moment of inertia (r=0.51, CI [0.45, 0.56]); however, add/abd moment was not sensitive to thigh moment of inertia. Hip add/abd was moderately sensitive to the medial/lateral

position of the center of mass of the thigh and weakly sensitive to the center of mass of the shank (thigh: *r*=0.47, CI [0.41, 0.56]; shank: *r*=0.26, CI [0.22, 0.34]; foot: *r*=-0.06, CI [-0.09, 0.11]) (Table 5.3). The joint moment-segment mass relationship produced the largest impact on joint moment outputs for a one standard deviation change in segment mass compared to the other BSPs. For example, the hip flex/ext moment would change 1.06 N·m in response to a one standard deviation change in shank mass (Table 5.4).

In general, muscle force outputs were highly sensitive to changes in maximum isometric force and tendon slack length; however, this was not consistent across muscles (Table 5.3).The gluteus muscles were highly sensitive to uncertainty in maximum isometric force (*e.g.* gluteus medius3: *r*=0.72, CI [0.70, 0.74]) and weak to moderately sensitive to uncertainty in tendon slack length (*e.g.* gluteus medius3: r=0.24, CI [0.20, 0.27]). The gluteus muscle force would change 34.82 N in response to a one standard deviation change in maximum isometric force compared to 16.53 N in response to a one standard deviation change in tendon slack length. By contrast, the vasti muscles were highly sensitive to tendon slack length (*e.g.* vastus lateralis: r = -0.83, CI [-0.84 -0.82]), and would change 13.70 N in response to a one standard deviation change in tendon slack length compared to 3.17 N for maximum isometric force.

For both body segment and muscle parameters, the strength and sign (+/-) of correlations were dependent on where in the gait cycle the sensitivity analysis was performed. During the initial portion of the gait cycle, hip flexion moment was most sensitive to uncertainty in thigh mass with little sensitivity to uncertainty in shank or foot mass. However, after transitioning to the swing period, hip flexion moment was most sensitive to uncertainty in foot mass and least sensitive to uncertainty in thigh mass

(Figure 5.5). Although muscle force was consistently sensitive to tendon slack length throughout the gait cycle, the direction of the relationship (+/-) changed throughout the gait cycle, particularly for the medial gastrocnemius and rectus femoris (Figure 5.5).

5.5: Discussion

This study demonstrated a systematic probabilistic approach to assess the impact of measurement error and parameter uncertainty on outputs from musculoskeletal simulations. Uncertainties in simulation inputs propagate through the simulation workflow and result in significant impacts on joint kinematics, joint moments, and muscle force prediction. Mean 5-95 confidence bounds ranged from 2.7 to 6.4 deg in joint kinematics, 2.7 to 8.1 N·m in joint moments, and 35.8 N to 130.8 N in muscle forces. Muscle parameter uncertainty had the largest impact on muscle force prediction, greater than the uncertainty carried forward from marker placement and movement artifact. When measurement error was propagated through inverse dynamics and muscle force prediction, movement artifact had the largest impact on joint moment outputs and a considerable impact on muscle force prediction. Impact of movement artifact depended on whether the swing or stance period was considered. Similarly, sensitivity to specific BSPs and muscle parameters were varied, and linked to where in the gait cycle they were calculated. Uncertainty sources also led to a range of outputs for peak muscle force timing that reached as high as 402 msec for gluteus medius. The impact of uncertainty in BSPs and muscle parameters may be mitigated by measuring and applying *in-vivo* joint moment/joint angle data to subject-specific scaling. Probabilistic analyses can improve

understanding and interpretation of simulation data and can be applied to musculoskeletal simulations without large computational expense.

Movement artifact impacted the range of outputs more than marker placement after each stage of the simulation. The effect of movement artifact varied throughout the gait cycle and contributed to the variable size of the 5-95 confidence bounds in both joint moments and muscle forces. Movement artifact is a more dynamic form of uncertainty than marker placement error, and can have a large influence on calculated segment accelerations. In this investigation, marker positions were used only for segment tracking; however, marker position error may result in a significant impact on joint kinematics when marker positions are used to identify joint center locations. For example, locating the hip joint center based on marker position can result in errors as high as 22% and 15% in hip flexion/extension moments and adduction/abduction moments, respectively.(Stagni et al., 2000) When evaluating which sources of uncertainty investigators can influence, uncertainty due to marker placement error has been reduced through the development of digital placement methods and marker sets designed to consider variations in subject populations.(Lerner et al., 2014) Reduction of movement artifact is difficult and not feasible in most motion capture based experiments because the markers will always be affixed over the skin, which highlights the need to understand its impact.

The sensitivity of joint moments and muscle forces to uncertainty in individual input parameters varied throughout the gait cycle. Overall, BSP uncertainty had a greater impact on joint moments during the swing period compared to stance (Figure 5.5). During the stance period, the foot mass made small contributions to the range of hip flexion moment values when compared to contributions from the thigh mass. However,

after the transition to the swing period, the foot mass is the dominant contributor to hip flexion moment output range. This shift corresponds to the role that ground reaction forces play in joint moment calculations during each period.(Vaughan et al., 1992) Without the ground reaction forces in the swing period, the importance of the BSPs on joint moment predictions are higher compared to the stance period. Although the sensitivity of muscle forces to tendon slack length was statistically significant for all muscles, and a one standard deviation change in tendon slack length produced a muscle force change up to 42 N, the strength of sensitivity and direction of influence (sign of correlation coefficient) depended on the muscle length at the point of peak muscle force generation. Changes in tendon slack have a direct influence on the region of the force-length curve a muscle operates. Therefore, the sensitivity of muscle force output to this parameter changes sign based on whether the muscle is on the "ascending" or "descending" portion of the force-length curve(Ackland et al., 2012) (Figure 5.5). Representing sensitivity by calculating the relationship at a single time point in the gait cycle or over a period (swing and stance) does not fully characterize the relationship over the entire motion. For the most relevant representation of sensitivity, we recommend that each investigator assess the strength of sensitivity at the time point of clinical or scientific interest.

The highly sensitive nature of outputs to BSPs and muscle parameters highlights the importance of applying accurate subject-specific parameters. Parameter specification is commonly performed by scaling each BSP and muscle parameters based on segment dimensions. However, few parameters reliably scale based on segment dimensions alone.(Ward et al., 2005) Incorporating easily measured subject-specific parameters such

as joint moment/angle data into subject-specific models may limit the impact of uncertainties in BSPs and muscle parameters, which are difficult to determine. The joint moment/angle relationship(Herzog et al., 1991) and the sarcomere length/joint angle relationship(Lieber et al., 1997) are not uniform for all subjects. Functional scaling that relies on *in-vivo* data has been used to generate subject-specific models that accurately represent joint moment/angle relationships.(Garner and Pandy, 2003; Lloyd and Besier, 2003) Another option that results in high model accuracy is to introduce length constraints that preserve the normalized muscle fiber length/angle relationship for each muscle when scaling optimum fiber length and tendon slack length.(Winby et al., 2008)

This study uniquely considered the interaction of measurement error and parameter estimation, and systematically followed their impact through the processing stages commonly used in musculoskeletal simulation. Previous investigations have considered the impact of input uncertainty on results at individual simulation stages,(Ackland et al., 2012; Andrews and Misht, 1996; De Groote et al., 2010; Langenderfer et al., 2008; Nguyen and Reynolds, 2014; Reinbolt et al., 2007; Wesseling et al., 2014) but comparisons between studies can be difficult. De Groote *et al.*(De Groote et al., 2010) and Ackland *et al.*(Ackland et al., 2012) demonstrated a high level of sensitivity of peak force in lower-extremity muscles to tendon slack length when using Hill-type muscle models. Confidence bounds for muscles forces have not been previously reported based on uncertainty; however, the shape and magnitude of our muscle force predictions are similar to several studies that modeled healthy gait with subject-specific models. For example, maximum force for the gluteus medias has been reported to range from 900-1100 N during gait for subjects of similar size to the one modeled here, and

these values are within the 5-95% confidence bounds calculated for gluteus medius(Anderson and Pandy, 2001; van der Krogt et al., 2012). The confidence bounds calculated for joint moments as a result of uncertainty in BSPs were 25% smaller than bounds reported by Langenderfer *et al.*(Langenderfer et al., 2008) The differences are attributed to the use of a different bound size (1-99% versus 5-95%) and differences in the model used to generate joint kinematics and kinetics. Reinbolt *et al.*(Reinbolt et al., 2007) demonstrated that uncertainty in BSPs had only a mild effect on peak lower-extremity joint moments. Our data demonstrated that, for most joint moments, the impact of uncertainty depends on the portion of the gait cycle that is analyzed.

Several modeling decisions were made in the design of this study that should be evaluated when performing similar studies using probabilistic musculoskeletal simulations. First, outputs at each simulation stage will be affected by the model used and the number and location of the markers included in the model. We chose to use the OpenSim gait2392 model because it is widely used in gait analysis, and provides a consistent and accessible platform for investigators to make future comparisons. Second, several methods exist to calculate inverse kinematics, inverse dynamics, and predict muscle forces. Although the trends in output bounds and sensitivity will likely be similar, variations in these components will change the predicted results and should be evaluated on a problem-specific basis. Third, specific to the probabilistic musculoskeletal simulation, the input distributions will influence the simulation results. We recommend that researchers base their input distributions on experimental data whenever possible. Last, there are many more sources of uncertainty that can influence a simulation than included here such as model scaling, the muscle model chosen, and the number and

architecture of the muscles included. The purpose of this study was to evaluate recognized sources of uncertainty that affect the three major stages of the simulation process. The open source tools developed in this study will enable the widespread use of probabilistic methods and an improved understanding of the impact of uncertainty in musculoskeletal simulation.

In conclusion, this study demonstrated a systematic probabilistic approach to quantify and assess the impact of uncertainty propagation on musculoskeletal simulation of gait. These tools will enable researchers to perform these analyses on a variety of models at minimal computational cost. We anticipate that assessment of uncertainty will become standard practice within the musculoskeletal simulation community, allow researchers and clinicians to better understand the strengths and limitations of their musculoskeletal simulations, and improve use of computational simulations to evaluate hypotheses and inform clinical decisions.

Table 5.1: Maximum amount of variability (+/- 2 standard deviations) in marker placement expressed in coordinates of a segment coordinate system based on Della Croce *et al.*[9]

Anatomical Landmark	Maximum amount of variability (+/- 2 standard deviations)			
Hip	X (mm)	Y (mm)	Z (mm)	3D (mm)
Left Anterior Supior Iliac Spine	3.4	4	11	12.2
Right Anterior Supior Iliac Spine	10	11.5	14.5	21
Left Posterior Superior Iliac Spine	2.8	8.3	7.5	11.5
Right Posterior Superior Iliac Spine	5.7	10.7	4.6	13
Femur	X (mm)	Y (mm)	Z (mm)	3D (mm)
Greater Trocanter	12.2	11.1	7	17.9
Medial Epicondyle	5.1	5	6.7	9.8
Lateral Epicondyle	3.9	4.9	7.8	10
Lateral Patella	3.8	3.9	7.8	9.5
Medial Patella	5.2	2.4	10.8	12.2
Most Distal Point of Lateral Condyle	4.7	3.4	2.9	6.5
Most Distal Point of Medial Condyle	4.4	1.4	4.4	6.4
Tibia	X (mm)	Y (mm)	Z (mm)	3D (mm)
Tibial Tuberosity	1.2	1.8	4.3	4.8
fibula head	3.3	3.3	3.3	5.7
Medial Ridge of Medial Plateau	3.4	4.4	6.6	8.6
Lateral Ridge of the Lateral Plateau	8	2.1	5.6	10
Medial Malleolus	2.2	2.6	6.6	7.4
Lateral Malleolus	2.6	2.4	5.7	6.7
Foot	X (mm)	Y (mm)	Z (mm)	3D (mm)
Calcaneus	7	4.9	5.7	10.3
First metatarsal head	2.6	3.2	6.9	8
Second Metatarsal Head	2.2	6.3	6	9
Fifth Metatarsal Head	0.7	2	6.5	6.8

Table 5.2: Baseline value and (SD) of body segment and muscle parameters for each segment and muscle considered in the probabilistic analyses.

Body Segment Parameters:	Segment Baseline (SD)		
Parameter	Foot	Shank	Thigh
COM - Med/Lat (cm)	0 (0.93)	0 (0.37)	0 (0.29)
COM - Ant/Post (cm)	0 (0.93)	0 (0.37)	0 (0.29)
COM - Sup/Inf (cm)	0 (1.86)	-21.11 (0.75)	-17.91 (0.59)
I - Add/Abd ($kg \cdot m^2$)	0.004 (0.0009)	0.050 (0.005)	0.119 (0.026)
I - Int/Ext ($kg \cdot m^2$)	0.001 (0.0003)	0.004 (0.0004)	0.023 (0.005)
I - Flex/ext ($kg \cdot m^2$)	0.004 (0.0008)	0.049 (0.005)	0.124 (0.027)
Mass (kg)	1.43 (0.100)	3.39 (0.22)	8.50 (1.17)
Muscle Parameters:	Parameter Baseline (SD)		
Muscle	Maximum Isometric Force (N)	Tendon Slack Length (m)	Pennation angle (rad)
Rectus Femoris	1169 (76.7)	0.32426 (0.01479)	0.087 (0.061)
Vastus Medialis	1294 (109.9)	0.13229 (0.00485)	0.087 (0.120)
Vastus Lateralis	1871 (177.6)	0.16503 (0.00586)	0.087 (0.119)
Semitendinosus	410 (57.2)	0.27522 (0.02461)	0.087 (0.086)
Biceps Femoris	896 (65.4)	0.34844 (0.02376)	0 (0.096)
Gastrocnemius	1558 (135.8)	0.43873 (0.031858)	0.297 (0.077)
Gluteus Maximus 1	688 (53.0)	0.12730 (0.00981)	0.087 (0.104)
Gluteus Maximus 2	983 (64.9)	0.13027 (0.00860)	0 (0.104)
Gluteus Maximus 3	662 (45.9)	0.14877 (0.01031)	0.087 (0.104)
Gluteus Medius 1	983 (49.4)	0.07898 (0.00397)	0.140 (0.118)
Gluteus Medius 2	688 (56.6)	0.05368 (0.00442)	0 (0.118)
Gluteus Medius 3	784 (52.0)	0.05382 (0.00357)	0.332 (0.118)

Table 5.3: Sensitivity (correlation coefficient) calculated between muscle and body segment parameter inputs and the resulting maximum value of each output. Sensitivity is highlighted based on correlation coefficient strength. Weakly Sensitive: *r*=0.2-0.4 (green); Moderately Sensitive: *r*=0.4-0.6 (blue); Highly Sensitive: *r*=0.6-1.0 (red).

Body Segment Parameters:	Segment				
Center of Mass	Ankle	Knee	Hip Flex/Ext	HipAdd/Abd	Hip Int/Ext
Foot Med/Lat	0.06	-0.07	0.06	-0.06	0.13
Foot Ant/Post	0.67	0.43	0.03	-0.04	0.11
Foot Sup/Inf	-0.10	-0.13	0.19	0.02	-0.01
Shank Med/Lat	-0.02	-0.02	-0.03	0.26	-0.33
Shank Ant/Post	0.00	0.46	0.05	-0.02	0.21
Shank Sup/Inf	0.04	0.13	0.07	-0.06	0.05
Thigh Med/Lat	0.00	0.00	0.01	0.47	-0.58
Thigh Ant/Post	0.00	-0.01	0.18	0.00	0.60
Thigh Sup/Inf	0.03	0.02	-0.28	-0.14	0.00
Moment of Inertia	Ankle	Knee	Hip Flex/Ext	HipAdd/Abd	Hip Int/Ext
Foot AA	0.00	-0.02	0.00	0.02	-0.01
Foot IE	-0.06	-0.01	-0.03	0.00	-0.05
Foot FE	0.44	0.07	-0.05	0.02	0.03
Shank AA	0.03	-0.03	0.03	0.01	-0.05
Shank IE	-0.01	0.00	0.01	-0.01	-0.02
Shank FE	0.01	0.29	-0.08	0.02	0.02
Thigh AA	0.01	-0.01	0.01	-0.09	-0.15
Thigh IE	0.00	-0.02	-0.02	-0.01	-0.06
Thigh FE	0.04	0.01	0.51	0.02	0.19
Mass	Ankle	Knee	Hip Flex/Ext	HipAdd/Abd	Hip Int/Ext
Foot	0.58	0.29	0.11	0.14	0.00
Shank	0.03	0.64	0.64	0.33	-0.19
Thigh	0.01	0.00	0.42	0.75	0.02

Muscle Parameters:	Parameter		
Muscle	Maximum Isometric Force	Tendon Slack Length	Pennation Angle
Rectus Femoris	0.17	0.29	0.00
Vastus Medialis	0.33	-0.63	-0.07
Vastus Lateralis	0.28	-0.83	-0.10
Semitendinosus	0.76	0.51	-0.05
Biceps Femoris	0.53	0.39	-0.03
Gastrocnemius	0.53	0.51	-0.39
Gluteus Maximus1	0.59	-0.72	0.00
Gluteus Maximus2	0.62	-0.70	-0.04
Gluteus Maximus3	0.80	-0.47	-0.05
Gluteus Medius1	0.63	-0.57	-0.15
Gluteus Medius2	0.91	0.20	-0.12
Gluteus Medius3	0.72	0.24	-0.44

Table 5.4: The slope of sensitivity relationships calculated between muscle and body segment parameter inputs and the resulting maximum value of each output. Each parameter-output slope relationship was multiplied by one standard deviation of the input parameter. Sensitivity is highlighted based on correlation coefficient strength. Weakly Sensitive: *r*=0.2-0.4 (green); Moderately Sensitive: *r*=0.4-0.6 (blue); Highly Sensitive: *r*=0.6-1.0 (red).

Body Segment Parameters:	**Expected Change in Output for a +1 SD change in Input**				
Center of Mass	Ankle (N·m)	Knee (N·m)	Hip Flex/Ext (N·m)	HipAdd/Abd (N·m)	Hip Int/Ext (N·m)
Foot Med/Lat	0.01	-0.02	0.10	-0.03	0.01
Foot Ant/Post	0.04	0.06	0.02	-0.01	0.00
Foot Sup/Inf	-0.03	-0.07	0.62	0.02	0.00
Shank Med/Lat	0.00	-0.01	-0.06	0.14	-0.03
Shank Ant/Post	0.00	0.13	0.09	-0.01	0.02
Shank Sup/Inf	0.00	0.04	0.11	-0.03	0.00
Thigh Med/Lat	0.00	0.00	0.02	0.25	-0.05
Thigh Ant/Post	0.00	0.00	0.30	0.00	0.05
Thigh Sup/Inf	0.00	0.00	-0.46	-0.07	0.00
Moment of Inertia	Ankle (N·m)	Knee (N·m)	Hip Flex/Ext (N·m)	HipAdd/Abd (N·m)	Hip Int/Ext (N·m)
Foot AA	0.00	-0.01	-0.01	0.01	0.00
Foot IE	-0.01	0.00	-0.06	0.00	0.00
Foot FE	0.06	0.02	-0.08	0.01	0.00
Shank AA	0.00	-0.01	0.04	0.00	0.00
Shank IE	0.00	0.00	0.01	0.00	0.00
Shank FE	0.00	0.08	-0.13	0.01	0.00
Thigh AA	0.00	0.00	0.02	-0.05	-0.01
Thigh IE	0.00	0.00	-0.04	0.00	0.00
Thigh FE	0.01	0.00	0.84	0.01	0.01
Mass	Ankle (N·m)	Knee (N·m)	Hip Flex/Ext (N·m)	HipAdd/Abd (N·m)	Hip Int/Ext (N·m)
Foot	0.08	0.08	0.18	0.08	0.00
Shank	0.00	0.18	1.06	0.18	-0.02
Thigh	0.00	0.00	0.70	0.41	0.00

	Muscle Parameters		
Muscle	Maximum Isometric Force	Tendon Slack Length	Pennation Angle
Rectus Femoris (N)	0.49	0.92	0.00
Vastus Medialis (N)	2.83	9.83	-1.57
Vastus Lateralis (N)	3.53	-16.71	-2.78
Semitendinosus (N)	16.02	11.22	-1.32
Biceps Femoris (N)	29.43	22.52	-2.98
Gastrocnemius (N)	74.69	42.30	-27.96
Gluteus Maximus1 (N)	13.25	-16.01	0.07
Gluteus Maximus2 (N)	18.17	-19.74	-1.98
Gluteus Maximus3 (N)	8.72	-5.18	-0.73
Gluteus Medius1 (N)	12.35	-10.93	-3.68
Gluteus Medius2 (N)	31.70	7.01	-7.12
Gluteus Medius3 (N)	20.28	6.69	-12.19

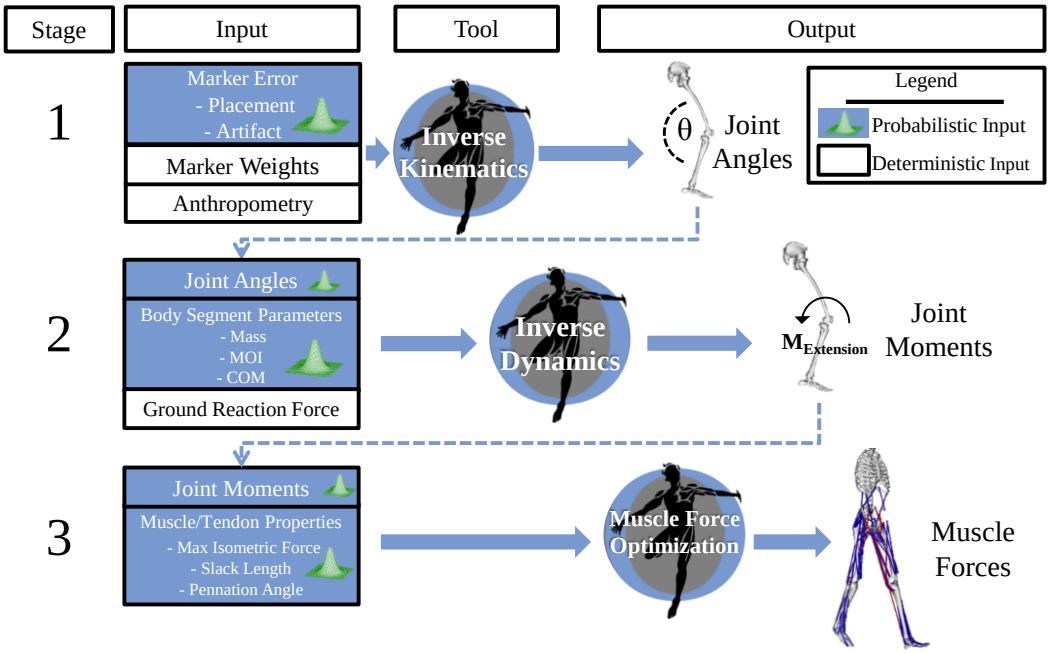

Figure 5.1: A gait trial was analyzed using OpenSim across three stages: Inverse Kinematics, Inverse Dynamics, and Muscle Force Optimization. Distributions of sources of uncertainty were inputs to each tool in a probabilistic simulation. To assess the propagation of uncertainty, output distributions from each tool were input into the next tool in the workflow. Output of each tool was used to calculate 5-95 confidence bounds and the sensitivity of the output to each source of uncertainty.

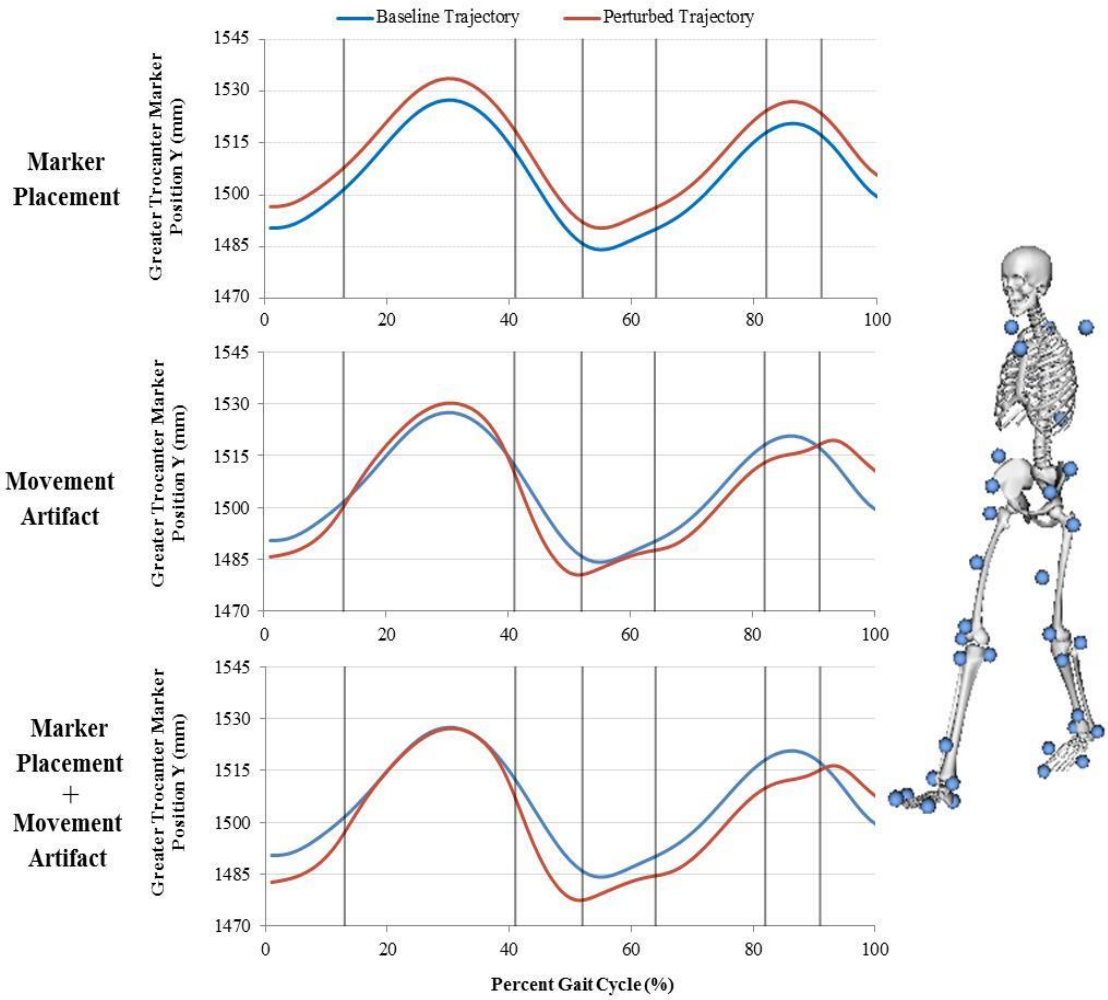

Figure 5.2: Representative marker trajectory that illustrates simulation of marker placement uncertainty, movement artifact uncertainty, and the combination of the two sources. Marker placement uncertainty was modeled as a constant offset throughout the gait cycle. Movement artifact was modeled using a trajectory that varied within each phase of the gait cycle (each phase separated by vertical lines). The marker set used for segment tracking is represented on the right

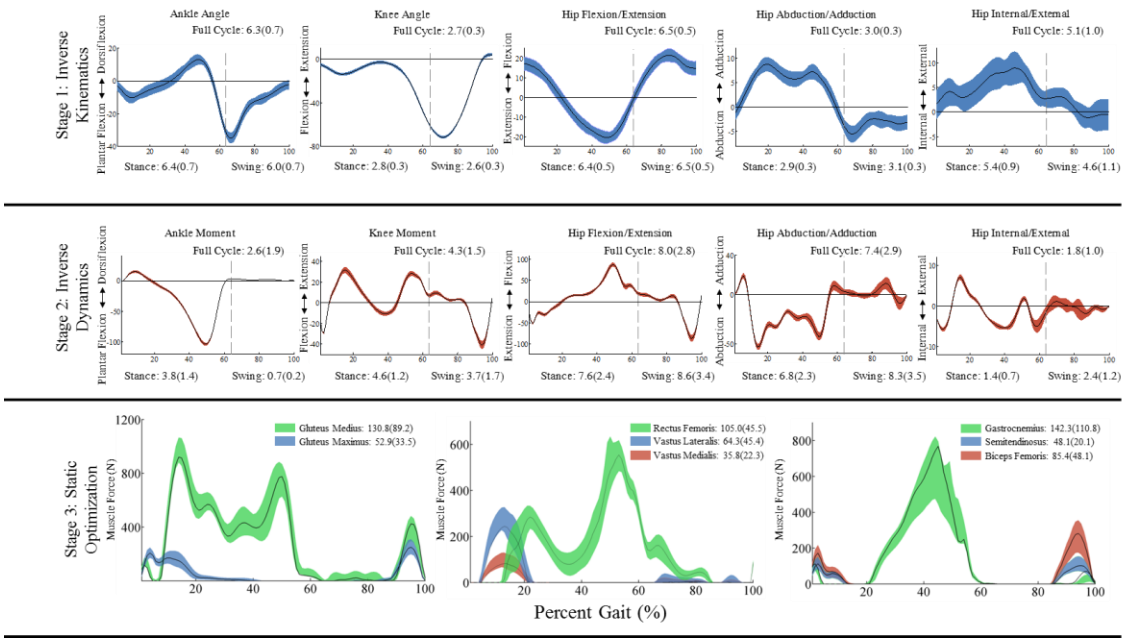

Figure 5.3: 5-95 confidence bounds for each simulation stage output following inverse kinematics (Stage 1), inverse dynamics (Stage 2) and static optimization (Stage 3). Values for the calculated mean 5-95 confidence bounds are displayed. Kinematic and kinetic degrees of freedom were divided into stance and swing periods. The baseline simulation output is represented by the black line

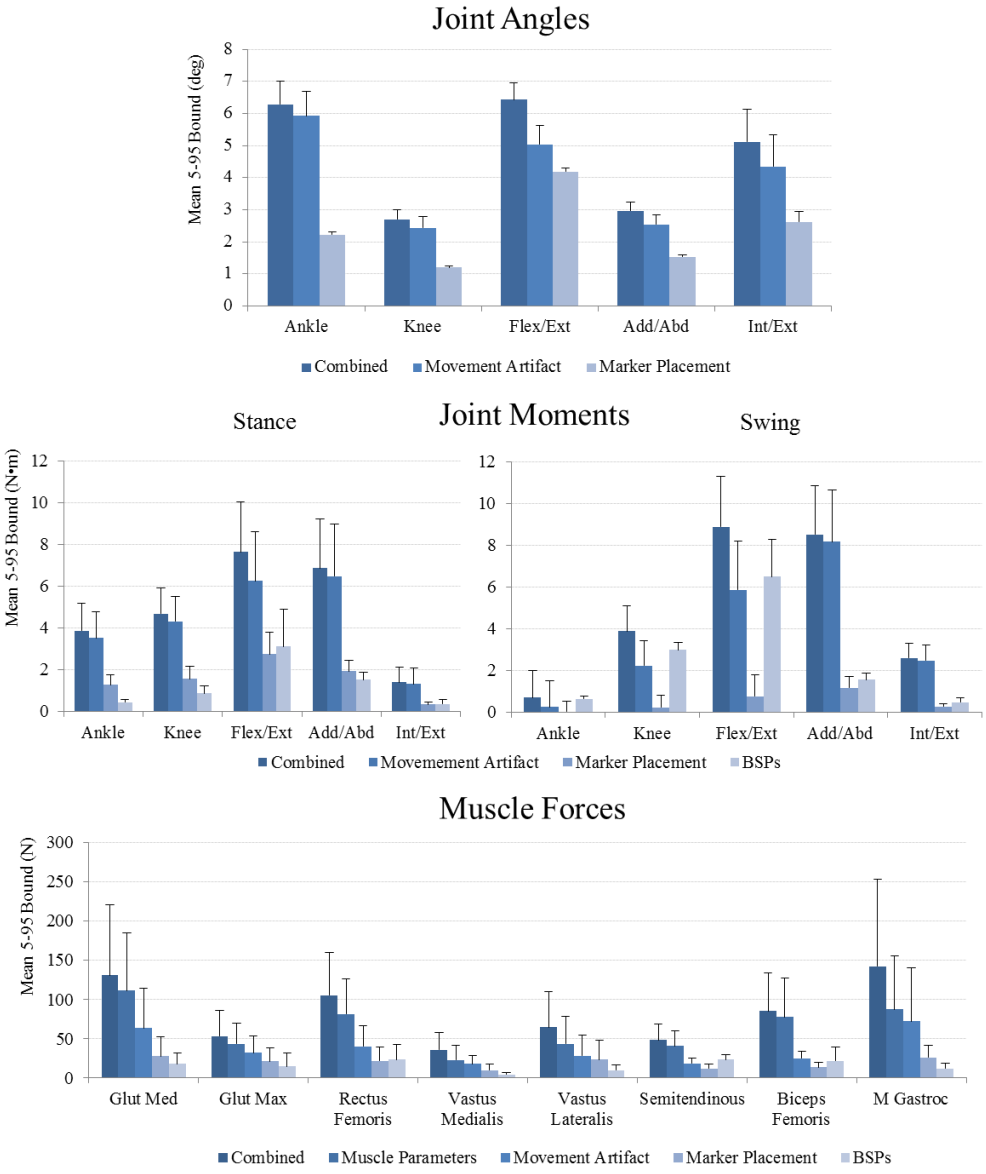

Figure 5.4: Mean 5-95 confidence bounds for each individual source of uncertainty for kinematics, joint moments and muscle forces. 5-95 confidence bounds calculated for joint moments were divided into stance and swing periods.

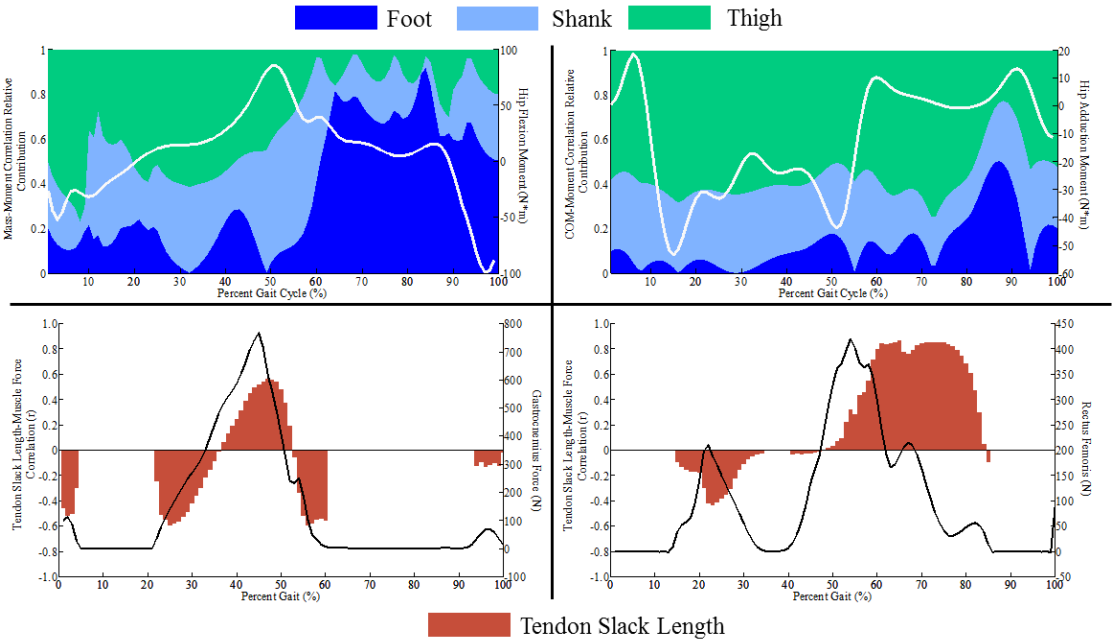

Figure 5.5: Upper: Relative sensitivity of flexion/extension and adduction/abduction hip moments to foot, shank, and thigh body segment parameters for each time point during the gait cycle. Relative sensitivity is presented as the segment correlation coefficient divided by the sum of the foot, shank, and thigh coefficients. Segment mass to hip flexion moment (Left), medial lateral position of the center of mass and hip adduction moment (Right). **Lower:** Sensitivity of predicted muscle force to tendon slack length calculated at each time point throughout the gait cycle for medial gastrocnemius (Left) and rectus femoris (right). Uncertainty in tendon slack length influences the point on the force-length curve that these two biarticular muscles operate on throughout the gait cycle. Note: no sensitivity reported when the muscle force is 0.

CHAPTER 6 – PROBABILISTIC MODELING OF REGIONAL INTERDEPENDENCE IN PATIENTS WITH TOTAL HIP ARTHROPLASTY

This chapter will present two studies that use the OpenSim probabilistic tool to improve on current modeling methodology and demonstrate how the tool can be used to inform rehabilitation practice in patients with total hip arthroplasty.

Study 1 – Incorporating Patient-Specific Strength and Parameter Uncertainty into Musculoskeletal Modeling of Patients with Total Hip Arthroplasty

6.1: Abstract

The in-vivo loading conditions predicted from musculoskeletal simulations used in combination with finite element analyses can be used to improve outcomes for patients with total hip arthroplasty (THA). Prior studies have not accounted for the significant patient-specific strength adaptations that occur following the surgery. Additionally, model input parameters and the experimental data that are used to parameterize these models contain uncertainty that is not typically considered. The purpose of this study was to develop musculoskeletal models with patient-specific muscle strength parameters in key hip muscle groups and characterize the impact of input uncertainty on muscle force and joint contact force outputs. This analysis was performed in a two-stage approach on five THA patients. The first stage scaled patient-specific muscle strength parameters to

minimize differences between model-predicted and experimental joint torques for maximal isometric hip flexion, extension and abduction tasks. The second stage generated 5-95% confidence bounds and input parameter sensitivity factors by simulating uncertainty in the muscle model parameters of peak muscle force, optimal fiber length and attachment site using a Monte Carlo simulation. Scaled models required a 38.1±16.2% decrease in hip extensor strength, a 29.9±8.9% decrease in hip abductor strength and only a 4.7±14.8% change in flexor strength compared to the generic model. Uncertainty in attachment site had 2.7 times greater impact on joint contact force than optimal fiber length and 2.0 times greater impact than maximum isometric force. Incorporating patient specific strength and uncertainty assessments into musculoskeletal simulation provides robust solutions when using these outputs in combination with finite element analysis for informing implant design, surgical approach and rehabilitation strategy to improve patient outcomes.

6.2: Introduction

Studies of total hip arthroplasty (THA) that incorporate accurate muscle force and joint contact force predictions from musculoskeletal simulation into finite element modeling can be used to perform in-vivo analyses on implant design, surgical approach and rehabilitation practices and improve patient outcomes. Outputs calculated from musculoskeletal simulation have been valuable in combination with high fidelity finite element models to provide realistic loading conditions in innovative approaches to calculate soft tissue loading in pathologies such as osteoarthritis and ACL injury

(Fernandez et al., 2011; Shelburne et al., 2011). Fernandez et al. (2011) used lower limb muscle force predictions from a musculoskeletal model in combination with ground reaction forces and joint kinematics as inputs to a 3D deformable model of the knee to determine magnitudes and locations of the contact forces and pressures. They were able to identify cartilage loading conditions that are associated with patellar tendon adhesion and may be responsible for initiating the patellofemoral pain and knee joint structural damage observed following ACL reconstruction. There are examples of the integration of musculoskeletal simulation outputs with ground reaction forces into finite element analyses at the hip joint (Heller et al., 2005), but further developments can increase the impact of this approach on pathological conditions.

Postoperatively, the muscles groups surrounding the hip can regain strength at different rates and to a variable extent (Di Monaco et al., 2009; Judd et al., 2014). The surgery is performed using either a posterior or an anterolateral approach that can lead to long term strength differences for the muscles affected (Gore et al., 1982). Generic musculoskeletal models with hip strength parameters meant to represent healthy individuals may not accurately characterize the loading conditions in the hip joint following THA surgery. Patient-specific strength adaptations that occur following THA surgery may be important to consider in musculoskeletal simulation to maximize the benefits of combining musculoskeletal simulation with finite element analyses. Several factors affect the available strength in the muscles that cross the hip in patients following THA surgery. Variation in rehabilitation strategy can also influence the extent to which the muscle groups of the hip regain strength (Shih et al., 1994).

Additionally, model input parameters and the experimental data that are used in the design and validation of musculoskeletal simulation models contain uncertainty that is not typically considered. Uncertainty in the inputs to musculoskeletal models results from a variety of sources. Experimental data that is used during model parameter tuning to improve model predictions are subject to measurement error that results in uncertainty (Widler et al., 2009). Additionally, the identification of bony landmarks for muscle attachment sites are subject to identification errors (Kepple et al., 1994; White et al., 1989). Finally, cadaveric specimens that provide valuable information used to parameterize the musculoskeletal models can be widely variable and also influenced by measurement error (Friederich and Brand, 1990; Ward et al., 2009).

The purpose of this study was to 1) develop musculoskeletal models for a group of THA patients with patient-specific muscle strength parameters in key hip muscle groups and to 2) quantify the impact of input uncertainty on muscle force and joint contact force outputs during maximal muscle force output.

6.3: Methods

6.3.1: Patients

Five patients who had undergone THA (2 male, 3 female; age: 61±7.9 yrs; mass: 81.6±14.8 kg; height: 170.7±11.7 cm) participated in a laboratory testing session six weeks post-operatively that consisted of hip flexion, extension and abduction maximum isometric strength tests. Patients had received THA through a posterior approach and received similar rehabilitative care between the surgery and the testing session. Each

participant provided written, informed consent and the study was approved by the Colorado Multiple Institutional Review Board. Data from these patients were collect by researchers at the Anschutz Medical Campus at the University of Colorado under the direction of Dr. Cory Christensen and Dr. Jennifer Stevens-Lapsley and provided for further analysis in this dissertation.

6.3.2: Experimental Isometric Strength Testing

Strength of the hip flexors, extensors, and abductors was assessed using an electromechanical dynamomter (HUMAC NORM, CSMI Solutions, Stoughton, MA) connected to a Biopac Data Acquisition System (Biodex Medical Systems, Inc., Shirley, NY) running AcqKnowledge software (v 3.8.2). Strength was measured in the affected limb. Hip abductor strength was measured while participants were positioned side-lying with 0° of hip flexion/extension and 0° of hip abduction/adduction. For hip extensor and flexor strength assessment, participants were positioned in supine with the hip flexed to 40°.

Musculoskeletal simulation analysis was performed in a two-stage approach in which 1) models with patient-specific muscle parameters were created and 2) parameter uncertainty was evaluated for each patient.

6.3.3: Musculoskeletal Simulation Stage 1: Patient-Specific Strength Scaling

In the first stage, patient-specific hip muscle strength scaling was done using OpenSim (Delp et al., 2007). A musculoskeletal model was used for each patient that

included detailed hip musculature (Shelburne et al., 2010). Additional muscles and wrapping were added to the lower extremity models currently available in OpenSim. Each model was initially scaled by patient segment dimensions and mass. Forward dynamic simulations of each patient performing maximum isometric hip abduction, extension, and flexion were generated to mimic laboratory tests in which each muscle activation level was set to 1.0 for the muscles that make up the hip abductors, extensors, and flexors (Table 6.1). Patient-specific maximum isometric strength parameters of each hip muscle were increased or decreased to minimize differences between model-predicted and the measured maximum isometric joint torques for each task. Muscles in each group were all scaled by the same factor to maintain the strength ratios between muscles of the same group. Baseline muscle force and hip joint contact force were calculated for each task using the model parameterized with the patient-specific hip strength.

6.3.4: Musculoskeletal Simulation Stage 2: Muscle Parameter Uncertainty

The second stage generated confidence bounds and input parameter sensitivity factors by simulating uncertainty in the muscle model parameters of peak muscle force, muscle attachment site, and optimal fiber length using a Monte Carlo simulation. To simulate uncertainty in isometric strength measurement, a coefficient of variation of 4.7% was applied to the value of maximum isometric force for each muscle based on the variability present in the testing during these maximum isometric tasks (Judd et al., 2014). A coefficient of variation of 5.8% was applied to the optimal fiber length of each muscle based on the average variation in this parameter among all the muscles considered

using cadaveric data (Friederich and Brand, 1990; Ward et al., 2009). Each value applied to the optimal fiber length was also applied to the tendon slack length in the opposite direction to ensure that the overall muscle length was held constant. A standard deviation of 5 mm was used for all the coordinates in reference to the segments body fixed frame (anterior/posterior (A/P), superior/inferior (S/I) and medial/lateral (M/L)) of the muscle origin and insertion sites, taken from the range of landmark location errors reported in literature (Kepple et al., 1994; White et al., 1989).

6.3.5: Data Analysis

The difference between model predicted and measured joint torques was calculated for each task (abduction, extension, and flexion) following model scaling. Additionally, the differences in the muscle isometric strength parameters for each muscle were compared between the generic model and the patient-specific scaled model.

Confidence bounds (5-95%) were calculated for hip joint contact forces and for each muscle force at the point of peak force. These bounds indicate a 90% probability that the true result of the simulation output lies between the lower and upper confidence bounds. The force outputs were normalized to body weight and averaged across all five patients. Monte Carlo simulations of 2000 trials were sufficient for convergence with differences in the average confidence bounds of less than 0.5 N for muscle force and joint contact force.

Sensitivity of joint contact force to individual muscle parameters was quantified by Pearson Product-Moment Correlation between the input parameter and the maximum

value of hip contact force. To objectively assess if a correlation was meaningful, a 95% confidence interval (CI) was calculated for the correlation coefficient. Correlations were considered statistically significant when the CI did not include zero with an alpha level of 0.05 (Curran-Everett, 2009). Strengths of the correlations that were statistically significant were categorized as weakly sensitive (r=0.2-0.4), moderately sensitive (r=0.4-0.6), or highly sensitive (r=0.6-1.0). The slope of each relationship was calculated and multiplied by the standard deviation of the input parameter to quantify the change in each muscle force and joint contact force output (Myers et al., 2014). Correlation coefficients, confidence intervals and the change in the output variable for a one standard deviation in the input were averaged across the five patients.

6.4: Results

6.4.1: Patient-Specific Strength Scaling

Following the first stage model scaling, the model-predicted and experimental torque matched within 0.1 Nm for each isometric task. The scaled isometric force muscle parameters differed from the values used in the generic musculoskeletal model and varied across muscle group and across the five patients. On average, models required a 38.1±16.2% decrease in hip extensor strength and a 29.9±8.9% decrease in hip abductor strength. Hip flexors were the least affected (4.7±14.8%), with 2 patients resulting in slight increases in strength to reproduce experiment hip flexion torque.

6.4.2: Uncertainty Impact: Muscle Force

The impact of all uncertainty sources on muscle force varied across patients and depended on whether the muscle was primarily a flexor, extensor or abductor. The impact of uncertainty on hip muscle forces can be observed in representative force profiles from the maximum isometric tasks (Figure 6.1). Variability was present in the impact of the sources of uncertainty in hip muscles across subjects. In the representative subject, uncertainty in maximum isometric force had approximately the same influence as uncertainty in attachment site, except for in the flexors where it was 1.3 times greater (Figure 6.1). However, on average for all patients attachment site 5-95 bound sizes were 2.7 times greater than optimal fiber and 1.8 times greater than maximum isometric force for all tasks. Additionally, 5-95 bounds in the flexor group were 5.1 times greater than extensors and 3.5 times greater than abductors (Figures 6.2).

6.4.3: Uncertainty Impact: Hip Joint Contact Force

On average, uncertainty had the greatest effect in flexion which produced hip joint reaction force confidence bounds that were 1.8 times greater than in abduction and 2.4 times greater than in extension for all parameters considered. Uncertainty in attachment site had 2.7 times greater impact on joint contact force than optimal fiber length and 2.0 times greater impact than maximum isometric force (Figure 6.2).

6.4.4: Joint Contact Force Sensitivity to Individual Hip Muscles

Statistically significant correlations between muscle parameters and hip joint contact force demonstrated the muscles of the abductors, extensors and flexors that had the greatest influence on joint contact force and quantified the magnitude of the impact that each source of uncertainty had on hip joint contact force. When considering the hip abductor muscles, hip joint contact force was most sensitive to changes in gluteus medius isometric force. Hip joint contact force was moderately sensitive to each section of the gluteus medius (glut_med1: r=0.47±0.04, CI [0.44 0.49]; glut_med2: r=0.40±0.01, CI [0.37 .42]; glut_med3: r=0.45±0.04 CI [0.41 0.49]) (Table 6.2) and resulted in a combined 0.0326±0.0126 BW change in contact force for one standard deviation change in gluteus medius maximum isometric force. Additionally, hip joint contact force also demonstrate statistically significant sensitivity to piriformis muscle properties of maximum isometric force (r=0.26±0.3, CI [0.21 0.31]), origin M/L (r=0.29±0.04, CI [0.25 0.33]), insertion S/I (r=-0.25±0.04, CI [0.20 0.29]), insertion M/L (-0.27±0.05, CI [0.21 0.32]) and optimal fiber length (0.25±0.11, CI [0.21 0.29]) (Table 6.1). Of these parameters, origin M/L location resulted in the largest change in hip joint contact force (0.0215±0.0079 BW) for a one standard deviation change (Table 6.3)

When considering the hip extensor muscles, hip joint contact force was most sensitive to the middle fascicle gluteus maximus (glut_med2) parameters of maximum isometric force (r=0.67±0.10, CI [0.65 0.69]), origin S/I(r=0.40±0.11, CI [0.35 0.42]), insertion S/I (r=-0.34±0.15, CI [0.30 0.40]), and optima fiber length (r=0.53±0.24, CI [0.48 0.55]) (Table 6.4). However, statistically significant relationships between hip joint

contact force and hip extensors parameter resulted in, on average, 53.7% less change in hip joint contact force compared to abductors and 82.9% less compared to hip flexors (Table 6.5).

Hip joint contact force was more sensitive to changes in the hip flexor group than the abductors and extensors. One standard deviation changes in statistically significant parameter relationships resulted changes to hip joint contact force that ranged from 0.0176 BW to 0.0539 BW. The muscle with the greatest influence was the psoas with significant relationships to hip joint contact force between maximum isometric force ($r=0.59\pm0.03$, CI [0.55 0.61]), origin S/I ($r=0.41\pm0.04$, CI [0.37 0.43]), insertion A/P ($r=-0.36\pm0.03$, CI [0.31 0.42]) and optimal fiber length ($r=0.45\pm0.04$, CI [0.40 0.49]) (Tables 6.6&6.7).

6.5: Discussion

This study demonstrates a patient-specific hip muscle strength scaling approach that provides the ability to capture post-operative THA strength adaptions in musculoskeletal simulations. This approach is required to match experimental data and provide realistic muscle and joint force outputs in the THA patient population. Further, assessment of the impact of uncertainty and identification of the most influential parameters quantify the range of possible results for outputs to describe model confidence and support broader applications in combination with finite element analysis to address implant design, surgical planning and rehabilitation strategy.

The patient-specific muscle strength scaling required to minimize differences between model predicted torque and experimentally collected torque illustrate the importance of careful parameterization in each muscle group of the hip. On average, muscles required a 24% change in strength to reproduce experimentally collected joint torques to within 0.1 Nm. However, these changes differed between patients and between muscle groups. The large changes required for hip extensors (38.1±16.2%) compared to hip flexors (4.7±14.8%) may be explained by the posterior surgical approach used on these patients and would likely be reversed in patients with an anterolateral approach. Strength difference between muscle groups persist throughout the recovery period as patients regain strength and function to varying degrees for years following the procedure (Di Monaco et al., 2009). Without scaling practices that match patient-specific experimentally measured joint torques, outputs from musculoskeletal simulation may not accurately represent loading conditions in a patient population, particularly those that experience significant muscular adaptations in response to pathology.

Further highlighting the need to apply patient-specific parameters, the impact of uncertainty was greatest when considering variability in muscle attachment site. Muscle attachment has a direct relationship with the muscle moment arm (Pal et al., 2007), altering joint torques and contact forces. Incorporating imaging data to inform the location of muscle attachment site may help to reduce the impact of this source of uncertainty. However, this may not be feasible in all musculoskeletal simulation studies. Therefore, it is necessary to understand and quantify the impact of uncertainty in muscle

force and joint contact force outputs before incorporating into finite element analyses and evaluating hypotheses.

The sensitivity of joint contact forces to individual muscle parameters identified the muscles with the largest influence on hip joint loading, and may be an important factor to consider during THA surgical planning. The muscles that resulted in the highest sensitivity (change in hip joint contact force for a one standard deviation change in any muscle parameter) all came from the flexor muscle group: psoas, rectus femoris and iliacus. This likely occurred because these muscles were much stronger on average than any in the abductor or extensor muscle groups. The analysis also identified interesting relationships for muscles that are considered secondary to the larger, prime movers. For example, the piriformis muscle, one of the weaker hip muscles based on strength, resulted in significant relationships to hip joint contact force for all three parameters considered. This is likely due to its location and orientation relative to the hip joint. The most influential muscles to hip joint loading may be left unaltered during surgery to improve patient outcomes.

Several limitations to this study should be considered. First, this cohort may not represent the THA population because we considered a sample group with only five patients. Second, maximum isometric abduction, extension and flexion tasks were only performed in one position for each task, and therefore, do not serve as a validation of the muscle parameters in the model. For true validation of model predictions with laboratory observations, additional experimental maximal joint torque values in varying position would be necessary. Finally, the output distributions for hip joint contact force and

muscle forces were dependent on the input distributions selected. We chose our probabilistic input parameters based on experimental data when possible and on values found in the literature. We recommend that other researchers select input distributions based on the best experimental data available.

6.6: Conclusion

Incorporating patient specific strength and uncertainty assessments into musculoskeletal simulation provides robust solutions when using these outputs in combination with finite element analysis to inform implant design, surgical approach and rehabilitation strategy. The patient-specific approach used in this study provides the ability to capture post-operative strength adaptions to generate realistic hip loading conditions in patients with THA. Further, assessment of the impact of uncertainty is needed to improve confidence in musculoskeletal modeling and should be considered when using results in hypothesis testing and clinical decision making.

Study 2 – Simulated Hip Abductor Strengthening Reduces Peak Joint Contact Forces During Step Down Task in Patients with Total Hip Arthroplasty

6.7: Abstract

It is common for lower extremity muscle strength training to be a focus of rehabilitation following total hip arthroplasty (THA). The strength of the hip abductor muscle group is an important predictor of overall function following THA due to the link between hip abductor function and joints other than the hip. The purpose of this study was to

investigate the effects of hip abductor strengthening following rehabilitation on joint contact forces (JCFs) in the lower extremity and low back during a high demand step down task. Five patients who had undergone THA performed lower extremity maximum isometric strength tests and a stair descent task from a height of 20 cm. Patient-specific musculoskeletal models were created in OpenSim using maximum isometric strength parameters scaled to minimize differences between model-predicted and measured preoperative maximum isometric joint torques in hip flexion, extension, and abduction as well as knee flexion and extension. A baseline forward dynamic simulation of each subject performing the stair descent was constructed using their corresponding patient-specific model to predict JCFs at the ankle, knee, hip, and low back. The hip abductor muscle strength was increased relative to baseline over a range of possible strength increases (0-30%) in a probabilistic framework using the advanced mean value method to predict bounds (0.5-99.5%) for peak JCF at each joint. Simulated hip abductor strengthening resulted in peak JCFs bounds that were reduced relative to baseline for all five patients at the hip (18.9-23.8±16.5%) and knee (20.5-23.8±11.2%). Four of the five patients had reductions at the ankle (7.1-8.5±11.3%) and low back (3.5-7.0±5.3%) with one patient demonstrating no change. Simulated hip abductor strengthening reduced JCF at the hip joint and at joints other than the hip demonstrating the dynamic and mechanical interdependencies of the knee, hip and spine that can be targeted in early THA rehabilitation and may lead to higher overall patient function.

6.8: Introduction

Rehabilitation following total hip arthroplasty (THA) is designed to reduce the impairments associated with the surgery and to optimize overall functional recovery. It is common for lower extremity muscle strength training to be a focus of rehabilitation as strength deficits are strongly associated with decreased overall function. Through the use of rehabilitation, investigators have reported improvement in muscle strength in the first six months of recovery compared to preoperative values. Lower extremity muscle strength gains from rehabilitation can range from 0-30% (Suetta et al., 2008), with more common gains of 15-20% (Judd et al., 2014). While strength deficits relative to the uninvolved limb may persist, early stage strength gains may be beneficial to long-term function and in reducing the loading experienced by the implant.

The strength of the hip abductor muscle group is an important predictor of overall function following THA. This may be due to its influence on the internal joint contact force (JCF), where weakness in the hip abductor group results in greater hip joint contact forces during walking (Valente et al., 2013). Increased joint loading can lead to loosening of the implanted components and overall functional deficits during tasks with high muscular demand (Long et al., 1993). Targeting deficits in hip abductor muscles may improve overall functional recovery following surgery by influencing the loading at the hip joint and potentially at joints other than the hip.

A clinical link has been established between the hip abductor muscle group and joints other than the hip. Individuals with patellofemoral pain syndrome demonstrate

deficits in hip abductor muscle strength and exhibit greater degrees of hip adduction and internal rotation during dynamic activities such as landing from a jump or a step down task (Lee et al., 2012; Powers, 2010; Salsich and Long-Rossi, 2011). Hip muscle force production is crucial for whole body balance in minimizing the acceleration of the body center of mass in response to postural perturbations, which has been linked to variety of injury mechanisms (Aramaki et al., 2001). However, the relationship between hip abductor strength and JCF in the lower extremity and lower back has not been fully investigated, particularly during tasks with high muscle demand. Additionally, identifying which abductor muscles have the most impact on JCF can direct rehabilitation strategy and inform surgical approach.

The purpose of this study was to investigate the effects of typical changes in hip strength following rehabilitation on JCFs in the lower extremity and low back during a step down task. The step down task was chosen because it is representative of stair descent, and demands higher hip function than flat walking. We hypothesized that simulated increases in abductor muscle strength would influence peak JCFs at joints other than the hip.

6.9: Methods

Five patients with THA (2 M, 3F; age: 63±7.5 yrs; BMI: 27.5±2.0) participated in a preoperative laboratory testing session that was repeated six weeks postoperatively. Each patient provided written, informed consent and the study was approved by the Colorado Multiple Institutional Review Board. Data from these patients were collect by

researchers at the Anschutz Medical Campus at the University of Colorado under the direction of Dr. Cory Christensen and Dr. Jennifer Stevens-Lapsley and provided for further analysis in this dissertation.

6.9.1: Experimental Testing Sessions

Strength of the hip flexors, extensors, and abductors as well as the knee flexors and extensors was assessed using an electromechanical dynamometer (HUMAC NORM, CSMI Solutions, Stoughton, MA) connected to a Biopac Data Acquisition System (Biodex Medical Systems, Inc., Shirley, NY) running AcqKnowledge software (v 3.8.2). Strength was measured in the affected limb. For hip flexor and extensor strength assessment, participants were positioned in supine with the hip flexed to 40°. Hip abductor strength was measured while participants were positioned side-lying with 0° of hip flexion/extension and 0° of hip abduction/adduction. Knee extensor and flexor strength was measured in a seated position with a with a shoulder harness and waist strap for stabilization. Patients were placed in 85° of hip flexion and 60° of knee flexion for testing.

32 reflective markers were used to define anatomical landmarks while an 8 motion camera motion capture system (Vicon, Centennial, CO) collected at 100 Hz. Patients performed a single step down task with their involved limb from a height of 20 cm onto a force plate collecting at 2000 Hz.

6.9.2: Probabilistic Musculoskeletal Simulation

Musculoskeletal simulations were performed in OpenSim (Delp et al., 2007). A musculoskeletal model was used for each patient that included detailed hip musculature (Shelburne et al., 2010). Additional muscles and wrapping were added to the lower extremity models currently available in OpenSim. Each model was initially scaled by patient segment dimensions and mass. Patient-specific muscle maximum isometric strength values of each model were then scaled to minimize differences between model-predicted and the measured maximum isometric joint torques for each task (see Study 1).

A baseline forward dynamic simulation of each patient performing the step down task was constructed using their corresponding patient-specific model to predict lower extremity muscle forces and JCFs at the ankle, knee, hip, and low back. The hip abductor muscle strength for gluteus medius (glut med), gluteus minimus (glut min), anterior section of the gluteus maximum (glut max), tensor fasciae latae (tfl), piriformis (piri) and gemellus (gem) were then increased relative to baseline in a series of probabilistic analyses. A range of possible strength increases was simulated with a mean of 15% and a standard deviation of 5% to result in a ±3 standard deviation range of 0-30% of possible increase in abductor muscle strength.

Probabilistic analyses were performed using both Monte Carlo methods and advance mean value (AMV) (Wu, Y et al., 1990). AMV is beneficial for probabilistic modeling involving long running simulations because it is more computational efficient compared to Monte Carlo. Fewer trials are necessary with AMV to obtain a solution for a

given probability level, resulting in decreased computational time compared to the Monte Carlo method. To verify convergence, data from one patient were analyzed using both the AMV and Monte Carlo methods and joint contact force outputs were compared. After confirming excellent agreement between the Monte Carlo and AMV methods for one patient, the AMV method was used.

The output range of peak JCF at each joint was generated by calculating the values with 0.5% (lower) and 99.5% (upper) probability. These bounds represent the greatest range possible without including the extreme tails of the output distribution. A final simulation of the step down task was performed in which each patient-specific model was scaled to the measured strength in the hip abductor group at the six-week postoperative test. The peak JCFs of each patient's strength adaptation at six weeks were compared to the predicted range from the probabilistic analyses

Within the probabilistic analysis, muscle strengths were varied per muscle. This enabled the calculation of sensitivity factors from the advanced mean value method for each muscle. Sensitivity factors were calculated in the standard normal variate space as the unit vector from the origin to the point that represents the combination of input parameter values that predict performance at the two specified probability levels. The Sensitivity factors are a measure of the relative impact of increased strength of each muscle on the peak JCF. The sum of squares of all sensitivities for each joint will equal one.

6.10: Results

6.10.1: Experimental Strength Testing

Three of the five patients demonstrated increases in hip abductor strength postoperatively that were on average 11.3% greater than preoperative strength (Table 6.8).

6.10.2: Simulated Strengthening

Results generated from the AMV analysis agreed with those from a Monte Carlo simulation of 3000 trials. 0.5% and 99.5% bounds calculated from AMV were on average 97.6% accurate for joint contact force estimations when compared to Monte Carlo. This verified the convergence of the AMV analysis to Monte Carlo. The results reported below were taken from the AMV analysis.

Simulated hip abductor strengthening resulted in peak JCFs at lower and upper bounds that were smaller than baseline peak JCFs for all five patients at the hip (18.9-23.8±16.5%) and knee (20.5-23.8±11.2%) (Figure 6.3). Four of the five patients had reductions at the ankle (7.1-8.5±11.3%) and low back (3.5-7.0±5.3%) with one patient demonstrating no change. Reductions at the ankle and low back were smaller than the hip and knee, but demonstrate the ability of the hip abductor group to influence loading at these joints in some patients (Figure 6.4).

The large variability in percent reduction in JCF was associated with preoperative strength. In general, patients with weaker preoperative strength resulted in the greatest reductions in JCF in response to simulated strengthening. Further, two patients with weaker hip abductors at the 6-week follow up compared to preoperatively, demonstrated,

on average, greater hip (34.9±20.3%) and knee (20.7±7.1%) JCFs compared to baseline, while patients with increased strength demonstrated reductions in JCFs that were within the upper and lower simulated strength bounds (Figure 6.3).

Simulated strengthening resulted in a redirection of JFCs at the lower extremity joints as demonstrated by changes to the force components. The largest differences occurred in the vertical component at each joint and accounted for 82.5±13.1% of the JCF reductions, on average (Table 6.9).

The two posterior sections of the gluteus medius had a 20.3% greater effect on low back JCF than any other joint, while the anterior section had 46.3% greater effect on knee JCF than any other joint. The smaller muscles (tfl, gem) had the greatest influence overall for the relative increase in hip strength. Knee JCFs demonstrated sensitivity factors of 0.24±0.8 and 0.26±0.8 for the tfl and gem, respectively, and were the highest of any individual muscle-joint relationship. However, sensitivity factors varied between subjects, likely due to differences in anthropometry and stair descent kinematics that can influence moment arm and muscle mechanics (Figure 6.5).

6.11: Discussion

Simulated strengthening of the hip abductor muscle group produced reductions in hip and knee JCF and smaller reductions at the low back and ankle when muscle demand was high. This indicates that targeting this muscle group in early THA rehabilitation may lead to higher overall patient function with reduced JCF on the implant. In addition, JCF was most sensitive to simulated strengthening in what may be considered minor muscles

of the hip, and may play an important role in surgical approach and rehabilitation planning.

Strengthening of the hip abductor group is capable of reducing JCF at joints other than the hip, confirming our initial hypothesis. While simulated strengthening of the hip abductors had the greatest influence on the hip JCF (18.9 to 23.8%), reductions in JCF that ranged from 3.5% to 20.5% were also demonstrated in the low back, knee and ankle. Increasing the strength alone, of a vital muscle group, while maintaining kinematics and anthropometrics, resulted in a redirection of contact forces and redistribution across muscles that lead to potentially beneficial force reductions. It is likely this was a result of dynamic coupling between the body segments where each muscle force contributes to the angular accelerations of all the joints at each instant of the task (Pandy, 2001; Zajac and Gordon, 1989). Because the articular contact forces are a function of the joint angular accelerations, it follows that each muscle force also contributes to the contact force transmitted by each joint. Therefore, muscles that do not cross a specific joint are capable of contributing to the contact force at that joint. For example during gait, the vasti, soleus and gastrocnemius contribute greater than 0.5 BW to hip contact force (Correa et al., 2010).

The sensitivity factors calculated also identify the influence of the hip abductor muscle on each of the joints assessed. Within the same muscle, the three different sections of the gluteus medius were capable of influencing loading to different degrees at the knee, hip and low back. Likely as a result of the architecture and the moment arm of each section, the most anterior section of the gluteus medius had the largest influence

over the knee JCF, while the two posterior sections had a greater influence over the low back. Additionally, knee JCF demonstrated the greatest sensitivity factors to the gem and tfl, muscles that might be considered minor muscles of the hip in comparison the gluteal muscles. These sensitivity results offer clinicians muscles to target when designing strength based rehabilitation strategy. Surgeons may also use these data in consideration of surgical planning when assessing approach and the muscles that are affected to the greatest extent.

This is the first study to assess the influence of simulated hip muscle strengthening on joint loading; however, there have been in-vitro study designs that support our findings. For example, the influence of the gluteal muscles on joint loading has been demonstrated using in-vitro models. Cristofolini et al., (1995) simulated the forces of ten thigh muscles during early stance in gait on cadaveric femurs and found that the gluteus medius and minimus had over two times greater influence on vertical femur strain than muscles that included gluteus maximus, the quadriceps muscles and adductor magnus. High demand, landing tasks have been simulated at the knee, where increasing quadriceps force over a physiological possible range demonstrated a redirection of ground reaction forces and reductions in ACL strain (Hashemi et al., 2010). While not specifically at the hip joint, this study also quantified evidence of the interrelationship between muscle forces and accelerating body segments in the presence of ground reaction forces during high-demand tasks.

This study implemented the AMV approximation method to enable the use of probabilistic methodology with musculoskeletal simulation in an efficient and accurate

way. The method was originally designed for structural and aerospace applications, but has been used in certain orthropaedic applications (Langenderfer et al., 2009, 2008; Laz and Browne, 2010). AMV is attractive for applications with high computational costs like the forward simulations used in this study, because it requires fewer evaluations than Monte Carlo to generate similar outputs. However, the AMV method cannot be used in every musculoskeletal modeling application. The number of trials needed for AMV analysis is determined by $n+1+m$, where n is the number of random variables and m is the number of specified probability levels. As study complexity increases, computational savings is reduced and the more robust Monte Carlo method should be used. Additionally, when multiple combinations of input parameters result in the same output, the method will have difficulty converging on a meaningful solution. We recommend that prior to proceeding, AMV outputs should always be compared to Monte Carlo outputs.

There are limitations to this study should be considered. First, this was a controlled condition that assessed only the influence of increased muscle strength. It is possible that step down kinematics, ground reaction forces and as well as anthropometric variables could change following a strengthening rehabilitation protocol which would influence the resulting JCFs. Second, simulated strengthening assumed that the maximum isometric strength of each muscle was independent. It is not known how the different muscles of the hip abductor group respond to typical strengthening rehabilitation. Additionally, this allowed for the calculation of sensitivity factors for each muscle in the abductor group.

6.12: Conclusion

Simulated hip abductor strengthening produced reductions in JCF when muscle demand was high at the hip joint as well as at the knee and low back. This is evidence of the dynamic and mechanical interdependencies of the knee, hip and spine that can be targeted in early THA rehabilitation and may lead to higher overall patient function with reduced JCF on the implant. In addition, JFC was most sensitive to simulated strengthening in what may be considered minor muscles of the hip, and may play an important role in surgical approach and rehabilitation planning.

Table 6.1: The muscles that make up the abductor, extensor and flexor groups of the hip with the abbreviations for each muscle. The abbreviations are consistent with those used in OpenSim.

Abductors	Extensors	Flexors
Gluteus Maximus: 1 fascicle Anterior (glut_max1) Gluteus Medius: 3 fascicles Anterior (glut_med1) Middle (glut_med2) Posterior (glut_med3) Gluteus Minimus: 3 fascicles Anterior (glut_min1) Middle (glut_min2) Posterior (glut_min3) Piriformis (piri) Tensor Fasciae Latae (tfl) Gemellus (gem)	Adductor Magnus: 3 fascicles Superior (add_mag1) Middle (add_mag2) Inferior (add_mag3) Gluteus Maximus: 2 fascicles Middle (glut_max2) Posterior (glut_max3) Gracilis Quadratus femoris (quad_fem)	Adductor Longus (add_long) Iliacus Pectineus (pect) Psoas Rectus Femoris (rect_fem) Sartorius (sar)

Table 6.2: Average correlation coefficient (SD) across five patients between hip joint contact force magnitude and hip muscle parameters of the abductor group. Sensitivity is highlighted based on correlation coefficient strength. Weakly Sensitive: *r*=0.2-0.4 (green); Moderately Sensitive: *r*=0.4-0.6 (yellow); Highly Sensitive: *r*=0.6-1.0 (red).

	glut_max1	glut_med1	glut_med2	glut_med3	glut_min1	glut_min2	glut_min3	piri	tfl	gem
Max Iso	0.29 (0.04)	0.47 (0.04)	0.40 (0.01)	0.45 (0.04)	0.18 (0.03)	0.19 (0.02)	0.23 (0.03)	0.26 (0.03)	0.17 (0.04)	0.14 (0.11)
Origin A/P	0.00 (0.03)	0.08 (0.04)	0.02 (0.04)	0.03 (0.02)	-0.01 (0.04)	0.00 (0.02)	0.01 (0.03)	-0.12 (0.02)	0.01 (0.03)	-0.01 (0.02)
Origin S/I	0.15 (0.07)	0.26 (0.07)	0.06 (0.02)	0.15 (0.02)	0.02 (0.03)	0.02 (0.04)	0.10 (0.08)	0.18 (0.02)	0.01 (0.03)	0.15 (0.06)
Origin M/L	0.06 (0.04)	0.13 (0.03)	0.10 (0.02)	0.09 (0.02)	0.02 (0.07)	0.01 (0.06)	0.02 (0.05)	0.29 (0.05)	0.00 (0.03)	0.17 (0.11)
Insert A/P	0.07 (0.01)	-0.07 (0.01)	0.01 (0.03)	0.00 (0.02)	0.02 (0.02)	-0.01 (0.03)	-0.01 (0.04)	0.09 (0.01)	0.00 (0.04)	0.03 (0.04)
Insert S/I	-0.11 (0.03)	-0.31 (0.07)	-0.09 (0.02)	-0.11 (0.04)	0.01 (0.03)	-0.02 (0.02)	-0.07 (0.03)	-0.25 (0.04)	0.00 (0.03)	-0.16 (0.06)
Insert M/L	-0.02 (0.03)	-0.14 (0.05)	-0.05 (0.02)	-0.07 (0.03)	-0.02 (0.02)	0.00 (0.02)	-0.07 (0.03)	-0.27 (0.05)	-0.03 (0.01)	-0.21 (0.09)
Fiber Len	0.58 (0.11)	0.31 (0.10)	0.05 (0.03)	0.14 (0.08)	0.19 (0.08)	0.00 (0.01)	-0.01 (0.01)	0.25 (0.11)	0.03 (0.04)	0.00 (0.01)

Table 6.3: Average change in hip contact force in BW for 1 SD change in input parameter (SD) across five patients between hip joint contact force magnitude and hip muscle parameters of the abductor group. Sensitivity is highlighted based on correlation coefficient strength. Weakly Sensitive: *r*=0.2-0.4 (green); Moderately Sensitive: *r*=0.4-0.6 (yellow); Highly Sensitive: *r*=0.6-1.0 (red).

	glut_max1	glut_med1	glut_med2	glut_med3	glut_min1	glut_min2	glut_min3	piri	tfl	gem
Max Iso	0.0072 (0.0031)	0.0114 (0.0045)	0.0100 (0.0037)	0.0112 (0.0044)	0.0043 (0.0016)	0.0046 (0.0018)	0.0056 (0.0024)	0.0061 (0.0022)	0.0039 (0.0010)	0.0028 (0.0009)
Origin A/P	0.0006 (0.0019)	0.0066 (0.0042)	0.0017 (0.0026)	0.0020 (0.0019)	-0.0009 (0.0031)	-0.0005 (0.0018)	0.0013 (0.0019)	-0.0089 (0.0035)	0.0013 (0.0023)	-0.0008 (0.0015)
Origin S/I	0.0122 (0.0068)	0.0202 (0.0085)	0.0048 (0.0026)	0.0113 (0.0042)	0.0015 (0.0024)	0.0024 (0.0035)	0.0080 (0.0064)	0.0134 (0.0047)	0.0007 (0.0020)	0.0107 (0.0031)
Origin M/L	0.0035 (0.0023)	0.0099 (0.0037)	0.0074 (0.0017)	0.0069 (0.0031)	0.0047 (0.0038)	0.0040 (0.0028)	0.0045 (0.0024)	0.0215 (0.0079)	0.0019 (0.0014)	0.0115 (0.0055)
Insert A/P	0.0051 (0.0021)	-0.0056 (0.0024)	0.0002 (0.0015)	-0.0004 (0.0017)	0.0012 (0.0017)	-0.0005 (0.0023)	-0.0007 (0.0031)	0.0064 (0.0018)	0.0002 (0.0038)	0.0023 (0.0029)
Insert S/I	-0.0084 (0.0040)	-0.0240 (0.0105)	-0.0071 (0.0026)	-0.0091 (0.0047)	0.0008 (0.0024)	-0.0018 (0.0019)	-0.0055 (0.0030)	-0.0189 (0.0081)	0.0007 (0.0026)	-0.0108 (0.0015)
Insert M/L	-0.0021 (0.0022)	-0.0108 (0.0058)	-0.0037 (0.0018)	-0.0052 (0.0024)	-0.0016 (0.0017)	0.0000 (0.0014)	-0.0057 (0.0035)	-0.0203 (0.0083)	-0.0023 (0.0011)	-0.0149 (0.0057)
Fiber Len	0.0097 (0.0039)	0.0052 (0.0028)	0.0008 (0.0005)	0.0027 (0.0021)	0.0032 (0.0021)	-0.0001 (0.0002)	-0.0001 (0.0001)	0.0043 (0.0031)	0.0007 (0.0006)	0.0001 (0.0003)

Table 6.4: Average correlation coefficient (SD) across five patients between hip joint contact force magnitude and hip muscle parameters of the abductor group. Sensitivity is highlighted based on correlation coefficient strength. Weakly Sensitive: *r*=0.2-0.4 (green); Moderately Sensitive: *r*=0.4-0.6 (yellow); Highly Sensitive: *r*=0.6-1.0 (red).

	Add_mag1	Add_mag2	Add_mag3	glut_max2	glut_max3	gracilis	Quad Fem
Max Iso	0.20 (0.08)	0.22 (0.09)	0.30 (0.14)	0.67 (0.10)	0.39 (0.10)	0.21 (0.19	0.21 (0.06)
Origin A/P	-0.17 (0.07)	-0.13 (0.05)	-0.05 (0.03)	-0.03 (0.11)	-0.03 (0.03)	-0.04 (0.05)	-0.18 (0.05)
Origin S/I	0.09 (0.02)	0.07 (0.05)	0.01 (0.03)	0.40 (0.11)	0.06 (0.01)	0.01 (0.01)	0.16 (0.03)
Origin M/L	0.14 (0.07)	0.06 (0.03)	0.03 (0.03)	0.16 (0.09)	0.04 (0.02)	0.01 (0.02)	0.04 (0.02)
Insert A/P	0.07 (0.04)	0.06 (0.02)	-0.03 (0.01)	0.19 (0.05)	0.03 (0.04)	0.00 (0.03)	0.03 (0.04)
Insert S/I	-0.20 (0.07)	-0.10 (0.06)	-0.05 (0.03)	-0.34 (0.15)	-0.04 (0.06)	0.00 (0.06)	-0.21 (0.06)
Insert M/L	-0.11 (0.08)	-0.05 (0.07)	-0.04 (0.04)	-0.02 (0.09)	-0.03 (0.04)	-0.01 (0.01)	-0.04 (0.05)
Fiber L	0.22 (0.17)	0.22 (0.17)	0.01 (0.04)	0.53 (0.24)	-0.01 (0.02)	-0.01 (0.03)	0.02 (0.01)

Table 6.5: Average change in hip contact force in BW (SD) for one standard deviation change in input parameter across five patients between hip joint contact force magnitude and hip muscle parameters of the extensor group. Sensitivity is highlighted based on correlation coefficient strength. Weakly Sensitive: *r*=0.2-0.4 (green); Moderately Sensitive: *r*=0.4-0.6 (yellow); Highly Sensitive: *r*=0.6-1.0 (red).

	Add_mag1	Add_mag2	Add_mag3	glut_max2	glut_max3	gracilis	Quad Fem
Max Iso	0.0043 (0.0035)	0.0046 (0.0036)	0.0059 (0.0045)	0.0128 (0.0060)	0.0077 (0.0053)	0.0039 (0.0036)	0.0041 (0.0026)
Origin A/P	-0.0049 (0.0038)	-0.0038 (0.0031)	-0.0016 (0.0016)	-0.0017 (0.0043)	-0.0009 (0.0009)	-0.0009 (0.0011)	-0.0051 (0.0036)
Origin S/I	0.0028 (0.0025)	0.0020 (0.0015)	0.0004 (0.0005)	0.0109 (0.0062)	0.0010 (0.0015)	0.0002 (0.0017)	0.0045 (0.0030)
Origin M/L	0.0038 (0.0031)	0.0018 (0.0016)	0.0006 (0.0008)	0.0039 (0.0022)	0.0011 (0.0007)	0.0004 (0.0009)	0.0011 (0.0007)
Insert A/P	0.0022 (0.0021)	0.0014 (0.0008)	-0.0009 (0.0007)	0.0048 (0.0022)	0.0011 (0.0014)	-0.0001 (0.0007)	0.0008 (0.0011)
Insert S/I	-0.0057 (0.0041)	-0.0030 (0.0026)	-0.0012 (0.0007)	-0.0089 (0.0045)	-0.0013 (0.0019)	0.0003 (0.0019)	-0.0057 (0.0035)
Insert M/L	-0.0028 (0.0022)	-0.0016 (0.0021)	-0.0013 (0.0017)	-0.0007 (0.0024)	-0.0009 (0.0014)	-0.0004 (0.0003)	-0.0009 (0.0016)
Fiber L	0.0017 (0.0012)	0.0017 (0.0012)	0.0001 (0.0004)	0.0044 (0.0019)	-0.0001 (0.0001)	0.0000 (0.0003)	0.0001 (0.0002)

Table 6.6: Average correlation coefficient (SD) across five patients between hip joint contact force magnitude and hip muscle parameters of the flexor group. Sensitivity is highlighted based on correlation coefficient strength. Weakly Sensitive: *r*=0.2-0.4 (green); Moderately Sensitive: *r*=0.4-0.6 (yellow); Highly Sensitive: *r*=0.6-1.0 (red).

	Add_Long	Iliacus	Pect	psoas	rect_fem	sar
Max Iso	0.29 (0.00)	0.64 (0.02)	0.16 (0.05)	0.59 (0.03)	0.39 (0.01)	0.02 (0.01)
Origin A/P	-0.08 (0.03)	-0.17 (0.07)	0.00 (0.03)	-0.14 (0.03)	-0.26 (0.02)	-0.03 (0.03)
Origin S/I	0.20 (0.05)	0.32 (0.04)	0.13 (0.03)	0.41 (0.04)	0.38 (0.04)	0.01 (0.03)
Origin M/L	0.06 (0.04)	0.03 (0.04)	0.05 (0.05)	0.14 (0.02)	0.02 (0.02)	0.03 (0.02)
Insert A/P	-0.09 (0.03)	-0.31 (0.04)	-0.07 (0.06)	-0.36 (0.03)	-0.01 (0.01)	-0.01 (0.04)
Insert S/I	-0.19 (0.04)	-0.10 (0.04)	-0.13 (0.02)	-0.14 (0.04)	-0.01 (0.02)	-0.03 (0.01)
Insert M/L	-0.09 (0.03)	-0.11 (0.04)	-0.07 (0.03)	-0.09 (0.02)	0.00 (0.03)	-0.03 (0.02)
Fiber L	0.32 (0.05)	0.33 (0.02)	0.17 (0.02)	0.45 (0.04)	0.71 (0.03)	0.02 (0.03)

Table 6.7: Average change in hip contact force in BW (SD) for one standard deviation change in input parameter across five patients between hip joint contact force magnitude and hip muscle parameters of the flexor group. Sensitivity is highlighted based on correlation coefficient strength. Weakly Sensitive: *r*=0.2-0.4 (green); Moderately Sensitive: *r*=0.4-0.6 (yellow); Highly Sensitive: *r*=0.6-1.0 (red).

	Add_Long	Iliacus	Pect	psoas	rect_fem	sar
Max Iso	0.0176 (0.0044)	0.0389 (0.0096)	0.0106 (0.0029)	0.0365 (0.0070)	0.0280 (0.0067)	0.0016 (0.0012)
Origin A/P	-0.0104 (0.0041)	-0.0203 (0.0055)	-0.0001 (0.0027)	-0.0171 (0.0021)	-0.0333 (0.0078)	-0.0042 (0.0051)
Origin S/I	0.0253 (0.0029)	0.0425 (0.0143)	0.0171 (0.0050)	0.0539 (0.0185)	0.0482 (0.0087)	0.0024 (0.0038)
Origin M/L	0.0078 (0.0048)	0.0038 (0.0034)	0.0057 (0.0042)	0.0179 (0.0058)	0.0030 (0.0030)	0.0039 (0.0019)
Insert A/P	-0.0111 (0.0043)	-0.0405 (0.0125)	-0.0081 (0.0064)	-0.0484 (0.0171)	-0.0005 (0.0017)	-0.0009 (0.0053)
Insert S/I	-0.0252 (0.0109)	-0.0135 (0.0075)	-0.0173 (0.0052)	-0.0194 (0.0090)	-0.0019 (0.0027)	-0.0039 (0.0025)
Insert M/L	-0.0119 (0.0045)	-0.0146 (0.0068)	-0.0084 (0.0040)	-0.0121 (0.0043)	-0.0008 (0.0035)	-0.0038 (0.0026)
Fiber L	0.0179 (0.0062)	0.0187 (0.0055)	0.0095 (0.0027)	0.0249 (0.0071)	0.0401 (0.0092)	0.0011 (0.0018)

Table 6.8: Maximum isometric torque (N/kg) at each muscle group for all patients

Subject #	Quadriceps	Hamstrings	Flexors	Extensors	Pre-Abductors	Post-Abductors
1	1.40	0.43	0.91	0.33	0.81	0.55
2	1.70	0.76	0.73	0.78	0.96	1.10
3	1.08	0.42	0.86	0.73	0.85	0.80
4	2.69	1.09	1.70	0.77	1.56	1.76
5	1.42	0.50	0.78	1.04	0.61	0.65
Avg	1.66	0.64	1.00	0.73	0.96	0.97
SD	0.62	0.29	0.40	0.25	0.36	0.49

Table 6.9: Mean (SD) joint contact forces in body weight for ankle (A), knee (K), hip, (H) and low back (B) in anterior-posterior (x), vertical (y), and medial-lateral (z) components across 5 subjects. Included is the difference between the lower and upper (L/U) probability levels.

	Ax	Ay	Az	||A||	Kx	Ky	Kz	||K||	Hx	Hy	Hz	||H||	Bx	By	Bz	||B||
Baseline (pre-op)	-0.31 (.31)	-3.36 (.68)	-0.34 (.38)	3.64 (1.05)	0.21 (.77)	-3.42 (1.35)	-0.31 (.26)	3.51 (1.36)	0.03 (.50)	-3.30 (.34)	0.81 (.31)	3.43 (.38)	0.08 (.08)	1.56 (.60)	0.04 (.06)	1.56 (.60)
Lower (0.5%)	-0.33 (.31)	-3.25 (.67)	-0.30 (.33)	3.53 (.93)	0.22 (.71)	-2.65 (.92)	-0.22 (.19)	2.84 (.86)	0.19 (.35)	-2.61 (.37)	0.65 (.16)	2.80 (.45)	0.07 (.07)	1.51 (.65)	0.06 (.06)	1.51 (.65)
Upper (99.5%)	-0.35 (.31)	-3.28 (.67)	-0.31 (.33)	3.50 (.93)	0.19 (.69)	-2.76 (.82)	-0.24 (.19)	2.73 (.96)	0.16 (.35)	-2.71 (.44)	0.59 (.15)	2.70 (.40)	0.06 (.07)	1.46 (.66)	0.05 (.06)	1.46 (.66)
L/U Diff	0.02	0.03	0.01	0.04	0.03	0.10	0.02	0.11	0.04	0.10	0.05	0.10	0.01	0.05	0.01	0.05

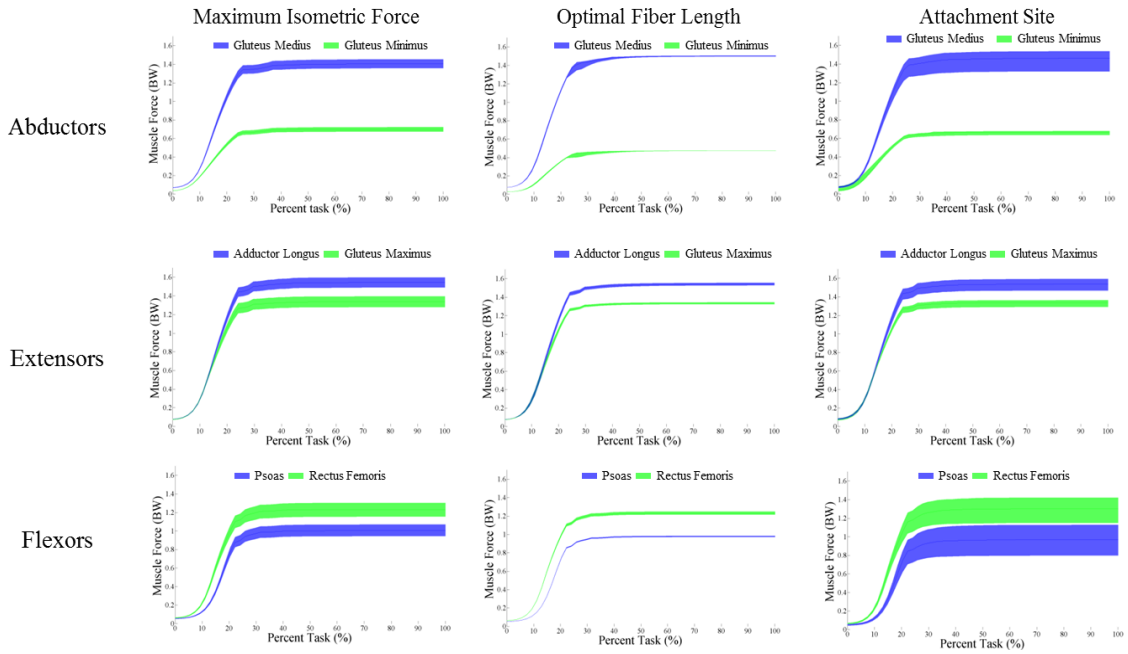

Figure 6.1: Representative muscle force outputs from each muscle group (abductors, extensors and flexors) from one patient. 5-95% confidence bounds are plotted for each source of uncertainty for two muscles in each group: the gluteus medius and gluteus minimus (abductors), adductor longus and gluteus maximus (extensors), and the psoas and

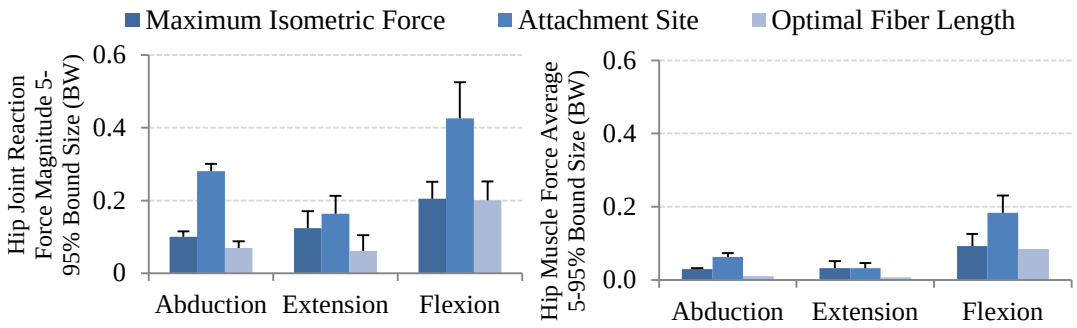

Figure 6.2: Average 5-95% confidence bounds for hip joint contact force (left) and muscle force (right) for each muscle group and uncertainty source.

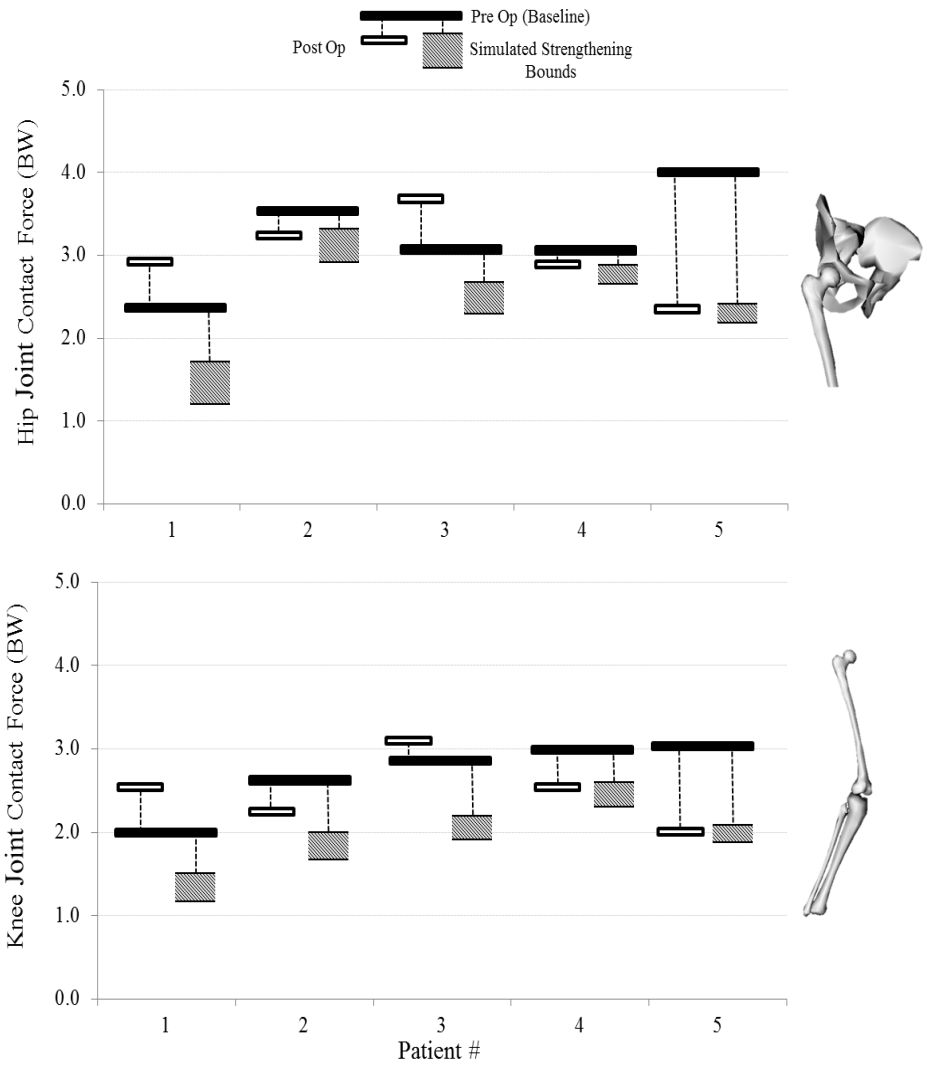

Figure 6.3: Hip and Knee joint contact forces (JCFs) during step down with preoperative (baseline) strength and with postoperative hip abductor strength. Shaded regions indicate the upper and lower bounds from simulated hip abductor strengthening. Reductions in JCF resulting from strengthening were greatest for the weaker patients (patients 1, 3, 5). Postoperatively, Patients that had increased hip abductor strength (2,4,5) demonstrated reduced hip JCFs that were within the upper and lower simulated strengthening bounds and reduced knee JCFs that were within the upper and lower strengthening bounds for two of the three subjects.

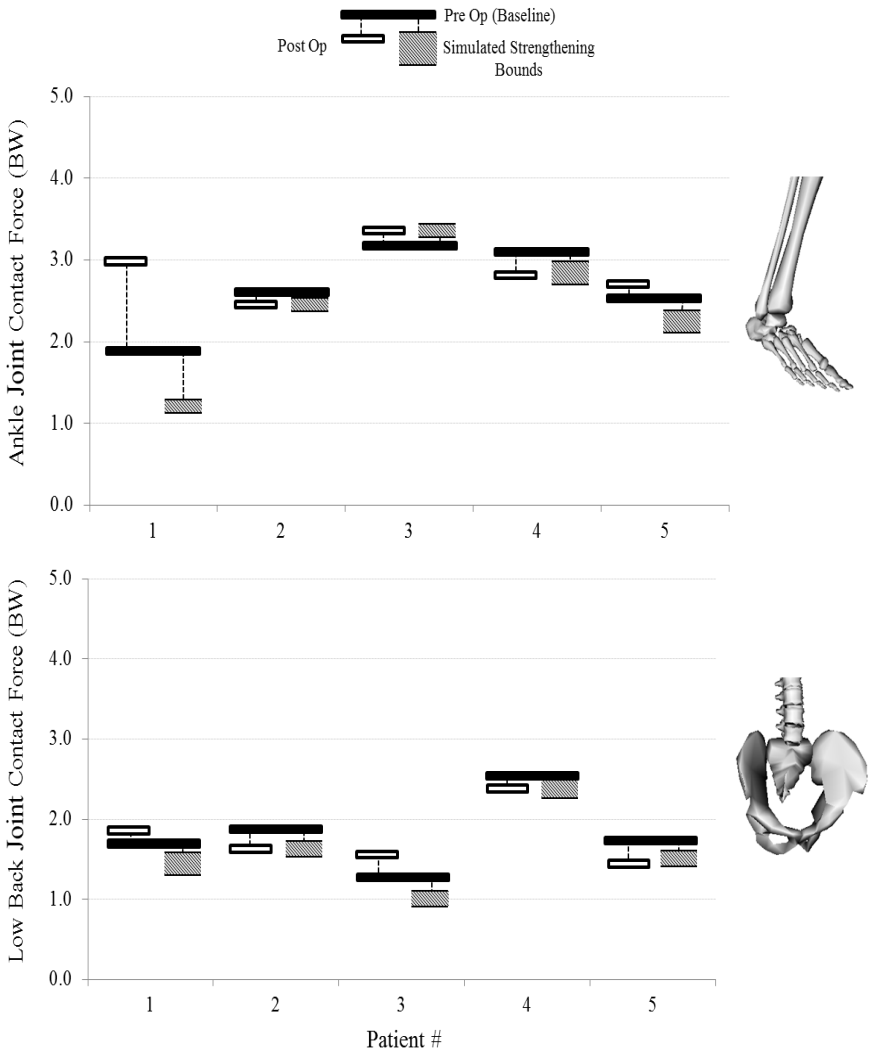

Figure 6.4: Ankle and low back joint contact forces (JCFs) during step down with preoperative (baseline) strength and with postoperative hip abductor strength. Shaded regions indicate the upper and lower bounds from simulated hip abductor strengthening. Reductions in JCF at the ankle and low back were smaller than at the hip and knee but were still apparent for four of the five subjects.

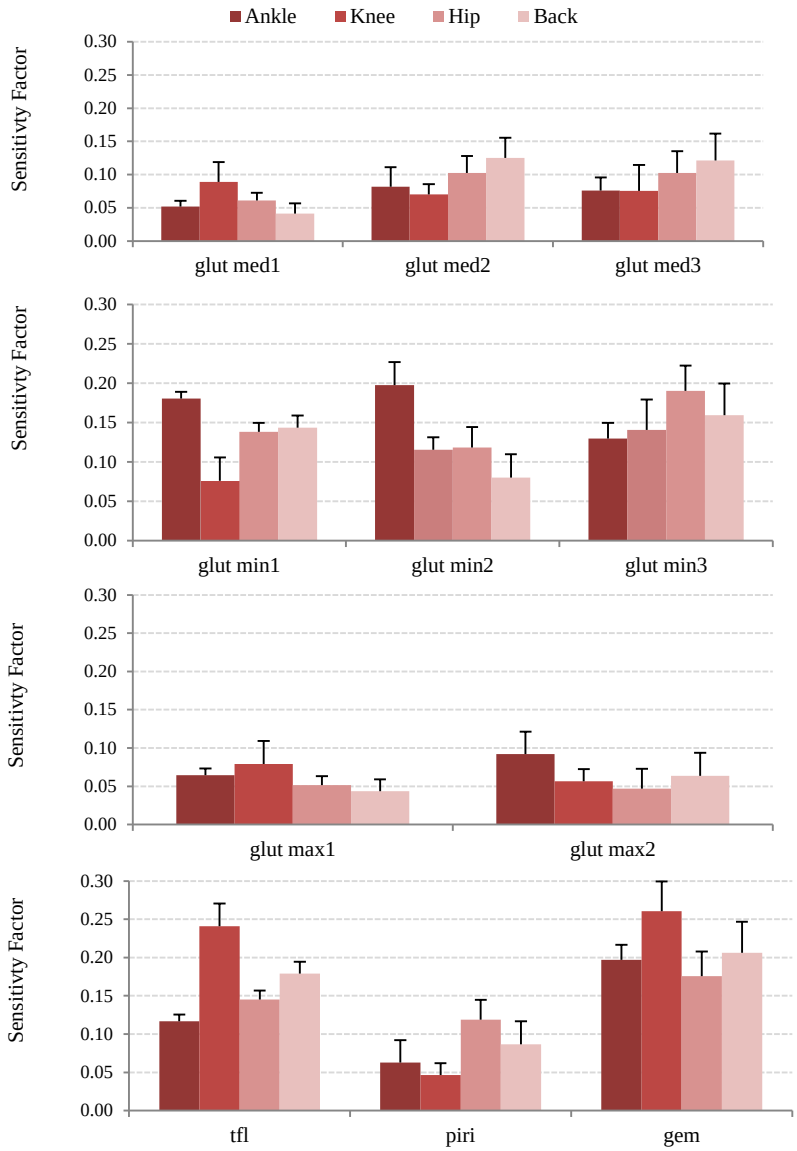

Figure 6.5: Sensitivity factors for hip abductor muscles with respect to ankle, knee, hip and low back joint contact forces.

CHAPTER 7 – POPULATION-BASED PROBABILISTIC MUSCULOSKELETAL MODELING

This chapter will present a feasibility study to address challenges to performing population-based musculoskeletal modeling through the development of a statistical model using principal component analysis. The chapter describes our approach in a specific application on a population of patients with total knee arthroplasty, and the expected outcomes and future work from the application of population-based probabilistic musculoskeletal modeling.

7.1: Introduction

Evidence-based practice, which is defined as "the use of mathematical estimates of the risk of benefit and harm, derived from high-quality research on population samples, to inform clinical decision-making... [regarding] individual patients" (Greenhalgh, 2010), is the standard for clinical decision-making within rehabilitation therapy. Rehabilitation clinicians develop patient-specific rehabilitation strategies from properly powered randomized clinical trials that compare treatments across a population. Therefore, outputs from musculoskeletal simulations that include muscle force and joint contact forces would be valuable in evidence-based practice for prescription of rehabilitation and movement retraining in patient populations following lower extremity joint surgery.

The effects of rehabilitation can be difficult to represent in musculoskeletal simulation studies because of high inherent inter-patient variability and widely varying treatment effects. Typical simulation studies are based on limited sample sizes on the order of 5-15 patients that attempt to extrapolate findings to draw conclusions for the population as a whole. Modeling populations in musculoskeletal simulation has not been prevalent within the musculoskeletal simulation community. Musculoskeletal modeling platforms are designed to create the most accurate patient-specific models possible and significant effort has been made to improve the anatomic detail of these models (Arnold et al., 2010; Ward et al., 2005). Provided the simulation is properly designed and parameterized, the results of a patient-specific simulation are applicable only to that particular patient from which the data are obtained. For example, Shull et al. (2013) demonstrated gait modifications that led to reduced knee adduction moments in 12 patient-specific models; however, it is unknown how well this subset represents the osteoarthritis patient population.

Generating the amount of patient-specific models necessary to represent a population is costly and not feasible. However, probabilistic tools that have been combined with musculoskeletal simulation (Myers et al., 2014; Valente et al., 2013) are capable of quantifying the influence of inter-patient variability in model input parameters on simulation outputs. The ability to realistically model treatment effects that include variable interactions and movement variability can improve the impact of musculoskeletal simulation on rehabilitation therapy (Figure 7.1).

Previous studies demonstrate that population-based variability in measures used in clinical decision making can be generated from smaller patient cohorts by combining

probabilistic methods with principal component analysis (PCA) (Bryan et al., 2009; Fitzpatrick et al., 2011b; Galloway et al., 2012). PCA has been used in population-based applications to create statistical models from training sets of 20-30 patients that quantify relationships between parameters and provide predictive capability between variables that are related. For example, PCA has been used to predict patellofemoral kinematics and contact pressures using patient geometry and kinematics (Fitzpatrick et al., 2011a). Additionally, tibiofemoral kinetics during gait have been successfully predicted with high accuracy in a population of patients with total knee arthroplasty (TKA) using PCA (Galloway et al., 2012). By repeatedly sampling from these models, unique new instances of the variables of interest can be generated that capture the inter-patient variability from the training data. Using the OpenSim probabilistic plugin, the combined probabilistic-PCA approach could be implemented to perform population-based study designs with musculoskeletal simulations

There are two key challenges to address in implementing the previously designed probabilistic tools in population-based musculoskeletal simulation studies. First, it is not known if the variables used in the generation of musculoskeletal simulations (*e.g.* anthropometry, kinematics, kinetics) are correlated to the extent that is necessary to establish an accurate predictive statistical model. Second, if a predictive model can be established, it is necessary to identify the level of accuracy that can be expected from using predicted variables as inputs into musculoskeletal simulation tools. Accordingly, the purpose of this study is to demonstrate the feasibility of population-based probabilistic musculoskeletal modeling by using PCA to build a statistical model of the

relationships between simple anthropometric variables, kinematic variables and variables collected from a force plate for a population of TKA patients performing a sit-to-stand task (STS) that can be used to predict new instances of kinematic and force plate variables not included in the model. An OpenSim simulation will be performed to determine the feasibility of using predicted values as inputs to simulations that calculate muscle force and joint reaction force.

7.2: Methods

Development and accuracy assessment was performed using three sequential stages: 1) Anthropometric, kinematic and force plate data from a sample of 28 TKA patients performing a STS task were collected and processed. 2) PCA was performed to establish a statistical model of the anthropometric, kinematic and force plate variables and the predictive ability of the model was assessed. 3) Predicted inputs and outputs were used in an OpenSim simulation of the STS task using static optimization to assess the accuracy of generating muscle force and joint contact force outputs.

7.2.1: Experimental Sit-to-Stand Task

Twenty-eight pre-operative TKA patients (mass: 80.9±15.6 Kg; height: 1.70±0.10 m; age: 67.3±8.4 yrs) performed a five time STS test as part of a larger investigation. Each patient provided written, informed consent and the study was approved by the Colorado Multiple Institutional Review Board. Data from these patients were collect by researchers at the Anschutz Medical Campus at the University of Colorado under the direction of Dr.

Cory Christensen and Dr. Jennifer Stevens-Lapsley and provided for further analysis in this dissertation.

The five time STS test is a test of dynamic balance (Whitney et al., 2005) and measures the time it takes to stand from and sit in a chair five times (Bohannon, 2006). Each patient was seated in a standard chair (height 46 cm) and instructed to transfer to a standing position and return to a sitting position five times. Participants were instructed not to use the arms of the chair. For the purposes of this study, the last of the five trials was used as a representative STS for each patient. Thirty-two reflective markers were used to define anatomical landmarks while an 8 motion camera motion capture system (Vicon, Centennial, CO) collected at 100 Hz. Patients placed each foot on a force plate collecting at 2000 Hz while performing the test.

OpenSim was used with the gait2392 model to calculate kinematics that included right and left ankle plantarflexion/dorsiflexion, knee flexion/extension, hip flexion/extension, abduction/adduction, internal/external rotation, lumbar flexion/extension, lateral bending, axial rotation as well as translations and rotations of the pelvis relative to the ground. Models were scaled to patient mass and height. Force plate data collected in the lab was transformed into the OpenSim global coordinate system and included: right and left ground reaction forces (GRFs); anterior-posterior (Fx) vertical (Fy), medial-lateral (Fz), center of pressure; anterior-posterior (Px) medial-lateral (Pz) and the free moment (Tz). All variables were time normalized to one hundred percent of the task. Force moment variables were normalized to body weight, with both normalized and un-normalized results presented.

7.2.2 Predictive Model Using Principal Component Analysis

A predictive statistical model was created by using PCA to establish the relationships between inputs of patient mass, height and kinematic variables and outputs of the force plate variables. PCA was carried out using methods described by Fitzpatrick et al., (2011b). In the presence of strong correlations between input and output variables, the model can be used to predict new instances of inputs and outputs not included in the training set. Each set of patient data was arranged in a 1x*n* vector with each anthropometric, kinematic and kinetic variable (*n*) and combined into an *N*x*n* training matrix for all subjects (*N*). An *N*x*n* matrix of correlation coefficients was calculated between the *n* variables. Eigenvectors and eigenvalues were solved for the correlation coefficient matrix. Principal component (PC) values were calculated as linear combinations of the variables from each subject, weighted according to the eigenvectors. PC values were mapped to their constituent variables, which consisted of both the inputs and outputs. A PC value for a set of variables can be divided into separate contributions from the input and output variables.

The ability of the PCA approach to predict ground reaction forces, moments and center of pressure was assessed using a leave-one-out approach. The number of PCs included in the predictive model was determined by how many are necessary to represent 95% of the variance in the model. A total of 28 repeated trials were run where the input and output variables for one subject were not included in the development of the model and were used as a validation set. The model, based on the remaining 27 subjects, was used to predict the kinematic variables of the validation set. Using the validation set and height, weight and kinematics as the inputs and force plate variables as the outputs,

kinematics, the ground reaction forces, moments and center of pressure were predicted. The root mean square (RMS) differences between validation set and predicted variables were calculated and averaged across the right and left side for each patient and then across all of the patients to calculate the prediction error.

7.2.3 Accuracy of Sit-to-Stand Simulation Using Predicted Inputs

A STS static optimization was then performed in OpenSim using the predicted kinematics with the predicted ground reaction forces, moment and center of pressure. The average residuals, which are non-physical forces and moments applied in each plane to the model that account for inconsistencies between experimental GRFs and joint accelerations estimated from experimental markers, were assessed to quantify how well the kinematics and kinetics agreed.

7.3: Results

Including 18 PCs represented 95.5% of the variation in the model and was used to predict kinematic and force plate variables**.**

7.3.1: Kinematic Variables

When predicting joint angles, the average RMS error for all variables was 2.25±0.23 deg. Average RMS error was lowest for lumbar bending (1.34±0.59 deg) and lumbar rotation (1.65±0.60) (Table 7.1) The kinematic and force plate data used in the creation of the predictive model represented a wide range in each variable, illustrating the

number of different ways the STS task was performed within the patient cohort (Figures 7.2&7.3).

The rotations and translations of the pelvis relative to the global coordinate system resulted in RMS error between actual and predicted that were 25.2% less that joint angle error for all variables (Table 7.2).

7.3.2: Force Plate Variables

Average RMS error for GRFs were greater in the vertical direction (0.074±0.035 BW) compared to anterior-posterior (0.017±0.011 BW) and medial-lateral (0.0090±0.0033 BW) (Table 7.3). Additionally, error was greater for center of pressure predictions in the anterior-posterior direction (3.37±1.74 cm) compared to medial-lateral (2.21±1.43 cm). Average RMS error in the free moment was 0.0058±0.0028 BW.

7.3.3: OpenSim Simulation from Model Predictions

After implementing the predicted kinematic variables and force plate variables in an OpenSim static optimization of the STS task, average force residuals for Fx, Fy and Fz were 26.5 N, 34.46 N and 7.88 N respectively. Average moment residuals for Mx, My, Mz were 6.40 Nm, 39.4 Nm, and 7.56 Nm.

7.4: Discussion

The statistical model of anthropometric, kinematic and force plate variables created in this study demonstrated the capability to predict STS kinematics and force plate variables

that can be used to generate a population of kinematic and force plate variables to be used in population-based OpenSim studies. Average RMS error between actual and predicted variables was less than 3.5 degrees for joint angle variables and less than 0.1 BW for all ground reaction force variables. The results of this feasibility study indicate that this model can be combined with probabilistic modeling to perform population-based assessments of inter-patient variability in anthropometric, kinematics, and force plate variables that represent movement strategies used during simple tasks of daily living in TKA patients. However, these data also indicate that model refinement will be necessary to use predicted kinematic and force plate variables as inputs into musculoskeletal modeling tools with confidence.

The average RMS error of predicted force plate variables generated from the model was below expected values based on a previous study that used a similar approach. Galloway et al., (2012) created a statistical model of tibiofemoral kinetic variables during that was capable of generating a population of new knee kinetic variables representative of a training data set. The median RMS error for knee force variables were 0.033 BW in anterior-posterior, 0.086 BW in the axial direction, and 0.008 BW in medial-lateral. These agree well with the average RMS error in ground reaction force components that we found for anterior-posterior (0.017 BW), vertical (0.074 BW) and medial-lateral (0.0090).

The size of the errors between validation set and predicted set kinematic and force plate variables provide confidence that this is a feasible approach to performing population-based musculoskeletal modeling. The model established between joint kinematics and force plate variables could be used in a population-based application to

characterize the movement strategies that are associated with detrimental asymmetric ground reaction force loading. For example, during the STS task, patients often preferentially weight the uninvolved limb and adopt a large range of hip motion, that may be indicative of poor overall function (Doorenbosch et al., 1994).

The model was marginally successful at predicting kinematic and force plate variables to a level of accuracy necessary for use as inputs in musculoskeletal modeling tools. The quality of an OpenSim simulation is based on the size of the residuals, or the non-physical forces and moments applied in each plane to the model that account for inconsistencies between experimental GRFs and joint accelerations estimated from experimental markers. The residuals from the predicted kinematics and force plate variables input into OpenSim were outside the range that is recommended for best practices (forces: less than 10 N; moments less than 30 Nm). However, the strong relationships identified between anthropometric, kinematic and force plates variables that were successful in generating an accurate predictive model provide confidence that similar models could be created with anthropometric and kinematic inputs and musculoskeletal simulation outputs of muscle force and joint contact force that are valuable to clinicians. This would require the generation of 20-30 accurate patient-specific models in simulations to use as a training set that would be costly but not unfeasible.

Improvements to the anthropometric, kinematic and force plate variable statistical model can be made that could improve its predictive ability. A training set that included a greater number of subjects would improve the predictive ability of the model. The kinematics were generated from a marker set that was not intended for use in

musculoskeletal simulation. A marker set that is designed for use with OpenSim could improve the quality of the kinematics generated from the inverse kinematic tool to include in the training set. Additionally, a marker set designed for use in musculoskeletal modeling would provide the opportunity to improve the scaling of the initial models used to generate kinematics and further improve the quality of kinematic data.

Proposed future work is to combine the statistical model developed in this chapter with the previously described probabilistic tool to investigate the impact of variability in hip strategy on joint loading at the knee, hip and spine. Variability in the hip angle profile that is based on the range that was observed in the training set will be applied to the statistical model to fully characterize the range of potential hip angle strategies and repeatedly output the corresponding kinematic and force plate variables. These will then be used as inputs to OpenSim in order to calculate the joint loads at the knee, hip and spine. Confidence bounds and sensitivity factors will then be calculated on the range of potential joint loads based on variability in hip angle strategy. Additionally, this method will quantify the interactions between the hip angle strategy and the other kinematic variables as well as the loading variables. Results from this proposed study can be directly applied in the mathematical estimates generated during evidence-based practice of the risk of benefit and harm used in clinical decision making of rehabilitation and movement retraining in patient populations following lower extremity joint surgery.

7.5 Conclusion

This study demonstrated the feasibility of performing population-based musculoskeletal modeling that would use principal component analysis combined with probabilistic methods. Population-based musculoskeletal modeling studies will improve the interpretation of findings from patient-specific analyses and offer high impact to clinicians who compare treatments across a population when designing rehabilitation protocol.

Table 7.1: Average and standard deviation of RMS errors of each joint angle kinematic variable (deg)

	Hip Flex/Ext	Hip Add/Abd	Hip Int/Ext	Knee Angle	Ankle Angle	Lumbar Flex/Ext	Lumbar Bending	Lumbar Rotation
Average	3.49	1.77	2.16	3.37	1.69	2.52	1.34	1.65
SD	1.22	0.73	0.91	0.96	0.60	1.03	0.59	0.60

Table 7.2: Average and standard deviation of RMS error between actual and predicted pelvic rotations and translations in all three planes about the global coordinate system

	Pelvis Rx (deg)	Pelvis Ry (deg)	Pelvis Rz (deg)	Pelvis dx (cm)	Pelvis dy (cm)	Pelvis dz (cm)
Average	2.82	1.15	1.41	1.81	2.13	0.76
SD	1.14	0.46	1.05	1.07	1.11	0.37

Table 7.3: Average (±SD) root mean square error between actual and predicted ground reaction forces in both body weight and Newtons

	Fx	Fy	Fz
Body Weight (BW)	0.017 (0.011)	0.074 (0.035)	0.0090 (0.0033)
Newtons (N)	13.2 (9.0)	57.5 (27.0)	7.0 (2.5)

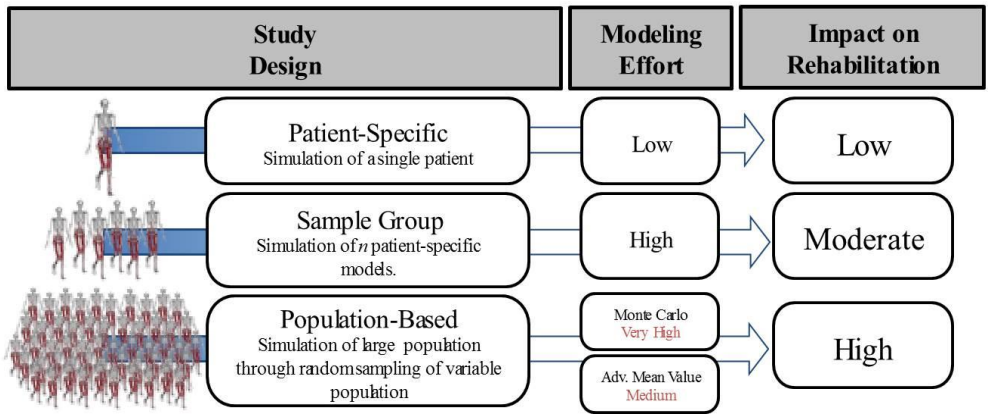

Figure 7.1: The modeling effort and impact on rehabilitation for different simulation study designs.

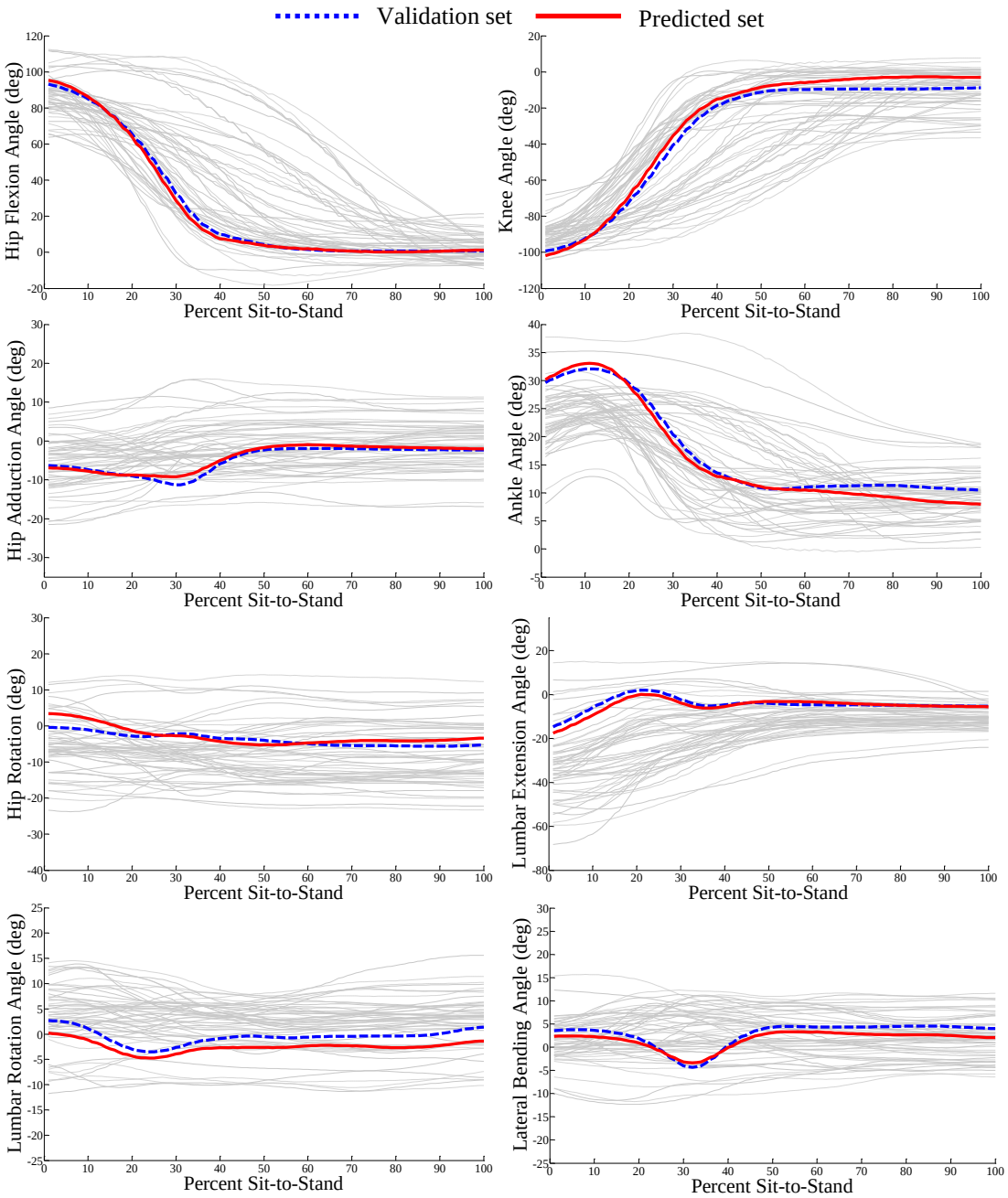

Figure 7.2: Comparison between validation set and predicted set joint angles shown for a representative patient with errors close to the average RMS error. Actual and predicted data for the other patients in the population on shown in grey.

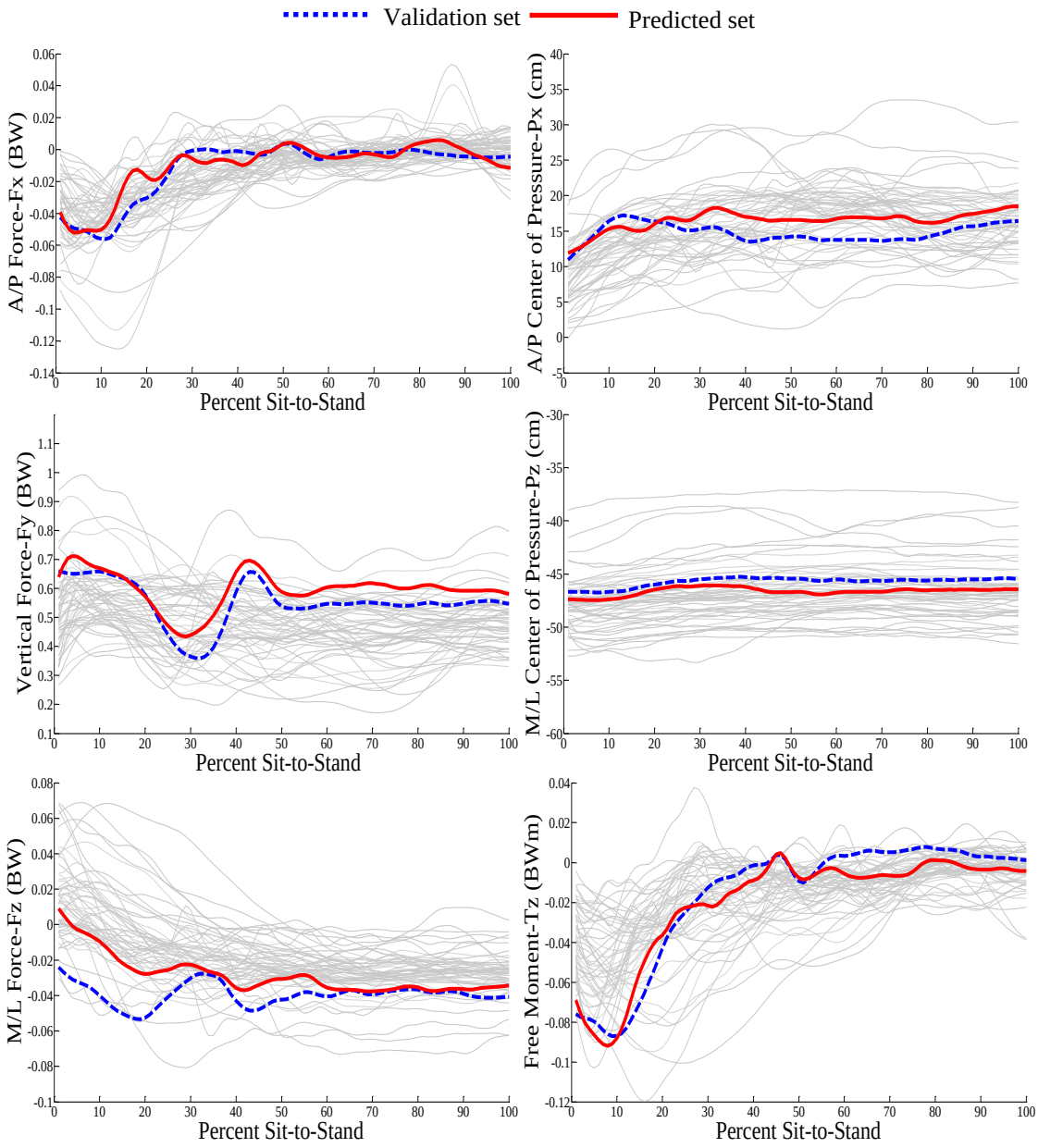

Figure 7.3: Comparison between validation set and predicted set right foot ground reaction forces (Fx, Fy, Fz), free moment (Tz) and center of pressure (Px,Pz) shown for a representative patient with errors close to the average RMS error. Actual and predicted data for the other patients in the population on shown in grey.

CHAPTER 8 – SUMMARY AND CONCLUSIONS

The studies presented in this dissertation represent a progression of work to analyze the interdependencies of the knee, hip, and spine using probabilistic musculoskeletal modeling. An initial experimental investigation provided biomechanical support for how an intervention applied to the hip abductor muscle group is capable of altering function of joints both inferior to the pelvis and superior to the pelvis during dynamics tasks. In order to address knee, hip, and spine regional interdependence using musculoskeletal modeling and to provide an innovative tool to the modeling community, a probabilistic plugin was designed and developed to interface with OpenSim and implement the probabilistic methods of Monte Carlo and advanced mean value. The four studies that were performed with the use of the probabilistic plugin improve the ability to translate outputs from musculoskeletal models to rehabilitation practice, demonstrate application of the plugin in rehabilitation strategies following total joint replacement and provide a foundation for future investigations that implement probabilistic musculoskeletal methods.

An original contribution from this dissertation was the creation of the open-source probabilistic plugin for OpenSim. The probabilistic plugin functions with any of the OpenSim tools (*e.g.* Inverse Dynamics, Static Optimization, etc.) and provides a graphical user interface to guide users through the setup of probabilistic analyses and generate visualizations of results for interpretation. A user manual with tutorial examples

was created (Appendix) and the tool was made available to OpenSim users (simtk.org/prob_tool). This plugin was used as the key design component to accomplish the objectives this dissertation. With the ability to efficiently implement probabilistic methods in musculoskeletal modeling, researchers and clinicians will better understand the strengths and limitations of their musculoskeletal simulations and more effectively use simulations to in complex study designs to inform clinical decisions.

In a novel study design in Chapter 5, propagation of uncertainty was performed by using the output distributions from one stage of the simulation as input distributions to subsequent stages and calculating confidence bounds and sensitivity factors for common simulation inputs. An important initial step in translating the outputs from musculoskeletal simulations into rehabilitation applications involving knee, hip, and spine regional interdependence was to demonstrate how understanding and reporting the output confidence and sensitivity of outputs to a range of known possible inputs can provide clinicians with valuable metrics for use in clinical decision making. This was done by quantifying the impact of input uncertainty propagation in a simulation of gait. The results of this study demonstrated how an uncertainty source such as, movement artifact that is used in the calculation of joint kinematics, can propagate into the final simulation stage of muscle force optimization. Additionally, high sensitivity to muscle parameters illustrated the importance of using experimental data in model scaling to reduce the impact of uncertainty and best represent patient characteristics.

When applying probabilistic methods in the analyses of a cohort of patients with THA, the conclusions from the initial probabilistic investigation were used to make key

improvements in modeling methodology beginning in the first study of Chapter 6. A two-stage patient-specific approach was designed where the first stage scaled patient-specific muscle strength parameters to minimize differences between model-predicted joint torques and joint torques collected from individual patients with THA during maximal isometric hip flexion, extension and abduction tasks. The second stage simulated uncertainty in the muscle model parameters to generate the range of possible outputs for muscle force and joint contact force when patient-specific strength parameters were used. This patient-specific approach provides the ability to capture post-operative strength adaptions to generate realistic hip loading conditions that consider input uncertainty. Outputs from this approach are useful in combination with finite element analysis to inform implant design, surgical approach and rehabilitation strategy.

The probabilistic plugin was further applied to the THA patient cohort in the second study of Chapter 6 on the role of hip abductor muscle strength in knee, hip and spine regional interdependence. This represents the first study to quantify the clinical concept of regional interdependence using musculoskeletal modeling. The patient-specific models of the cohort of patients with THA were used in a probabilistic analysis that systematically increased the strength of the hip abductor muscle group and calculate the effect on lower extremity joint loads and loads at the low back during a step down task. Simulated hip abductor strengthening produced reductions in joint contact force when muscle demand was high at the hip joint as well as at the knee and low back. Strengthened hip muscles can account for a greater percentage of contact loads compared to weakened muscles and redirect those loads, providing evidence for the dynamic and

mechanical interdependencies of the knee, hip and spine. These interdependencies can be targeted in early THA rehabilitation to establish a link between reduced contact loads at the knee, hip and spine and higher overall patient function.

In order to increase the impact of using outputs from musculoskeletal modeling to inform rehabilitation practice compared to what is possible from a patient-specific approach; the feasibility of performing population-based musculoskeletal modeling was demonstrated in Chapter 7. The study was performed on a population of patients with total knee arthroplasty performing a sit-to-stand task where a wide range of movement strategies are used. A predictive statistical model was created by using principal component analysis to establish the relationships between inputs of patient mass, height and kinematic variables and outputs of the force plate variables. The model demonstrated the capability to predict sit-to-stand kinematics and force plate variables that can be used to generate a population of kinematic and force plate variables for population-based OpenSim studies. By shifting away from a purely patient-specific approach, population-based musculoskeletal modeling studies can offer high impact to clinicians who compare treatments across a population when designing rehabilitation protocol.

In summary, the use of the probabilistic plugin designed and developed in this dissertation represents advancement in how outputs from musculoskeletal simulations can be applied to rehabilitation practices. The plugin was used in studies to further our understanding of knee, hip, and spine regional interdependence. Future investigations should continue to adapt the probabilistic plugin to address the broad range of questions impacting rehabilitation practice. Additionally, population-based musculoskeletal

modeling that was determined to be feasible in this dissertation represents a shift in how musculoskeletal modeling can be used to impact rehabilitation. The methods used to establish a predictive statistical model using variables present in musculoskeletal simulations should be applied to include the influence of movement strategy variability in assessments of rehabilitation effects to provide clinicians with a complete assessment of treatment protocols.

LIST OF REFERENCES

Ackland, D.C., Lin, Y.C., Pandy, M.G., 2012. Sensitivity of model predictions of muscle function to changes in moment arms and muscle-tendon properties: a Monte-Carlo analysis. J. Biomech. 45, 1463–71.

Aminaka, N., Pietrosimone, B.G., Armstrong, C.W., Meszaros, A., Gribble, P.A., 2011. Gluteal muscle activation during running in females with and without patellofemoral pain syndrome. J. Electromyogr. Kinesiol. 21, 645–51.

Anderson, F.C., Goldberg, S.R., Pandy, M.G., Delp, S.L., 2004. Contributions of muscle forces and toe-off kinematics to peak knee flexion during the swing phase of normal gait: an induced position analysis. J. Biomech. 37, 731–7.

Anderson, F.C., Pandy, M.G., 2001. Static and dynamic optimization solutions for gait are practically equivalent. J. Biomech. 34, 153–61.

Andrews, J.G., Misht, S.P., 1996. Methods for investigating the sensitivity of joint resultants to body segment parameter variations. J. Biomech. 29, 651–654.

Aramaki, Y., Nozaki, D., Masani, K., Sato, T., Nakazawa, K., Yano, H., 2001. Reciprocal angular acceleration of the ankle and hip joints during quiet standing in humans. Exp. Brain Res. 136, 463–73.

Arnold, E.M., Ward, S.R., Lieber, R.L., Delp, S.L., 2010a. A model of the lower limb for analysis of human movement. Ann. Biomed. Eng. 38, 269–79.

Arnold, E.M., Ward, S.R., Lieber, R.L., Delp, S.L., 2010b. A model of the lower limb for analysis of human movement. Ann. Biomed. Eng. 38, 269–79.

Barton, C.J., Lack, S., Malliaras, P., Morrissey, D., 2013. Gluteal muscle activity and patellofemoral pain syndrome: a systematic review. Br. J. Sports Med. 47, 207–14.

Beckman, S.M., Buchanan, T.S., 1995. Ankle inversion injury and hypermobility: effect on hip and ankle muscle electromyography onset latency. Arch. Phys. Med. Rehabil. 76, 1138–43.

Ben-galim, P., Ben-galim, T., Rand, N., Haim, A., Hipp, J., Dekel, S., Floman, Y., 2007. Hip-Spine Syndrome The Effect of Total Hip Replacement Surgery on Low Back Pain in. Spine (Phila. Pa. 1976). 32, 2099–2102.

Benoit, D.L., Ramsey, D.K., Lamontagne, M., Xu, L., Wretenberg, P., Renström, P., 2006. Effect of skin movement artifact on knee kinematics during gait and cutting motions measured in vivo. Gait Posture 24, 152–64.

Beynnon, B.D., Renström, P.A., Alosa, D.M., Baumhauer, J.F., Vacek, P.M., 2001. Ankle ligament injury risk factors: a prospective study of college athletes. J. Orthop. Res. 19, 213–20.

Blond, L., Hansen, L., 1998. Patellofemoral pain syndrome in athletes: a 5.7-year retrospective follow-up study of 250 athletes. Acta Orthop Belg 64, 393–400.

Bogduk, N., 2000. What's in a name? The labelling of back pain. Med. J. Austrailia 173, 400–410.

Bohannon, R.W., 2006. Reference values for the five-repetition sit-to-stand test: a descriptive meta-analysis o f data from elders. Percept. Mot. Skills 103, 215–222.

Bolgla, L.A., Uhl, T.L., 2005. Electromyographic analysis of hip rehabilitation exercises in a group of healthy subjects. J. Orthop. Sports Phys. Ther. 35, 487–494.

Boyle, J.K., Anthony, I.C., Jones, B.G., Wheelwright, E.F., Blyth, M.J.G., 2014. Influence of low back pain on total knee arthroplasty outcome. Knee 21, 410–4.

Brindle, T.J., Mattacola, C., McCrory, J., 2003. Electromyographic changes in the gluteus medius during stair ascent and descent in subjects with anterior knee pain. Knee surgery, Sport. Traumatol. Arthrosc. 11, 244–51.

Bryan, R., Nair, P.B., Taylor, M., 2009. Use of a statistical model of the whole femur in a large scale, multi-model study of femoral neck fracture risk. J. Biomech. 42, 2171–6.

Chandler, R.F., Clauser, C.E., McConville, J.T., Reynolds, H.M., Young, J.W., 1975. Investigation of inertial properties of the human body, AMRL-TR-74. Ohio.

Chaudhari, A.M.W., Jamison, S.T., McNally, M.P., Pan, X., Schmitt, L.C., 2014. Hip adductor activations during run-to-cut manoeuvres in compression shorts: implications for return to sport after groin injury. J. Sports Sci. 32, 1333–40.

Chiari, L., Della Croce, U., Leardini, A., Cappozzo, A., 2005. Human movement analysis using stereophotogrammetry. Part 2: instrumental errors. Gait Posture 21, 197–211.

Cibulka, M.T., 1999. Low back pain and its relation to the hip and foot. J. Orthop. Sports Phys. Ther. 29, 595–601.

Cibulka, M.T., Delitto, A., 1993. Comparison of Two Different Methods to Treat Hip Pain in Runners. J. Orthop. Sports Phys. Ther. 17.

Cliborne, A. V, Rhon, D.I., Judd, C.D., Fee, T.T., 2004. Clinical Hip Tests and a Functional Squat Test in Patients With Knee Osteoarthritis : Reliability , Prevalence of Positive Test Findings , and Short-Term Response to Hip. J. Orthop. Sports Phys. Ther. 34, 676–685.

Correa, T. a, Crossley, K.M., Kim, H.J., Pandy, M.G., 2010. Contributions of individual muscles to hip joint contact force in normal walking. J. Biomech. 43, 1618–22.

Cowan, S.M., Crossley, K.M., Bennell, K.L., 2009. Altered hip and trunk muscle function in individuals with patellofemoral pain. Br. J. Sports Med. 43, 584–8.

Cristofolini, L., Viceconti, M., Toni, A., Giunti, A., 1995. Influence of Thigh muscles on the axial strains in the proximal femur during early stance in gait. J. Biomech. 28, 617–624.

Crossley, K.M., Dorn, T.W., Ozturk, H., van den Noort, J., Schache, A.G., Pandy, M.G., 2012. Altered hip muscle forces during gait in people with patellofemoral osteoarthritis. Osteoarthr. Cartil. 20, 1243–9.

Curran-Everett, D., 2009. Explorations in statistics: confidence intervals. Adv. Physiol. Educ. 33, 87–90.

Currier, L.L., Froehlich, P.J., Carow, S.D., McAndrew, R.K., Cliborne, A. V, Boyles, R.E., Mansfield, L.T., Wainner, R.S., 2007. Development of a clinical prediction rule to identify patients with knee pain and clinical evidence of knee osteoarthritis who demonstrate a favorable short-term response to hip mobilization. Phys. Ther. 87, 1106–19.

De Groote, F., Van Campen, A., Jonkers, I., De Schutter, J., 2010. Sensitivity of dynamic simulations of gait and dynamometer experiments to hill muscle model parameters of knee flexors and extensors. J. Biomech. 43, 1876–83.

Della Croce, U., Cappozzo, A., Kerrigan, D., 1999. Pelvis and lower limb anatomical landmark calibration precision and its propagation to bone geometry and joint angles. Med. Biol. Eng. Comput. 37, 155–161.

Delp, S.L., Anderson, F.C., Arnold, A.S., Loan, P., Habib, A., John, C.T., Guendelman, E., Thelen, D.G., 2007. OpenSim: Open-source software to create and analyze dynamic simulations of movement. IEEE Trans. Biomed. Eng. 54, 1940–1950.

Delp, S.L., Arnold, A.S., Piazza, S.J., 1998. Graphics-based modeling and analysis of gait abnormalities. Biomed. Mater. Eng. 8, 227–40.

Delp, S.L., Arnold, A.S., Speers, R.A., Moore, C.A., 1996. Hamstrings and Psoas lengths during normal and crouch gait: implications for muscle-tendon surgery. J. Orthop. Res. 14, 144–151.

Delp, S.L., Hess, W.E., Hungerford, D.S., Jones, L.C., 1999. Variation of rotation moment arms with hip flexion. J. Biomech. 32, 493–501.

Delp, S.L., Loan, J.P., Hoy, M.G., Zajac, F.E., Topp, E.L., Rosen, J.M., 1990. An interactive graphics-based model of the lower extremity to study orthopaedic surgical procedures. IEEE Trans. Biomed. Eng. 37, 757–67.

Dempster, W.E., 1955. Space requirements of the seated operator. WADC-TR-55-159. Wright Air Development, Ohio.

DeWal, H., Maurer, S.L., Tsai, P., Su, E., Hiebert, R., Di Cesare, P.E., 2004. Efficacy of abduction bracing in the management of total hip arthroplasty dislocation. J. Arthroplasty 19, 733–738.

Deyle, G.D., Allison, S.C., Matekel, R.L., Ryder, M.G., Stang, J.M., Gohdes, D.D., Hutton, J.P., Henderson, N.E., Matthew, B., 2005. Research Report Effectiveness for Osteoarthritis of the Knee : A Randomized Comparison of Supervised Clinical Exercise and Manual Therapy Procedures Versus a. Phys. Ther. 85, 1301–1317.

Deyle, G.D., Henderson, N.E., Matekel, R.L., Ryder, M.G., Garber, M., Allison, S., 2000. Effectiveness of Manual Physical Therapy and Exercise in Osteoarthritis of the Knee. Ann. Intern. Med. 132, 173–181.

Di Monaco, M., Vallero, F., Tappero, R., Cavanna, A., 2009. Rehabilitation after total hip arthroplasty: a systematic review of controlled trials on physical exercise programs. Eur. J. Phys. Rehabil. Med. 45, 303–317.

Doorenbosch, C.A.M., Harlaar, J., Roebroeck, M.E., Lankhorst, G.J., 1994. Two strategies of transferring from sit-to-stand; the activation of monoarticular and biarticular muscles. J. Biomech. 27, 1299–307.

Dorn, T.W., Schache, A.G., Pandy, M.G., 2012. Muscular strategy shift in human running: dependence of running speed on hip and ankle muscle performance. J. Exp. Biol. 215, 1944–56.

Ellison, J.B., Rose, S.J., Shirley, A., 1990. Patterns of Hip Rotation Range of Motion : A comparison Between ~ e a l t h Subjects Patients with Low Back Pain. Phys. Ther. 70, 537–541.

Esola, M., McClure, P., Fitzgerald, G., Siegler, S., 1996. Analysis of lumbar spine and hip motion during forward bending in subjects with and with a history of low back pain. Spine (Phila. Pa. 1976). 21, 71–78.

Ferber, R., Noehren, B., Hamill, J., Davis, I., 2010. Competitive female runners with a history of iliotibial band syndrome demonstrate atypical hip and knee kinematics. J. Orthop. Sports Phys. Ther. 40, 52–58.

Fernandez, J.W., Akbarshahi, M., Crossley, K.M., Shelburne, K.B., Pandy, M.G., 2011. Model predictions of increased knee joint loading in regions of thinner articular cartilage after patellar tendon adhesion. J. Orthop. Res. 29, 1168–77.

Fitzpatrick, C.K., Baldwin, M. a, Laz, P.J., FitzPatrick, D.P., Lerner, A.L., Rullkoetter, P.J., 2011a. Development of a statistical shape model of the patellofemoral joint for investigating relationships between shape and function. J. Biomech. 44, 2446–52.

Fitzpatrick, C.K., Baldwin, M. a, Rullkoetter, P.J., Laz, P.J., 2011b. Combined probabilistic and principal component analysis approach for multivariate sensitivity evaluation and application to implanted patellofemoral mechanics. J. Biomech. 44, 13–21.

Fitzpatrick, C.K., Baldwin, M.A., Clary, C.W., Wright, A., Laz, P.J., Rullkoetter, P.J., 2012a. Identifying alignment parameters affecting implanted patellofemoral mechanics. J. Orthop. Res. 30, 1167–75.

Fitzpatrick, C.K., Clary, C.W., Laz, P.J., Rullkoetter, P.J., 2012b. Relative contributions of design, alignment, and loading variability in knee replacement mechanics. J. Orthop. Res. 30, 2015–24.

Fitzpatrick, C.K., Clary, C.W., Rullkoetter, P.J., 2012c. The role of patient, surgical, and implant design variation in total knee replacement performance. J. Biomech. 45, 2092–102.

Fregly, B.J., Besier, T.F., Lloyd, D.G., Delp, S.L., Banks, S.A., Pandy, M.G., D'Lima, D.D., 2012. Grand challenge competition to predict in vivo knee loads. J. Orthop. Res. 30, 503–13.

Fregly, B.J., Reinbolt, J.A., Rooney, K.L., Mitchell, K.H., Chmielewski, T.L., 2007. Design of patient-specific gait modifications for knee osteoarthritis rehabilitation. IEEE Trans. Biomed. Eng. 54, 1687–95.

Friederich, J.A., Brand, R.A., 1990. Muscle fiber architecture in the human lower limb. J. Biomech. 23, 91–95.

Galloway, F., Worsley, P., Stokes, M., Nair, P., Taylor, M., 2012. Development of a statistical model of knee kinetics for applications in pre-clinical testing. J. Biomech. 45, 191–5.

Gao, B., Zheng, N.N., 2008. Investigation of soft tissue movement during level walking: translations and rotations of skin markers. J. Biomech. 41, 3189–95.

Garner, B.A., Pandy, M.G., 2003. Estimation of Musculotendon Properties in the Human Upper Limb. Ann. Biomed. Eng. 31, 207–220.

Goehler, C.M., Murray, W.M., 2010. The sensitivity of endpoint forces produced by the extrinsic muscles of the thumb to posture. J. Biomech. 43, 1553–9.

Gore, D., Murray, M., Sepic, S., Gardner, G., 1982. Anterolateral compared to posterior approach in total hip arthroplasty: differences in component positioning, hip strength, and hip motion. Clin. Orthop. Relat. Res. 165, 180–187.

Greenhalgh, T., 2010. How to Read a Paper: The basics of Evidence-Based Medicine. Wiley-Blackwell.

Grimaldi, A., Richardson, C., Stanton, W., Durbridge, G., Donnelly, W., Hides, J., 2009. The association between degenerative hip joint pathology and size of the gluteus medius, gluteus minimus and piriformis muscles. Man. Ther. 14, 605–10.

Halder, A., Mahadevan, S., 2000. Probability, Reliability and Statistical Methods in Engineering Design. John Wiley & Sons, Inc., New York, NY.

Hamby, D.M., 1994a. A review of the techniques for parameter sensitivity analysis of environmental models. Environ. Monit. Assess. 32, 135–154.

Hamby, D.M., 1994b. A review of techniques for parameter sensitivity analysis of environmental models. Environ. Monit. Assess. 32, 135–54.

Hashemi, J., Breighner, R., Jang, T.-H., Chandrashekar, N., Ekwaro-Osire, S., Slauterbeck, J.R., 2010. Increasing pre-activation of the quadriceps muscle protects the anterior cruciate ligament during the landing phase of a jump: an in vitro simulation. Knee 17, 235–41.

Heller, M.O., Bergmann, G., Kassi, J.-P., Claes, L., Haas, N.P., Duda, G.N., 2005. Determination of muscle loading at the hip joint for use in pre-clinical testing. J. Biomech. 38, 1155–63.

Herzog, W., Guimaraes, A.C., Anton, M.G., Carter-Erdman, K.A., 1991. Moment-length relations of rectus femoris muscles of speed skaters/cyclists and runners. Med. Sci. Sport. Exerc. 23, 1289–96.

Hodges, P.W., Richardson, C.A., 1997. Contraction of the abdominal muscles associated with movement of the lower limb. Phys. Ther. 77, 132–142.

Hoy, M.G., Zajac, F.E., Gordon, M.E., 1990. A musculoskeletal model of the human lower extremity: the effect of muscle, tendon, and moment arm on the moment-angle relationship of musculotendon actuators at the hip, knee, and ankle. J. Biomech. 23, 157–69.

Jo, H.J., Song, A.Y., Lee, K.J., Lee, D.C., Kim, Y.H., Sung, P.S., 2011. A kinematic analysis of relative stability of the lower extremities between subjects with and without chronic low back pain. Eur. spine J. 20, 1297–303.

Judd, D.L., Dennis, D. a, Thomas, A.C., Wolfe, P., Dayton, M.R., Stevens-Lapsley, J.E., 2014. Muscle strength and functional recovery during the first year after THA. Clin. Orthop. Relat. Res. 472, 654–64.

Kelly, B.T., Bedi, A., Robertson, C.M., Dela Torre, K., Giveans, M.R., Larson, C.M., 2012. Alterations in internal rotation and alpha angles are associated with arthroscopic cam decompression in the hip. Am. J. Sports Med. 40, 1107–12.

Kelly, B.T., Weiland, D.E., Schenker, M.L., Philippon, M.J., 2005. Arthroscopic Labral Repair in the Hip : Surgical Technique and Review of the Literature. Arthroscopy 21, 1496–1504.

Kepple, T.M., Arnold, A.S., Stanhope, S.J., Siegel, K.L., 1994. Assessment of a method to estimate muscle attachments from surface landmarks: A 3D computer graphics approach. J. Biomech. 21, 365–371.

Kibler, W.B., Press, J., Sciascia, A., 2006. The role of core stability in athletic function. Sport. Med. 36, 189–98.

Klein Horsman, M.D., Koopman, H.F.J.M., van der Helm, F.C.T., Prosé, L.P., Veeger, H.E.J., 2007. Morphological muscle and joint parameters for musculoskeletal modelling of the lower extremity. Clin. Biomech. 22, 239–47.

Langenderfer, J.E., Laz, P.J., Petrella, A.J., Rullkoetter, P.J., 2008. An efficient probabilistic methodology for incorporating uncertainty in body segment parameters and anatomical landmarks in joint loadings estimated from inverse dynamics. J. Biomech. Eng. 130, 014502.

Langenderfer, J.E., Rullkoetter, P.J., Mell, A.G., Laz, P.J., 2009. A multi-subject evaluation of uncertainty in anatomical landmark location on shoulder kinematic description. Comput. Methods Biomech. Biomed. Engin. 12, 211–216.

Laz, P.J., Browne, M., 2010. A review of probabilistic analysis in orthopaedic biomechanics. Proc. Inst. Mech. Eng. Part H J. Eng. Med. 224, 927–943.

Laz, P.J., Pal, S., Fields, A., Petrella, A.J., Rullkoetter, P.J., 2006. Effects of Knee Simulator Loading and Alignment Variability on Predicted Implant Mechanics : A Probabilistic Study. J. Orthop. Res. 24, 2212–2221.

Lee, D.C., Ham, Y.W., Sung, P.S., 2012. Effect of visual input on normalized standing stability in subjects with recurrent low back pain. Gait Posture 36, 580–5.

Lee, S.P., Souza, R.B., Powers, C.M., 2012. The influence of hip abductor muscle performance on dynamic postural stability in females with patellofemoral pain. Gait Posture 36, 425–9.

Leetun, D., 2004. Core stability measures as risk factors for lower extremity injury in athletes. Med. Sci. Sport. Exerc. 36, 926–934.

Lerner, Z.F., Board, W.J., Browning, R.C., 2014. Effects of an Obesity-Specific Marker Set on Estimated Muscle and Joint Forces in Walking. Med. Sci. Sport. Exerc. 46, 1261–1267.

Lieber, R.L., Ljung, B., Friden, J., 1997. Intraoperative sacromere length measurements reveal differential design of human wrist extensor muscles. J. Exp. Biol. 200, 19–25.

Liu, M.Q., Anderson, F.C., Schwartz, M.H., Delp, S.L., 2008. Muscle contributions to support and progression over a range of walking speeds. J. Biomech. 41, 3243–52.

Lloyd, D.G., Besier, T.F., 2003. An EMG-driven musculoskeletal model to estimate muscle forces and knee joint moments in vivo. J. Biomech. 36, 765–776.

Long, W., Dorr, L., Healy, B., Perry, J., 1993. Functional recovery of noncemented total hip arthroplasty. Clin. Orthop. Relat. Res. 288, 73–77.

Melchers, R.E., 2001. Structural reliability analysis and prediction. John Wiley & Sons, Inc., New York, NY.

Merchant, A.D., 1965. An experimental study of the influence of hip position with particular reference to rotation. Jounal Bone Jt. Surg. 47, 462–476.

Murata, Y., Takahashi, K., Yamagata, M., Hanaoka, E., Moriya, H., 2003. The knee-spine syndrome: Association between lumbar lordosis and extension of the knee. J. Bone Jt. Surg. 85, 95–99.

Myers, C. a, Laz, P.J., Shelburne, K.B., Davidson, B.S., 2014. A Probabilistic Approach to Quantify the Impact of Uncertainty Propagation in Musculoskeletal Simulations. Ann. Biomed. Eng.

Nelson-Wong, E., Gregory, D.E., Winter, D.A., Callaghan, J.P., 2008. Gluteus medius muscle activation patterns as a predictor of low back pain during standing. Clin. Biomech. 23, 545–53.

Neptune, R.R., Clark, D.J., Kautz, S.A., 2009. Modular control of human walking: a simulation study. J. Biomech. 42, 1282–7.

Neptune, R.R., Kautz, S.A., Zajac, F.E., 2001. Contributions of the individual ankle plantar flexors to support, forward progression and swing initiation during walking. J. Biomech. 34, 1387–1398.

NESSUS Theoretical Manual, 2001. . Southwest Research Institute, San Antonio, TX.

Nguyen, T.C., Reynolds, K.J., 2014. The effect of variability in body segment parameters on joint moment using Monte Carlo simulations. Gait Posture 39, 346–53.

Offerski, C., MacNab, I., 1983. Hip-spine syndrome. Spine (Phila. Pa. 1976). 8, 316–321.

Oliver, G.D., 2014. Relationship between gluteal muscle activation and upper extremity kinematics and kinetics in softball position players. Med. Biol. Eng. Comput. 52, 265–70.

Pal, S., Langenderfer, J.E., Stowe, J.Q., Laz, P.J., Petrella, A.J., Rullkoetter, P.J., 2007. Probabilistic modeling of knee muscle moment arms: effects of methods, origin-insertion, and kinematic variability. Ann. Biomed. Eng. 35, 1632–42.

Pandy, M.G., 2001. Computer modeling and simulation of human movement. Annu rev biomed eng 3, 245–273.

Parvizi, J., Pour, A.E., Hillibrand, A., Goldberg, G., Sharkey, P.F., Rothman, R.H., 2010. Back pain and total hip arthroplasty: a prospective natural history study. Clin. Orthop. Relat. Res. 468, 1325–30.

Pavol, M.J., Owings, T.M., Grabiner, M.D., 2002. Body segment inertial parameter estimation for the general population of older adults. J. Biomech. 35, 707–12.

Perry, J., 1992. Gait Analysis: Normal and Pathological Function. Stack, inc., Baltimore, MD.

Plummer, H.A., Oliver, G.D., 2014. The relationship between gluteal muscle activation and throwing kinematics in baseball and softball catchers. J. strength Cond. Res. 28, 87–96.

Popovich, J.M., Kulig, K., 2012. Lumbopelvic landing kinematics and EMG in women with contrasting hip strength. Med. Sci. Sports Exerc. 44, 146–53.

Porter, J., Wilkinson, A., 1997. Lumbar-hip flexion motion. A comparative study between asymptomatic and chronic low back pain in 18- to 36-year-old men. Spine (Phila. Pa. 1976). 22, 1513–1524.

Powers, C.M., 2010. The influence of abnormal hip mechanics on knee injury: a biomechanical perspective. J. Orthop. Sports Phys. Ther. 40, 42–51.

Radebold, A., Cholewicki, J., Polzhofer, G.K., Greene, H.S., 2001. Impaired postural control of the lumbar spine is associated with delayed muscle response times in patients with chronic idiopathic low back pain. Spine (Phila. Pa. 1976). 26, 724–30.

Rao, G., Amarantini, D., Berton, E., Favier, D., 2006. Influence of body segments' parameters estimation models on inverse dynamics solutions during gait. J. Biomech. 39, 1531–6.

Redmond, J.M., Gupta, A., Hammarstedt, J.E., Stake, C.E., Domb, B.G., 2014. The hip-spine syndrome: how does back pain impact the indications and outcomes of hip arthroscopy? Arthroscopy 30, 872–81.

Reeves, N.P., Everding, V.Q., Cholewicki, J., Morrisette, D.C., 2006. The effects of trunk stiffness on postural control during unstable seated balance. Exp. Brain Res. 694–700.

Reiman, M., Weisbach, P., Glynn, P., 2009a. The hips influence on low back pain: a distal link to a proximal problem. J. Sport. Rehabil. 18, 24–32.

Reiman, M., Weisbach, P.C., Glynn, P.E., 2009b. The hip's influence on low back pain: a distal link to a proximal problem. J. Sport. Rehabil. 18, 24–32.

Reinbolt, J.A., Haftka, R.T., Chmielewski, T.L., Fregly, B.J., 2007. Are patient-specific joint and inertial parameters necessary for accurate inverse dynamics analyses of gait? IEEE Trans. Biomed. Eng. 54, 782–93.

Riha, D.S., Thacker, B.H., Pleming, J.B., Walker, J.D., Mullin, S.A., Weiss, C.E., 2006. Verification and Validation for a Penetration Model Using a Deterministic and Probabilistic Design Tool. Int. J. Impact Eng. 33.

Rothbart, B.A., Estabrook, L., 1999. Excessive pronation: a major biomechanical determinant in the development of chondromalacia and pelvic lists. J. Manipulative Physiol. Ther. 29, 595–601.

Salsich, G.B., Long-Rossi, F., 2011. Do Females with Patellofemoral Pain have Abnormal Hip and Knee Kinematics during Gait. Physiother. Theory Pract. 26, 150–159.

Santos, F.G., Carmo, C.M., Francini, A.C., Pereira, R.R.P., Takara, K.S., Tanaka, C., 2013. Chronic low back pain in women: muscle activation during task performance. J. Phys. Ther. Sci. 25, 1569–1573.

Scott, R.E., Guskiewicz, K.M., Yu, B., 2005. Single-leg jump-landing stabilization times in subjects with functionally unstable ankles. J. Athl. Train. 40, 298–304.

Scovil, C.Y., Ronsky, J.L., 2006. Sensitivity of a Hill-based muscle model to perturbations in model parameters. J. Biomech. 39, 2055–63.

Shelburne, K.B., Decker, M., Peterson, D., Torry, M.R., Philippon, M.J., 2010. Hip joint forces during squatting exercise predicted with subject-specific modeling. In: Trans Annu Meet Orthop Res Soc. p. ISSN 0149–6433.

Shelburne, K.B., Kim, H.-J., Sterett, W.I., Pandy, M.G., 2011. Effect of posterior tibial slope on knee biomechanics during functional activity. J. Orthop. Res. 29, 223–31.

Shelburne, K.B., Pandy, M.G., 1998. Determinants of cruciate-ligament loading during rehabilitation exercise. Clin. Biomech. 13, 403–413.

Shelburne, K.B., Torry, M.R., Pandy, M.G., 2006. Contributions of muscles, ligaments, and the ground-reaction force to tibiofemoral joint loading during normal gait. J. Orthop. Res. 1983–1990.

Shelburne, K.B., Torry, M.R., Steadman, J.R., Pandy, M.G., 2008. Effects of foot orthoses and valgus bracing on the knee adduction moment and medial joint load during gait. Clin. Biomech. 23, 814–21.

Shih, C., Du, Y., Lin, Y., Wu, C., 1994. Muscular recovery around the hip joint after total hip arthroplasty. Clin. Orthop. Relat. Res. 302, 115–120.

Shull, P.B., Shultz, R., Silder, A., Dragoo, J.L., Besier, T.F., Cutkosky, M.R., Delp, S.L., 2013. Toe-in gait reduces the first peak knee adduction moment in patients with medial compartment knee osteoarthritis. J. Biomech. 46, 122–8.

Silverman, A.K., Neptune, R.R., 2012. Muscle and prosthesis contributions to amputee walking mechanics: a modeling study. J. Biomech. 45, 2271–8.

Sjolie, A.N., 2004. Low-back pain in adolescents is associated with poor hip mobility and high body mass index. Scand J Med Sci Sport. 14, 168–175.

Souza, R.B., Powers, C.M., 2009. Predictors of hip internal rotation during running: an evaluation of hip strength and femoral structure in women with and without patellofemoral pain. Am. J. Sports Med. 37, 579–87.

Stagni, R., Leardini, A., Cappozzo, A., Benedetti, M.G., Cappello, A., 2000. Effects of hip joint centre mislocation on gait analysis results. J. Biomech. 33, 1479–1487.

Sueki, D.G., Cleland, J.A., Wainner, R.S., 2013. A regional interdependence model of musculoskeletal dysfunction: research, mechanisms, and clinical implications. J. Man. Manip. Ther. 21, 90–102.

Suetta, C., Andersen, J.L., Dalgas, U., Berget, J., Koskinen, S., Aagaard, P., Magnusson, S.P., Kjaer, M., Sp, M., Resistance, K.M., 2008. Resistance training induces qualitative changes in muscle morphology , muscle architecture, and muscle function in elderly postoperative patients. J. Appl. Physiol. 105, 180–186.

Suter, E., McMorland, G., Herzog, W., Bray, R., 2000. Conservative Lower Back Treatment Reduces Inhibition in Knee-Extensor Muscles : A Randomized. J. Manipulative Physiol. Ther. 23, 76–80.

Tanaka, M.L., Ross, S.D., Nussbaum, M.A., 2010. Mathematical modeling and simulation of seated stability. J. Biomech. 43, 906–912.

Thacker, B.H., Riha, D.S., Fitch, S.H.K., Huyse, L.J., 2006. Probabilistic Engineering Analysis Using the NESSUS Software. Struct. Saf. 28, 83–107.

Thelen, D.G., Anderson, F.C., 2006. Using computed muscle control to generate forward dynamic simulations of human walking from experimental data. J. Biomech. 39, 1107–15.

Thijs, Y., Van Tiggelen, D., Willems, T., De Clercq, D., Witvrouw, E., 2007. Relationship between hip strength and frontal plane posture of the knee during a forward lunge. Br. J. Sports Med. 41, 723–7.

Valente, G., Taddei, F., Jonkers, I., 2013. Influence of weak hip abductor muscles on joint contact forces during normal walking: probabilistic modeling analysis. J. Biomech. 46, 2186–93.

Van der Krogt, M.M., Delp, S.L., Schwartz, M.H., 2012. How robust is human gait to muscle weakness? Gait Posture 36, 113–9.

Van Tulder, M., Koes, B., Bouter, L., 1997. Conservative treatment of acute and chronic nonspecific low back pain. A systematic review of randomized controlled trials of the most common interventions. Spine (Phila. Pa. 1976). 22, 2128–2156.

Vaughan, C.L., Davis, B.L., O'Connor, J.C., 1992. Dynamics of Human Gait, 2nd ed. Kiboho Publishers, Cape Town, South Africa.

Wainner, R.S., Whitman, J.M., Cleland, J.A., Flynn, T.W., 2007. Regional interdependence: A musculoskeletal examination model whose time has come. J. Orthop. Sports Phys. Ther. 37, 658–60.

Ward, S.R., Eng, C.M., Smallwood, L.H., Lieber, R.L., 2009. Are current measurements of lower extremity muscle architecture accurate? Clin. Orthop. Relat. Res. 467, 1074–82.

Ward, S.R., Smallwood, L.H., Lieber, R.L., 2005. Scaling of human lower extremity muscle architecture to skeletal dimensions. ISB XXth Congr. 29th Annu. Meet.

Wesseling, M., de Groote, F., Jonkers, I., 2014. The effect of perturbing body segment parameters on calculated joint moments and muscle forces during gait. J. Biomech. 47, 596–601.

White, S.C., Yack, H., Winter, D.A., 1989. A three-dimensional musculoskeletal model for gait analysis. Anatomical variability estimates. J. Biomech. 22, 885–893.

Whitney, S.L., Wrisley, D.M., Marchetti, G.F., Gee, M.A., Redfern, M.S., 2005. Clinical Measurement of Sit-to-Stand Performance in People With Balance Disorders: Validity of Data for the five-times-sit-to-stand test. Phys. Ther. 85, 1034–1045.

Widler, K.S., Glatthorn, J.F., Bizzini, M., Impellizzeri, F.M., Munzinger, U., Leunig, M., Maffiuletti, N. a, 2009. Assessment of hip abductor muscle strength. A validity and reliability study. J. bone Jt. Surg. 91, 2666–72.

Willson, J.D., Davis, I.S., 2008. Lower extremity mechanics of females with and without patellofemoral pain across activities with progressively greater task demands. Clin. Biomech. 23, 203–11.

Willson, J.D., Kernozek, T.W., Arndt, R.L., Reznichek, D.A., Straker, J.S., 2011. Gluteal muscle activation during running in females with and without patellofemoral pain syndrome. Clin. Biomech. (Bristol, Avon) 26, 735–40.

Wilson, E., 2005. Core stability: assessment and functional strengthening of the hip abductors. Strength Cond. J. 27, 21–23.

Winby, C.R., Lloyd, D.G., Kirk, T.B., 2008. Evaluation of different analytical methods for subject-specific scaling of musculotendon parameters. J. Biomech. 41, 1682–8.

Winter, S., 2015. Effectiveness of targeted home-based hip exercises in individuals with non-specific chronic or recurrent low back pain with reduced hip mobility: A randomised trial. J. Back Musculoskelet. Rehabil.

Wolfe, F., Hawley, D., Peloso, P., Wilson, K., Anderson, J., 1996. Back pain in osteoartritis of the knee. Arthritis care res 9, 376–383.

Wu, Y, T., Millwater, H.R., A, C.T., 1990. Advanced Probabilistic Structural Analysis Method for Implicit Performance Functions. AIAA 28, 1663–1669.

Xu, Y., Choi, J., Reeves, N.P., Cholewicki, J., 2010. Optimal control of the spine system. J. Biomech. Eng. 132, 051004.

Yoshimoto, H., Sato, S., Masuda, T., Kanno, T., Shundo, M., Hyakumachi, T., Yanagibashi, Y., 2005. Spinopelvic alignment in patients with osteoarthrosis of the hip: A radiographic comparison to patients with low back pain. Spine (Phila. Pa. 1976). 30, 1650–1657.

You, J.H., Kim, S.Y., Oh, D.W., Chon, S.C., 2014. The effect of a novel core stabilization technique on managing patients with chronic low back pain: a randomized, controlled, experimenter-blinded study. Clin. Rehabil. 28, 460–469.

Zajac, F.E., Gordon, M., 1989. Determining muscle's force and action in multi-articular movement. Exerc. Sport Sci. Rev. 17, 187–230.

Zajac, F.E., Neptune, R.R., Kautz, S.A., 2002. Biomechanics and muscle coordination of human walking. Part I: introduction to concepts, power transfer, dynamics and simulations. Gait Posture 16, 215–32.

Zazulak, B.T., Hewett, T.E., Reeves, N.P., Goldberg, B., Cholewicki, J., 2007. The effects of core proprioception on knee injury: a prospective biomechanical-epidemiological study. Am. J. Sports Med. 35, 368–73.

The OpenSim Probabilistic Plugin

An introductory guide to assess uncertainty in musculoskeletal modeling

Casey A. Myers
Kevin B. Shelburne
Peter J. Laz
Bradley S. Davidson

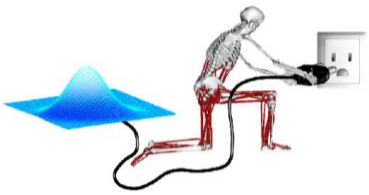

If you perform musculoskeletal simulations using OpenSim at any level, this Probabilistic Plugin is for you. The purpose of the Probabilistic Plugin is to enable OpenSim users to quantitatively assess confidence in outputs from your musculoskeletal simulations. This probabilistic approach provides a systematic framework to quantify uncertainty and report this information. The Probabilistic Plugin is open source, and should be adapted as needed to your specific project.

Where to Start

If you are new to probabilistic analyses, visit YouTube to view a presentation on common probabilistic methods in musculoskeletal simulation.

https://www.youtube.com/watch?v=ERtzZ7EY3SI&feature=youtu.be

If you have already configured the Matlab Scripting Environment in OpenSim, you are ready to work through the tutorials in order.

Contents

Initialize and Test Interface between OpenSim and Probabilistic Plugin

Set up the Matlab Scripting Environment in OpenSim

To connect Matlab and OpenSim API, follow the instructions on Scripting with Matlab within the OpenSim Confluence documentation.

Download the Probabilistic Plugin

Download zipfile that contains the Plugin distribution and files from https://simtk.org/home/prob_tool

Unzip the file and store folder on your computer.

Save the folder and add this folder name to the Matlab search path.

Test that the interface is correctly

To test that the interface is working correctly, type the following into the Matlab Command Window:

```
Model('YourFilePath/ProbModel_gait2392.osim)
```

Note: The ProbModel_gait2392.osim is a version of the gait2392 model that has been appropriately scaled for this data set.

Proceed to Tutorial 1 if 1) No errors occur and 2) A model object appears in the Matlab Workspace, proceed to Tutorial 1.

Tutorial 1: Inverse Dynamics and Uncertainty in Body Segment Parameters (Monte Carlo Simulation)

This self-guided tutorial will walk you through a simple analysis performed of the Probabilistic Plugin for OpenSim. A case study is presented that relies on Monte Carlo simulation as applied to lower extremity inverse dynamics in the presence of uncertainties in inertial properties.

Upon completing this tutorial, you will be able to:

- Create valid input distributions for body segment parameters
- Create and interpret outputs of probabilistic analyses: confidence bounds and sensitivity factors
- Develop intuition on convergence of Monte Carlo simulation
- Generate a set up file for future probabilistic analyses

How to consider the effects of uncertainty in inverse dynamics

Inverse dynamics is a fundamental metric in biomechanics

Modeling of inverse dynamics (net moment at a joint) during human movement is a foundational concept in biomechanics. Analyses of joint moments are:

- Taught in every course that covers human movement.
- Frequently applied to assess clinical outcomes.
- A foundational step toward estimating muscle forces (see Tutorial 2).

Where does uncertainty arise in inverse dynamics?

The inverse dynamics solution is mathematically straightforward and depends on three input variables (external reaction forces, segment kinematics, inertial parameters). Each of these inputs is prone to error in the measurement or estimation and is carried through the calculations to the output joint moments.

Effects of input uncertainty

Two important effects of input uncertainty that we should consider when developing a musculoskeletal model:

- The "correct output" at any given time point lies within a range of possible values that are linked to uncertainty in the input.
- The contributions of uncertainty in each input to the model outputs are not equal.

To quantify these effects, we will generate and interpret Confidence Bounds and Sensitivity Factors.

Preparation for Probabilistic Simulation

Create input distributions for body segment parameters

A challenging part of running a probabilistic analysis is correctly modeling the input distribution. The OpenSim Probabilistic Plugin currently accepts the mean and standard deviation to create the Gaussian distribution needed for sampling.

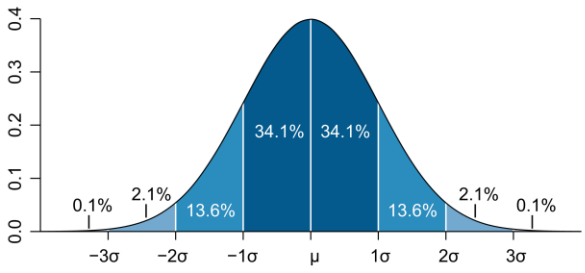

(image taken from Wikimedia commons)

$$f(x, \mu, \sigma) = \frac{1}{\mu\sqrt{2\pi}} e^{\frac{-(x-\mu)^2}{2\sigma^2}}$$

where μ is the mean value of the parameter and σ is the standard deviation of the parameter.

For your input distributions, we will take each value of μ from the starting model parameters, and define the input σ from previously reported literature.

Coefficient of variation for quantifying the distribution

To obtain a more generalized formulation applicable to all models, we can assume a constant coefficient of variation,

$$CV = \frac{\sigma}{|\mu|}$$

which assumes that the standard deviation is proportional to the magnitude of the mean.

For example, the means and standard deviations reported for the foot segment mass, tibia segment mass, and femur segment mass in Rao et al. (2006) were 0.85(0.11) kg, 2.89(0.19) kg, and 7.59(1.30) kg, respectively.

Therefore, the corresponding coefficients of variation are:

$$CV_{\text{femur}} = 0.171$$
$$CV_{\text{tibia}} = 0.066$$
$$CV_{\text{foot}} = 0.129$$

Make note of these for use when running the probabilistic simulation.

Appendix A. lists papers we have found helpful to quantify distributions for a variety of parameters.

Perform a Monte Carlo Simulation with the OpenSim Probabilistic Plugin

A Monte Carlo simulation is the most familiar probabilistic method. Monte Carlo is a class of data sampling techniques in which the simulation is run for multiple iterations. Each time, the input values are randomly selected from predetermined probability density functions associated with each parameter. The outputs of interest are random and distributed along their own probability density functions.

Run the baseline simulation

The Baseline Simulation is the initial deterministic simulation needed before the probabilistic methods can be performed. In this tutorial, the baseline parameters will be used as the mean values when defining the input distributions.

Type `ProbGUI_v8.m` **in the Matlab Command Window**
This launches the Probabilistic Plugin and you will see the following window.

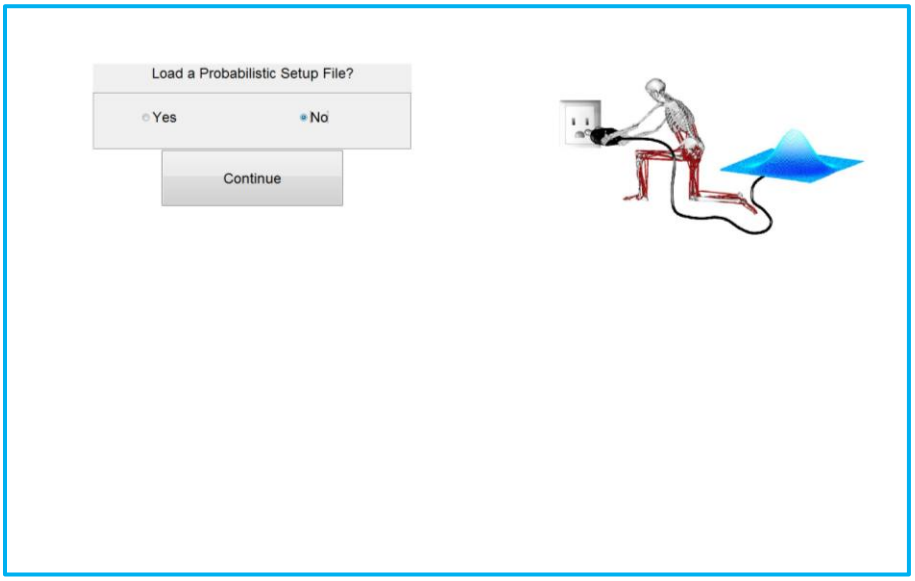

Select the "No" radio button, then "Continue"
The Probabilistic Setup File is a .xml file that allows the user to bypass the GUI setup. A modifiable setup file will be generated at the end this tutorial, and can be used for future simulations using the Probabilistic Plugin.

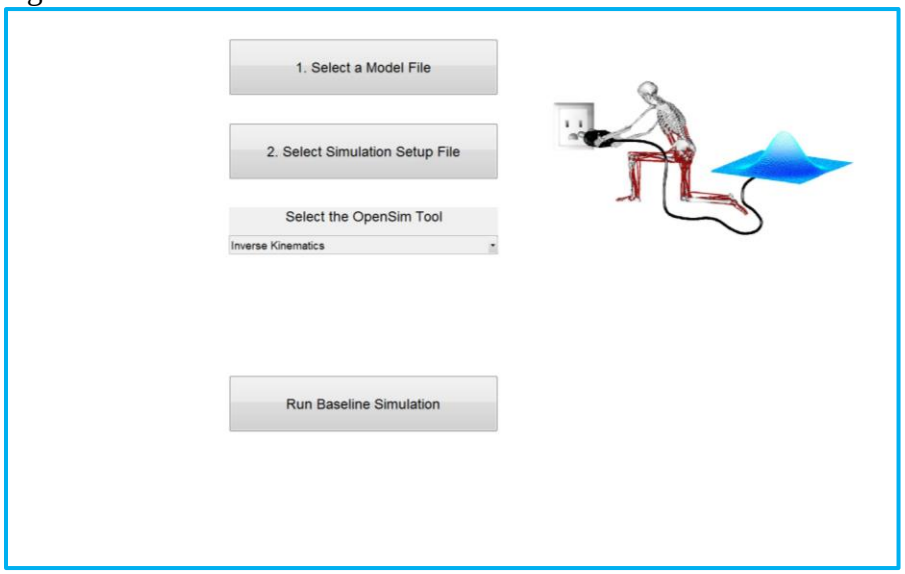

Click "1. Select a Model File"
Select ProbModel_gait2392.osim, which was included in the folder.

This file is the gait2392.osim model that has been appropriately scaled for use with the experimental data. The Probabilistic Plugin will generate a copy of this file and make changes to the copied file. If you restart the plugin, select the original model file.

Click "2. Select Simulation Setup File" and
Select the "OpenSimInverseDynamics_setup.xml" file, which was included in the folder.

!! Important !!
Before proceeding to the next step, open the simulation setup file and the external ground reaction force setup file and ensure that the file paths in these setup files are completely defined.

Select "Inverse Dynamics" from the OpenSim Tool dropdown menu.

Click "Run Baseline Simulation"

Check that "inverse_dynamics.sto" was written in the "Results" folder located in the current Matlab directory.

If you do not see "inverse_dynamics.sto" with a time stamp equivalent to running the simulation, **examine out.txt for errors that occurred during the baseline simulation.**
Out.txt is written at the conclusion of the baseline simulation and is located in the current Matlab folder.

The most common errors are related to improper path to locate the files needed for the Inverse Dynamics simulation. To correct this, ensure that all paths in the .xml setup files are correctly entered.

Close the Probabilistic Plugin and launch again after correcting the error.

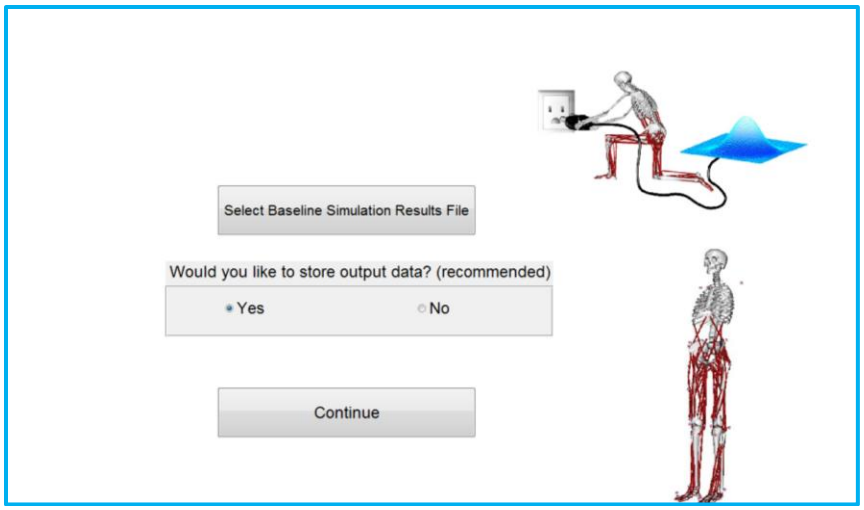

Click "Select Baseline Simulation Results File"
Select the "inverse_dyanmics.sto" file located in the Results folder.

Select the "Yes" radio button located under "Would you like to store the output data from each Monte Carlo simulation?"
The results from each iteration will be stored in the Results folder. The default is "Yes" to ensure future analysis.

Enter the input distributions

Define the parameters that will be perturbed and define the quantitative distributions.

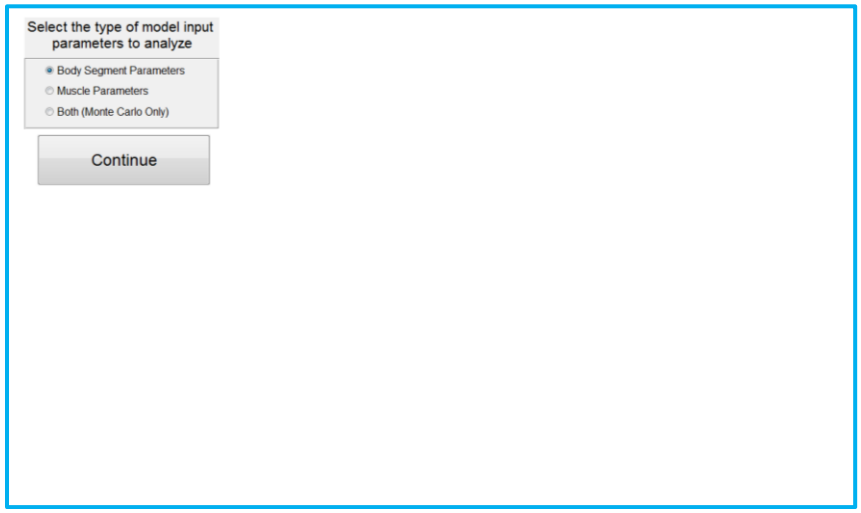

Select "Body Segment Parameters" radio button and click "Continue"

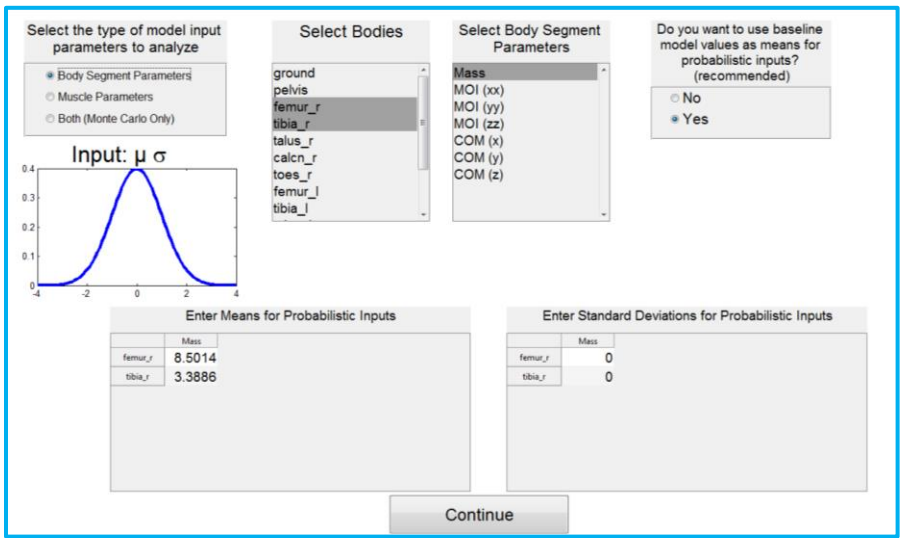

Select the "femur_r" and "tibia_r" segments in the list of bodies available to perform analyses.

note: To select multiple items in the list hold the Ctrl key.

Select "Mass" as the parameter to perturb on each segment.

note: Although Mass is already highlighted, you must click on it to avoid an error.

Select "Yes" radio button to indicate use the baseline model values.

Click "Continue"

Because we chose to use the segment parameters from the baseline model as the mean value for each distribution, the means table will be populated. If you chose "No", the means must be manually input into the table.

Calculate the standard deviations using the coefficients of variation defined in the earlier section and enter standard deviations in the GUI.

$$s_{\text{femur}} = CV_{\text{femur}} \times \left| m_{\text{femur}} \right| = 0.171 \times 8.5014 = 1.454$$
$$s_{\text{tibia}} = CV_{\text{tibia}} \times \left| m_{femur} \right| = 0.066 \times 3.3886 = 0.223$$

Click "Continue".

Initialize the Monte Carlo Simulation

After the distributions are defined, the probabilistic simulation must be initialized to perform the probabilistic analysis.

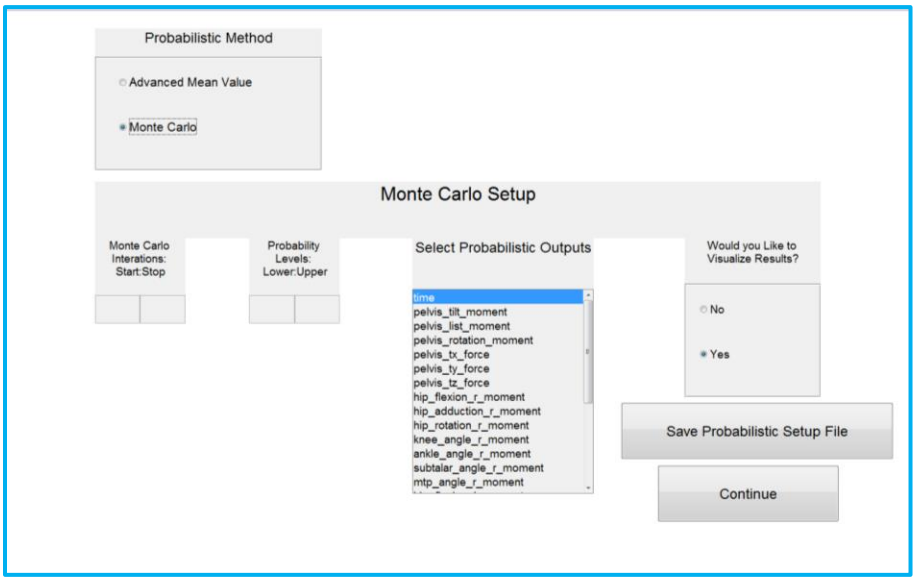

Select "Monte Carlo" radio button under Probabilistic Method. Click "Continue".

Enter 1 and 30 as the Monte Carlo iterations Start:Stop
This will run the Monte Carlo simulation 30 times.

Enter 5 and 95 as the lower and upper Probability Levels.
This specifies the program to create lower and upper limits of a 90% confidence bound (between the 5^{th} and 95^{th} percentiles of the distribution).

Select "hip_flexion_r_moment", "knee_angle_r_moment", and "ankle_angle_r_moment" as the Probabilistic Outputs.
This list is constructed from the possible outputs located in your Results File.

Select "Yes" under "Would you like to visualize the results?".

Click "Save Probabilistic Setup File".

Name the file "Tutorial1_MonteCarlo30_Setup" and save

This selection will generate an .xml file that can be loaded in place of the Probabilistic Plugin GUI.

Click "Continue"
The Monte Carlo Simulation will run and produce output information in the Matlab Command Window.

On a PC with 16.0 GB of RAM and a 3.60 GHz processor, 30 iterations in the Monte Carlo Simulation will take approximately 60 seconds.

Visualization from the Monte Carlo Simulation

After the simulation has completed, several plots will be displayed that include interpretable results and information about the simulation.

Confidence Bounds

Confidence bounds represent the range in which the output of the simulation can lie. In this tutorial, we chose a two-sided confidence bound with limits at 5^{th} and 95^{th} percentile of the output distribution.

> "There is a 90% probability that that true result of this simulation lies between the lower and upper confidence bounds."

Currently, standards do not exist on selection of confidence bound sizes.

Confidence Bounds versus a Confidence Interval

Confidence Bounds approximate the value of a model output and is calculated from repeated numerical simulations whereas a Confidence Interval approximates the mean of an entire population mean based on a sample data set that includes multiple participants (Curran-Everett, 2009). The

However, when the output distribution of your probabilistic simulation is Gaussian, the two-sided confidence bounds can be interpreted in a similar manner a confidence interval. For example, when the output distribution is Gaussian you can test if the outputs from two different models, given the same input data, are different by stating the null hypothesis (h_0) and alternative hypothesis (h_1) as

h_0: Model A Output = Model B Output.
h_1: Model A Output ≠ Model B Output

If the acceptable Type I Error is limited to 5%, then we reject h_0 when the two-sided 95% confidence bounds (2.5th percentile and 97.5th percentile) from each Monte Carlo Simulation do not overlap

Interpret sensitivity factors

A Sensitivity Factor is generated for every combination of input varied and the output of interest. The value of the sensitivity factor is quantified by Pearson Product-Moment Correlation between the input parameter and the output.

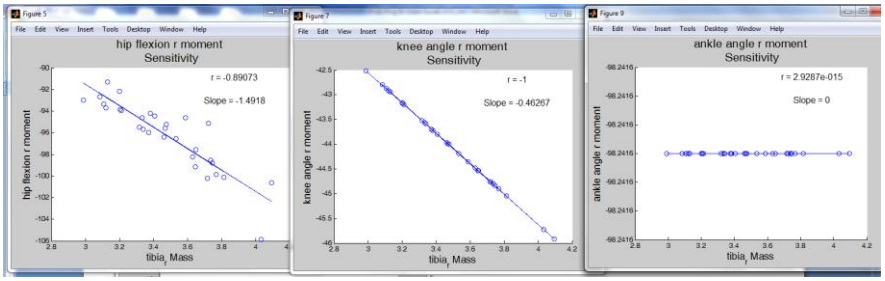

The value of Sensitivity Factor indicates the degree of sensitivity. For example: weakly sensitive (r=0.2-0.4), moderately sensitive (r=0.4-0.6), and highly sensitive (r=0.6-1.0).

We recommend categorizing the degree of sensitivity on Sensitivity Factors that are statistically different from zero (when the 95% confidence interval of the correlation coefficient does not contain zero).

In addition, the slope of the regression provides information about how the average change in the input will affect the output. Note that this interpretation assumes a linear relationship between the input and output.

Output Distribution

A plot is generated that shows the histogram of each output in the simulation and the normal probability plot. This information can be used to examine the qualitative features of your distribution.

If you intend to calculate a confidence interval (see panel above), the normal probability plot will help you decide if the data already satisfy the Gaussian criterion. If not, the value and histogram will assist deciding on an appropriate transform.

Use the Probabilistic Setup File to generate results with different parameter distributions

After completing the first simulation, the Plugin generated a new XML file that allows running the same or modified version of the probabilistic simulation without navigating the Plugin GUI each time.

Modify the probabilistic setup file

Navigate to the file named “filename.xml” which is located in the local directory with the Plugin files.

Open the file in an XML viewer of your choice

Explore the set up file created.
You will recognize many of the decisions you made when using the PlugIn GUI

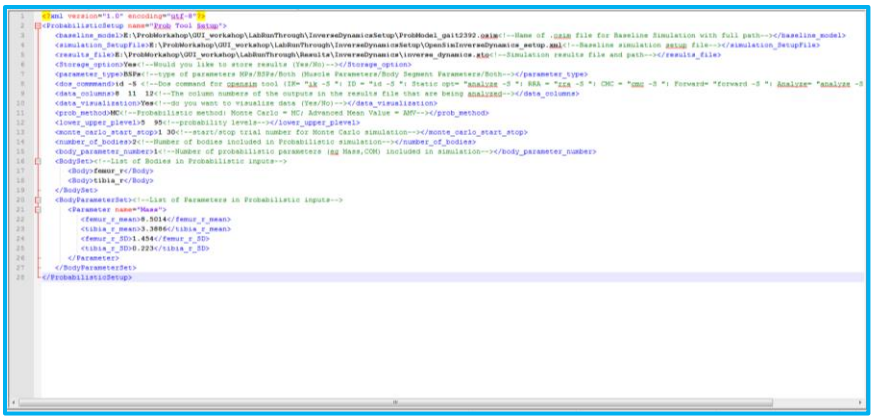

Change the standard deviations for the mass of the femur and tibia to 2x the original value.

```
<femur_r_SD>2.908<femur_r_SD>
<tibia_r_SD>0.466<tibia_r_SD>
```

Leave the number of iterations the same

Run the Monte Carlo Simulation with altered parameters

Type `ProbGUI_v8.m` in the Matlab Command Window

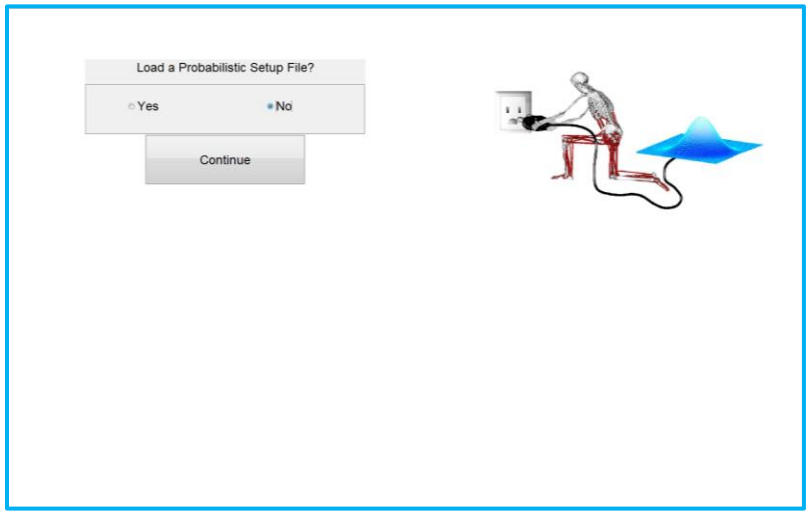

Select the "Yes" radio button, then "Continue".

Select the Probabilistic Setup file that you saved. The simulation will begin with the baseline simulation and then proceed to the Monte Carlo iterations.

Examine New Results

The updated plots of the 90% confidence bounds are now larger than in the initial simulation for the hip and knee.

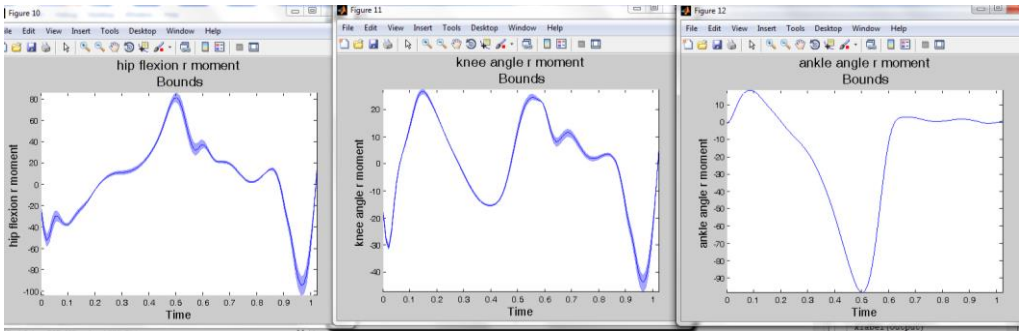

How many iterations are necessary in a Monte Carlo Simulation?

Accuracy of the Monte Carlo simulation improves with the number of iterations

It is important to perform enough iterations in the Monte Carlo simulation to obtain the results for interpretation. The confidence bounds and sensitivity will change with additional iterations.

There are multiple ways to examine convergence. The most common is to set a convergence criterion on the change on confidence bounds between iterations.

The plot below demonstrates how the bound size changed with each successive iteration of a Monte Carlo simulation that used bound size of the Vastus Lateralis muscle force. In the Monte Carlo simulation shown, the results converged around 3000 iterations.

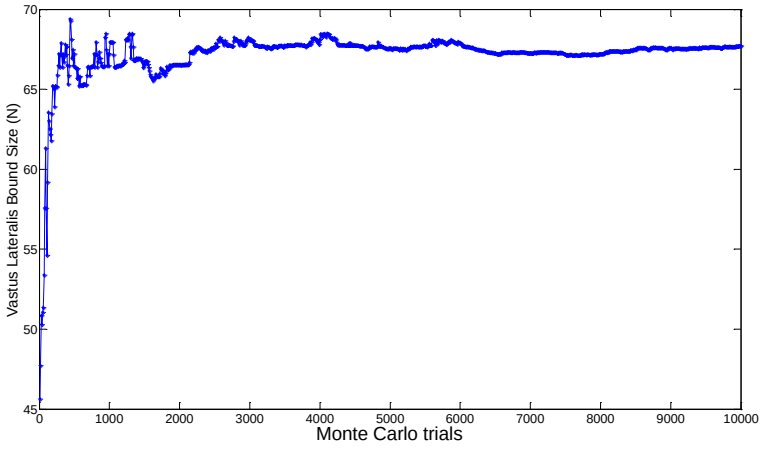

Without prior knowledge of how a system will behave in the Monte Carlos simulation, selecting the convergence criterion may be difficult. As a result, convergence may be assessed after the simulation.

To generate your own convergence for the inverse dynamics example, use the data in the results files created during the Monte Carlo Simulation, which are located in the results folder defined earlier and specified in the Probabilistic Setup File. The output you choose to converge upon must be plotted against the iteration using a custom Matlab script.

Refer to Valente et al. (2013) for an excellent example of reporting convergence of a Monte Carlo simulation.

Monte Carlo Simulation Exercises

Perform the following "homework assignments" to develop better understanding the Monte Carlo Simulation results and the file handling within the Probabilistic Plugin.

Exercise 1: Run full Monte Carlo Simulation

Modify the probabilistic input file to add 500 iterations to the last simulation. Did the 5^{th} and 95^{th} percentiles change compared to the simulation with 30 iteration?

Exercise 2: Create convergence plot

Write a Matlab script to plot the value of the 95^{th} percentile for peak hip extension moment for iterations 1 through 500. Steps:

1) Load the results file for an iteration from the output folder.
2) Find value for peak hip extension moment.
3) Using all previous iterations, calculate the 95^{th} percentile for that iteration
4) Plot results versus each iteration.

Tutorial 2: Muscle Force Prediction and Uncertainty in Muscle Properties (Advanced Mean Value)

This self-guided tutorial will walk you through using the Advanced Mean Value (AMV) method of the OpenSim Probabilistic Plugin.

Upon completing this tutorial, you will be able to:

- Run the AMV method within the Probabilistic Plugin GUI
- Create and interpret outputs of probabilistic analyses: confidence bounds and sensitivity factors
- Characterize the tradeoff of computational efficiency and amount of information available between Monte Carlo and AMV (within the number of most probable points selected)
- Generate and interpret importance factors

Muscle force prediction and uncertainty in muscle parameters

Static optimization and muscle force prediction

Static optimization is currently the most common tool used to resolve the over-determined system of muscles forces within a musculoskeletal model. In OpenSim, the Static Optimization Tool is standard in the GUI.

Uncertainty in muscle parameters

It is important to consider the effects of selecting muscle properties on force prediction processes. Muscles and parameters do not share equal importance in a given simulation. However, it is clear that muscles play an important role in accelerating segments they do not span (Zajac, 1993).

Large number of parameters included in the simulations

In a Hill-Type muscle model, multiple parameters must be quantified for each muscle. These include physiological cross-sectional area (PCSA), pennation angle, maximum velocity, tendon slack length. These values are specific to each muscle, and are quantified for each subject.

Most current lower-extremity models include large numbers of muscles to actuate the system. For example, the gait2392 model we are using for these tutorials includes 92 muscles. If we are required to quantify four parameters per muscle, then 92x4=368 parameters, each with a level of uncertainty.

Perform Most Probable Point Analysis (Advanced Mean Value method) on Muscle Forces

When the number of input parameters gets large, the computational expense can drastically increase. When this occurs, we can estimate the reliability metrics through an optimization procedure called the Most Probable Point (Wu et al., 1990). Like the Monte Carlo Simulation, the results provide confidence bounds; however, sensitivity factors are not possible because the entire input probability density function is not considered. A metric of sensitivity called an importance factor is available in the MPP methods.

Run the baseline simulation

The Baseline Simulation is the initial deterministic simulation needed before the probabilistic methods can be performed. In this tutorial, the baseline parameters will be used as the mean values when defining the input distributions.

Type `ProbGUI_v8.m` in the Matlab Command Window.

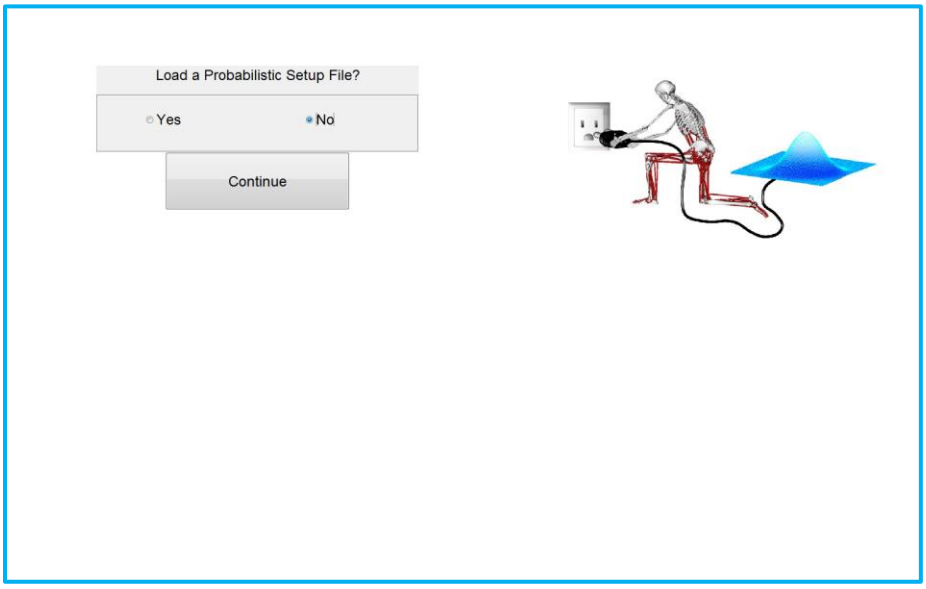

Select the “No” radio button, then “Continue”.

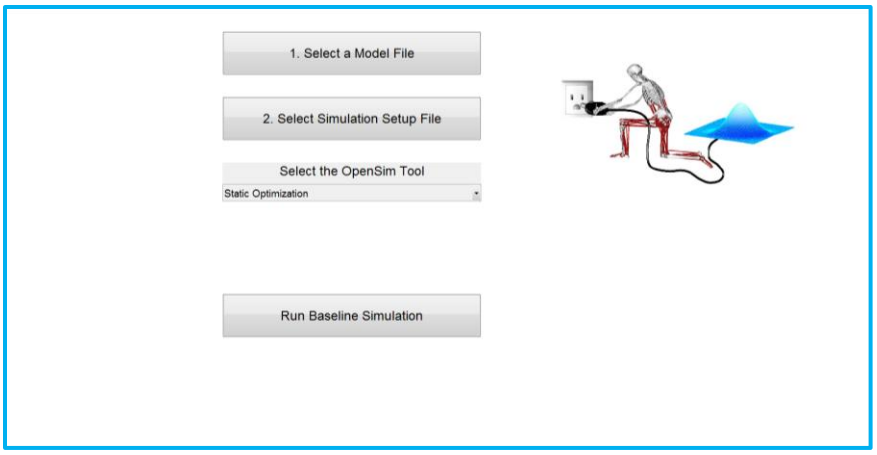

Click "1. Select a Model File" and
Select ProbModel_gait2392.osim.

Click "2. Select Simulation Setup File" and
Select the "ProbGait_StaticOp_Setup.xml" file.

!! Important !!

Before proceeding to the next step, open the simulation setup file and the external ground reaction force setup file and ensure that the file paths in these setup files are completely defined.

Select "Static Optimization" from the OpenSim Tool dropdown menu.

Click "Run Baseline Simulation".

Check that "_force.sto" was written in the "Results" folder located in the current Matlab directory.

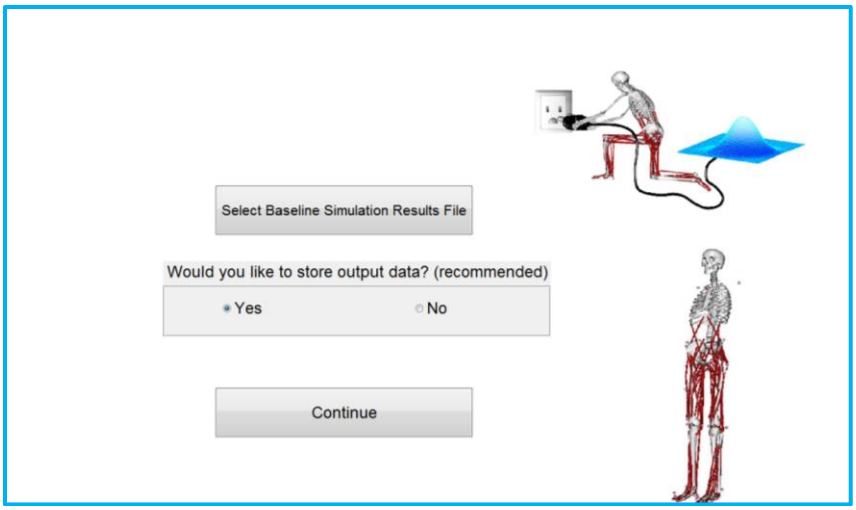

Click "Select Baseline Simulation Results File"
Select the "_force.sto" file located in the Results folder.

Select the "Yes" radio button located under "Would you like to store output data?"
The results from each iteration will be stored in the Results folder. The default is "Yes" to ensure future analysis.

Click "Continue".

Select your static optimization results file for '_force.sto'.

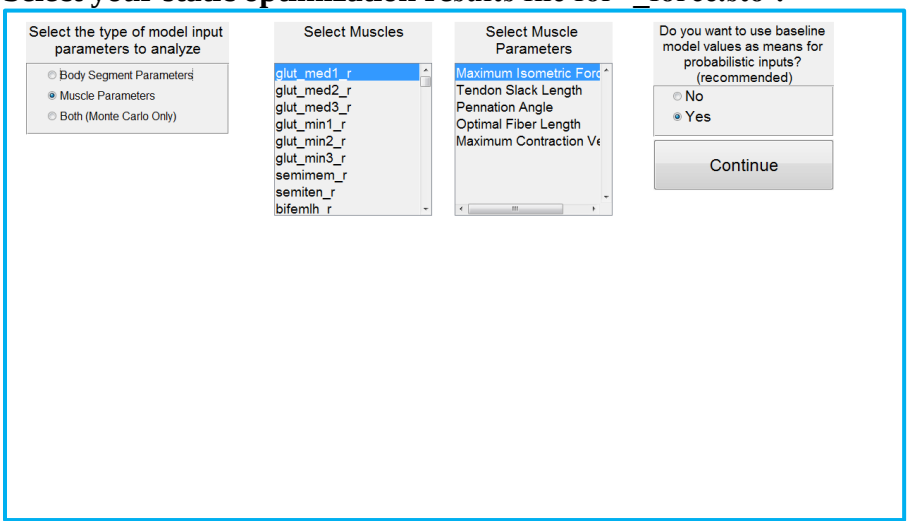

Select the Muscle Parameters radio button to analyze.

Select the biceps femoris long head (bifemlh_r) and rectus femoris (rect_fem_r) on the right side from the list of muscles in the model.

Select Maximum Isometric Force from the list of parameters.

Select the 'yes' radio button to use initial model values and continue.

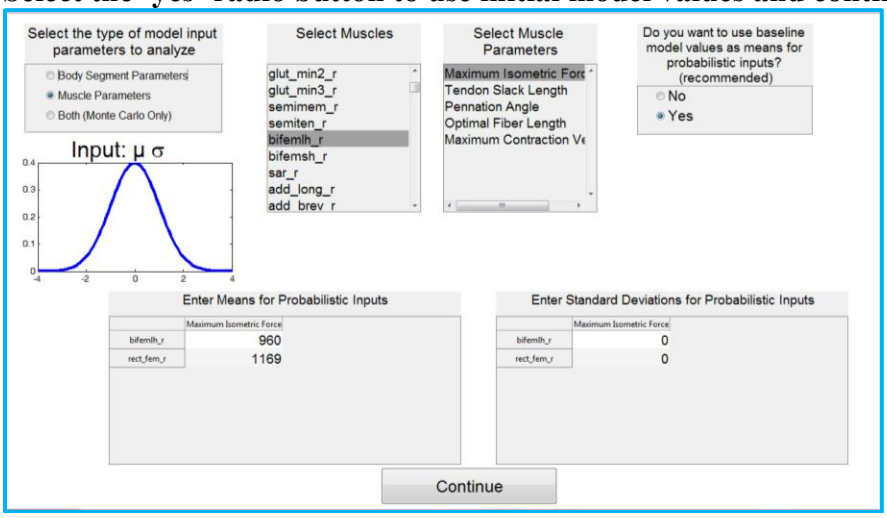

Enter values for standard deviations:

$$s_{BF} = CV_{BF} \times |m_{BF}| = 0.0682 \times 960 = 65.45$$

$$s_{RF} = CV_{RF} \times |m_{RF}| = 0.0456 \times 1169 = 76.71$$

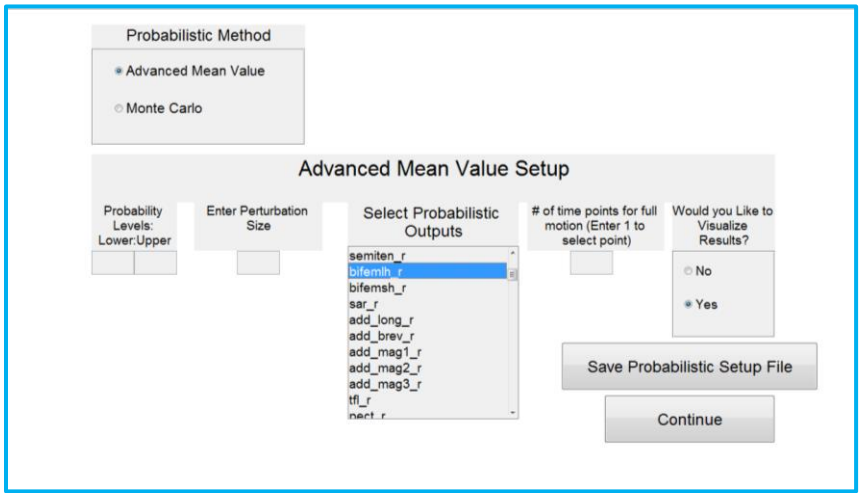

Select the Advanced Mean Value radio button.

Enter 5 and 95 for the upper and lower probability levels.

Enter 0.5 for the perturbation size. 0.5 is recommended but the user can use any.

Select the muscles that you chose in your analysis from the list of outputs to assess their results muscle force outputs. (bifemlh_r; rect_fem_r).

Enter 1 for '# the time points for full motion'.
When you continue you will be prompted to select where in the motion you would like the time point to be.

Save the probabilistic setup file, continue.

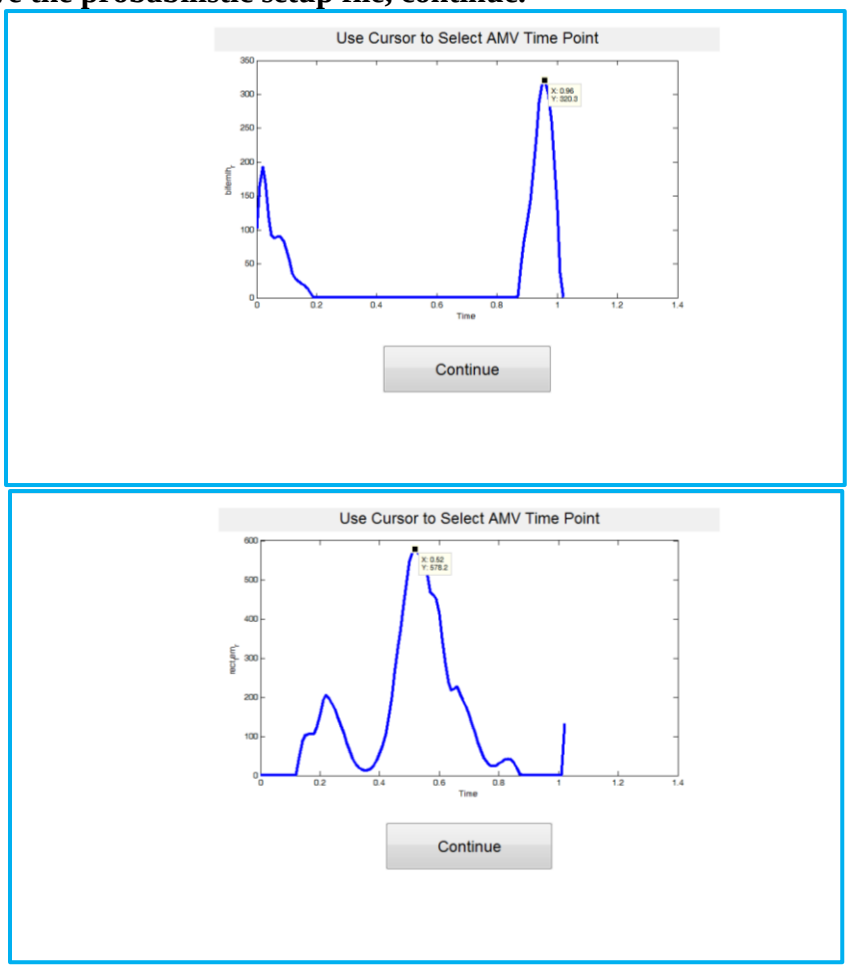

Use the cursor to select the point of maximum force outputs for each muscle, and click Continue.

Evaluate Results

Size of 5-95% bounds for the one time point are denoted by the height of the red line.
Does it make sense for the rectus femoris bounds to be so small? (Likely due to the peak force occuring during peak hip extension with the knee in a flexed position, putting the rectus femoris in a strentched position where changes in maximum isometric force would have a small effect).

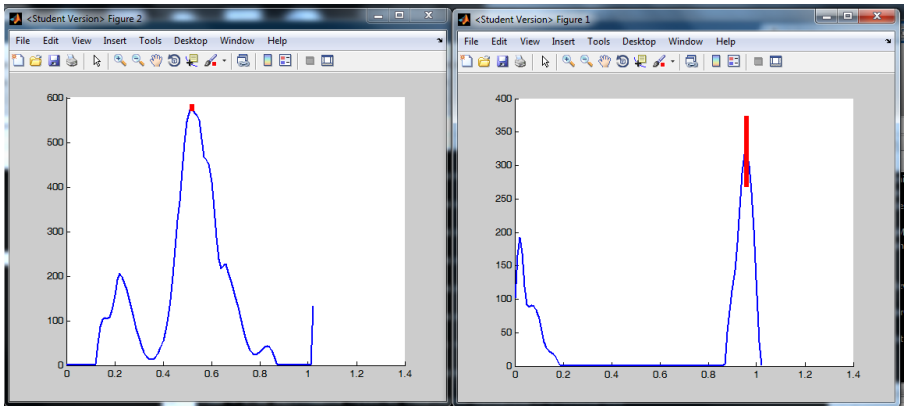

Open the Probabilistic setup file and change the number of time points from 1 to 10.

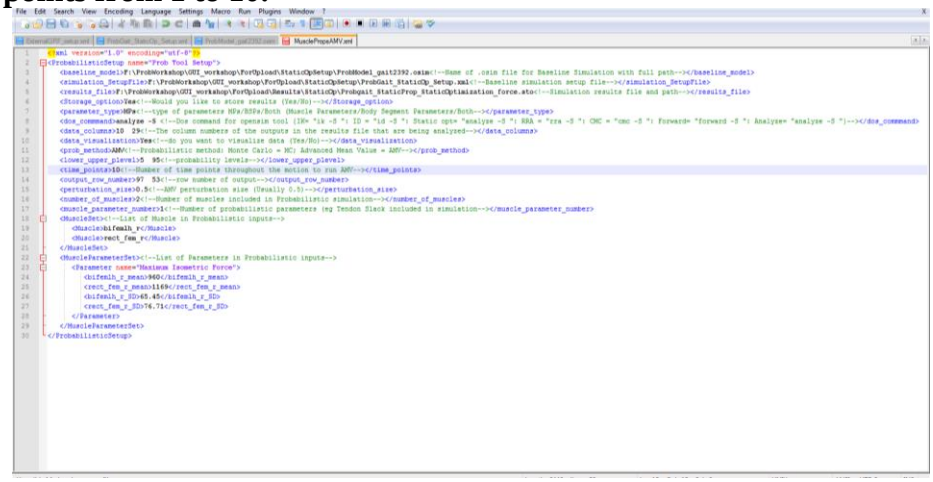

Re-run the simulation: evaluate results.

In the graphs you will see the bounds for a more complete gait cycle. Ten time points for this simulation should take approximately 25 minutes.

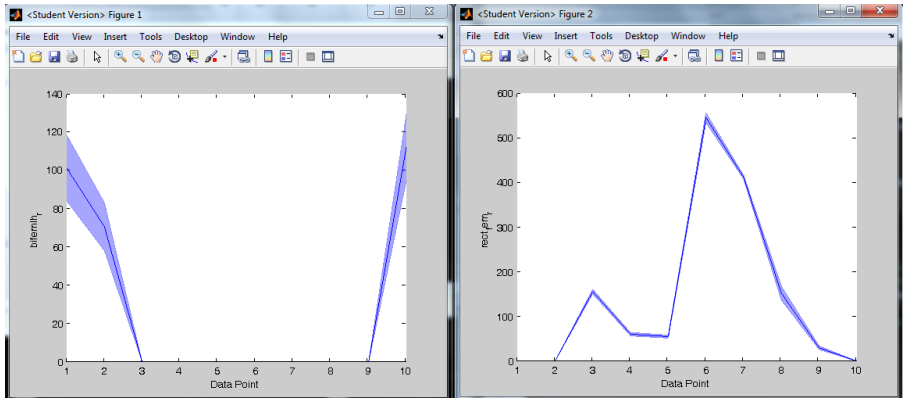

Try with even more points to increase the detail over the gait cycle. Next, take some time and run a Monte Carlo of 250 trials replicating the same same inputs

as the AMV (should complete in a little over 2 hours on a computer as decribed above). Compare the results for the size of the bounds. How many time points in AMV were needed to adequately follow the Monte Carlo result?

For Future analysis, results appear in three folders. First, the mean and each of the pertubations are run and stored in separate folders in the 'pertubations' folder. Second each muscle is run for the 5 and 95% probability level and results are stored for each time point.

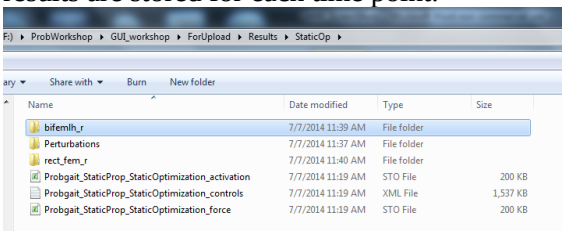

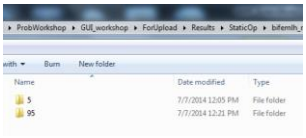

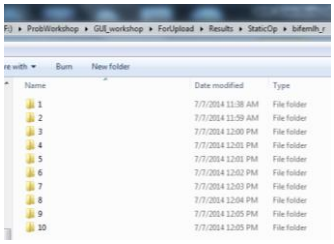

First Run:
One time point (max)
Two muscles (ham + quad)
Max isometric force

Second Time Point:
10 time points Multiple time points
Max isometric force

Assigmnent:
Run Monte Carlo Simualtion with Max isometric force

References

Curran-Everett, D., 2009. Explorations in statistics: confidence intervals. Adv. Physiol. Educ. 33, 87–90.

Valente, G., Taddei, F., Jonkers, I., 2013. Influence of weak hip abductor muscles on joint contact forces during normal walking: probabilistic modeling analysis. J. Biomech. 1–8.

Wu, Y.-T., Millwater, H., Cruse, T., 1990. Advanced probabilistic structural analysis method for implicit performance functions. AIAA J. 28, 1663–1669.

Zajac, F.E., 1993. Muscle coordination of movement: a perspective. J. Biomech. 26, 109–124.

Appendix A: Literature that contain quantitative information for parameter uncertainty

This list of peer-reviewed literature has been helpful for estimating the coefficients of variation for model parameters.

Marker Placement/Movement Artifact

Della Croce, U., A. Cappozzo, and D. Kerrigan. Pelvis and lower limb anatomical landmark calibration precision and its propagation to bone geometry and joint angles. *Med Biol Eng Comput* 37:155–161, 1999.

Benoit, D. L., D. K. Ramsey, M. Lamontagne, L. Xu, P. Wretenberg, and P. Renström. Effect of skin movement artifact on knee kinematics during gait and cutting motions measured in vivo. *Gait Posture* 24:152–64, 2006.

Gao, B., and N. N. Zheng. Investigation of soft tissue movement during level walking: translations and rotations of skin markers. *J Biomech* 41:3189–95, 2008.

Body Segment Parameters

De Leva, P. (1996). Adjustments to Zatsiorsky-Seluyanov's segment inertia parameters. *Journal of Biomechanics*, *29*(9), 1223–1230.

Langenderfer, J. E., Laz, P. J., Petrella, A. J., & Rullkoetter, P. J. (2008). An efficient probabilistic methodology for incorporating uncertainty in body segment parameters and anatomical landmarks in joint loadings estimated from inverse dynamics. *Journal of Biomechanical Engineering*, *130*(1), 014502.

Rao, G., Amarantini, D., Berton, E., and Favier, D., 2006, "Influence of Body Segments' Parameters Estimation Models on Inverse Dynamics Solutions During Gait," J. Biomech, **39**, pp. 1531–1536.

Reinbolt, J. a, Haftka, R. T., Chmielewski, T. L., & Fregly, B. J. (2007). Are patient-specific joint and inertial parameters necessary for accurate inverse dynamics analyses of gait? *IEEE Transactions on Biomedical Engineering*, *54*(5), 782–93.

Muscle Properties

Friederich, J. A., and R. A. Brand. Muscle fiber architecture in the human lower limb. *J Biomech* 23:91–95, 1990.

Ward, S. R., C. M. Eng, L. H. Smallwood, and R. L. Lieber. Are current measurements of lower extremity muscle architecture accurate? *Clin Orthop Relat Res* 467:1074–82, 2009.